

A STRONGLY MASS-CONSERVATIVE METHOD FOR THE COUPLED NAVIER–STOKES AND DARCY–FORCHHEIMER EQUATIONS

JINGYU LIU AND LINA ZHAO* 

Abstract. In this paper, we propose and analyze a strongly mass-conservative numerical scheme for the coupled Navier–Stokes and Darcy–Forchheimer system in both two and three spatial dimensions. The two subproblems are coupled through physically relevant interface conditions, including mass conservation, balance of normal forces, and the Beavers–Joseph–Saffman condition. We employ a staggered discontinuous Galerkin method for the Navier–Stokes equations and use standard mixed finite elements for the Darcy–Forchheimer problem. The proposed formulation incorporates the interface conditions directly, without introducing Lagrange multipliers on the interface or artificial numerical fluxes on the mesh skeleton. As a consequence, although discontinuous Galerkin elements are used in the free-flow region, the resulting discrete velocity field is globally $\mathbf{H}(\text{div})$ -conforming across the entire domain. In particular, the incompressibility constraint is satisfied exactly in the free-flow region, thereby yielding strong mass conservation over the entire computational domain. Under a suitable small-data assumption, we establish the well-posedness of the resulting nonlinear discrete system. Owing to the exact preservation of mass conservation, the proposed scheme exhibits a pressure-robust behavior, in the sense that the velocity approximation is insensitive to pressure effects. Numerical experiments are presented to illustrate the stability and robustness of the method, including its performance in regimes involving small viscosity, large pressure, and limited solution regularity.

Mathematics Subject Classification. 65M60, 65N22, 65N30, 74F10, 76M10.

Received March 18, 2025. Accepted February 19, 2026.

1. INTRODUCTION

The modeling and simulation of the interaction between free fluid and porous media pose persistent mathematical and computational challenges, due to the coexistence of different flow regimes and the coupling of fundamentally distinct governing equations across the interface. This framework is critical in diverse applications, such as modeling groundwater–riverbed interaction in karst aquifers and blood filtration across capillary walls in biomedical engineering. The development of robust numerical schemes for such coupled problems remains an active area of research, largely due to the presence of multiple interface conditions that must be enforced consistently across the fluid–porous interface. Among these conditions, mass conservation plays a particularly fundamental role, as it directly governs the continuity of normal fluxes and has a decisive impact on the stability

Keywords and phrases. Discontinuous Galerkin methods, mixed finite element method, strong mass conservation, pressure-robustness, Navier–Stokes equations, Darcy–Forchheimer problem.

Department of Mathematics, City University of Hong Kong, Kowloon Tong, Hong Kong SAR, P.R. China.

*Corresponding author: linazha@cityu.edu.hk

and robustness of the resulting numerical approximation. Existing approaches largely fall into two categories based on how interface conditions are enforced. The first category employs Lagrange multipliers on the interface to strongly enforce interface constraints, as seen in conforming finite element methods [22–24]. While such methods typically preserve strong mass conservation, this advantage comes at the cost of increased computational complexity and additional degrees of freedom. The second class avoids auxiliary interface variables and instead incorporates the coupling conditions weakly. Representative approaches include interior penalty discontinuous Galerkin methods [11, 25], domain decomposition methods [16], and staggered DG formulations [36, 39]. These methods are often more efficient in practice and easier to implement. Nevertheless, since the continuity of normal fluxes is not enforced explicitly, strong mass conservation is generally sacrificed. Recently, a class of hybridizable discontinuous Galerkin methods [8–10] has been proposed as an alternative approach for achieving strong mass conservation without the use of Lagrange multipliers. These methods are based on a velocity–pressure formulation in the free-flow region and require penalty stabilization on the mesh skeleton to ensure the well-posedness of the discrete system.

This paper proposes and analyzes a novel, strongly mass-conservative numerical scheme for the coupled Navier–Stokes and Darcy–Forchheimer system, without introducing any Lagrange multipliers or penalty terms on the interface. The coupled system is inherently nonlinear in both the free-flow and porous-media regions, which poses significant challenges for numerical approximation. The Navier–Stokes equations model viscous, incompressible fluid dynamics, capturing complex phenomena such as turbulence and high-velocity flows. Conversely, the Darcy–Forchheimer equations govern flow through porous media, where nonlinear inertial forces dominate at moderate velocities. The coupling is enforced through three interface conditions: (1) mass conservation, (2) balance of normal forces, and (3) the Beavers–Joseph–Saffman (BJS) condition, which prescribes the tangential slip velocity along the interface is proportional to the shear stress. Different from methods employing Lagrange multipliers to enforce interface constraints [7, 15, 21], our scheme treats the interface conditions as natural boundary conditions, leveraging compatible discretizations for each subdomain. Motivated by staggered DG schemes [28, 38], which preserve strong mass conservation for incompressible flows in a single domain, we adopt the framework proposed in [37] for coupled problems. In particular, staggered DG finite elements are employed in the free-flow region, whereas $\mathbf{H}(\text{div})$ -conforming Brezzi–Douglas–Marini elements (cf. [4]) are adopted for the Darcy–Forchheimer subproblem. As a result, the proposed discretization produces a globally $\mathbf{H}(\text{div})$ -conforming velocity and satisfies mass conservation exactly at the discrete level. As a consequence of strong mass conservation, the discrete velocity is structurally decoupled from the pressure variable. This property gives rise to a pressure-robust behavior of the scheme, in the sense that the velocity approximation is insensitive to pressure approximation, which is particularly important in regimes characterized by large pressure gradients and relatively small velocities, as illustrated in Examples 5.2 and 5.3. Moreover, in contrast to staggered DG scheme developed for the Navier–Stokes equations in a single domain [28], the presence of the fluid–porous interface requires a nontrivial modification of the trilinear convection terms. In our scheme, the interface contributions are reformulated through the BJS interface condition, which is essential for maintaining the stability of the coupled scheme.

The major contributions of this paper can be summarized as follows:

- (1) We propose a numerical scheme for the coupled Navier–Stokes and Darcy–Forchheimer system that does not rely on Lagrange multipliers on the interface or artificial numerical fluxes on the mesh skeleton. The well-balanced finite element discretizations employed in each subdomain allow all interface conditions to be incorporated naturally into the formulation.
- (2) We prove that the proposed scheme satisfies strong mass conservation (Lem. 4.10), in the sense that the normal component of the discrete velocity is continuous across all interior faces within each subdomain as well as across the interface, and that the discrete velocity is exactly divergence-free in the free-flow domain.
- (3) We establish the well-posedness of the resulting nonlinear discrete system under a suitable small-data assumption. The analysis is carried out within a fixed-point framework and relies on careful estimates of the nonlinear operators together with the structure-preserving properties of the discretization.

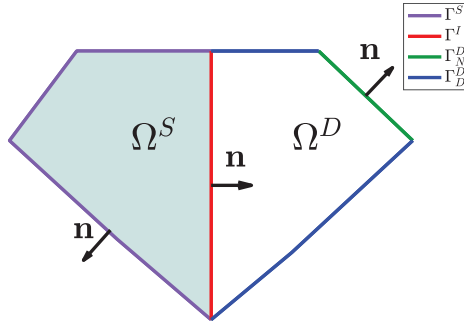


FIGURE 1. Schematic diagram of a diamond-shaped domain.

- (4) Numerical experiments are presented to illustrate the stability and robustness of the proposed method. Owing to the exact preservation of mass conservation, the scheme exhibits a pressure-robust behavior, in the sense that the velocity approximation is insensitive to pressure effects. To highlight this property, we investigate the performance of the method in challenging regimes involving small viscosity and large pressure in Examples 5.2 and 5.3, respectively. In addition, Example 5.4 is designed to examine the behavior of the scheme in the presence of limited solution regularity. These numerical results consistently demonstrate the stability and robustness of the proposed formulation.

The remainder of this paper is organized as follows. Section 2 presents the mathematical framework governing the coupled Navier–Stokes and Darcy–Forchheimer system. In Section 3, we detail the construction of the staggered discontinuous Galerkin discretization. Section 4 begins by recalling essential preliminary results, covering analytical properties of nonlinear operators and the degrees of freedom for the finite element spaces along with their corresponding projection operators. We then establish the well-posedness of the proposed scheme under a suitable small-data assumption. Numerical experiments are presented in Section 5 to validate the theoretical findings and demonstrate the robustness and accuracy of the method. To enhance the readability of this paper, complicated proofs are collected in Section 6.

2. THE CONTINUOUS PROBLEM

This section introduces the coupled Navier–Stokes and Darcy–Forchheimer equations governing the fluid-porous media interaction problem, including the background information, some notations, and existing results for the well-posedness.

2.1. Problem statement

Let Ω^S and Ω^D be two connected, bounded, non-overlapping polygonal (for $d = 2$) or polyhedral (for $d = 3$) domains in \mathbb{R}^d ($d = 2, 3$), sharing a common interface $\Gamma^I := \partial\Omega^S \cap \partial\Omega^D$, with $|\Gamma^I| > 0$. We define the exterior boundaries $\Gamma^S := \partial\Omega^S \setminus \Gamma^I$ and $\Gamma^D := \partial\Omega^D \setminus \Gamma^I$. The boundary Γ^D is further decomposed into two disjoint parts: $\Gamma^D := \Gamma_D^D \cup \Gamma_N^D$, where both $|\Gamma_D^D|, |\Gamma_N^D| \geq 0$. We denote by \mathbf{n} the unit normal vector. On the exterior boundary $\partial\Omega^S \cup \partial\Omega^D$, it points outward, while on the interface Γ^I , \mathbf{n} is taken to point from Ω^S into Ω^D . A schematic two-dimensional illustration of the diamond-shaped domain is shown in Figure 1.

In the free fluid domain Ω^S , the velocity \mathbf{u}^S and pressure p^S satisfy the incompressible Navier–Stokes equations

$$\begin{aligned} \nabla \cdot (\mathbf{u}^S \otimes \mathbf{u}^S) + \nabla p^S - \nabla \cdot (\mu \nabla \mathbf{u}^S) &= \mathbf{f}^S, & \text{in } \Omega^S, \\ \nabla \cdot \mathbf{u}^S &= 0, & \text{in } \Omega^S, \end{aligned}$$

$$\mathbf{u}^S = 0, \quad \text{on } \Gamma^S,$$

where $\mu > 0$ is the viscosity of the fluid.

In the porous media domain Ω^D , when kinematic effects dominate over viscous forces, the linear Darcy law for the velocity \mathbf{u}^D and pressure gradient ∇p^D no longer holds. Instead, the Darcy–Forchheimer model [18], a nonlinear system, is more appropriate for capturing the dynamics. The Darcy–Forchheimer model with mixed boundary conditions is given by

$$(\mu\kappa^{-1} + \beta|\mathbf{u}^D|)\mathbf{u}^D + \nabla p^D = \mathbf{f}^D, \quad \text{in } \Omega^D, \tag{2.1}$$

$$-\nabla \cdot \mathbf{u}^D = g^D, \quad \text{in } \Omega^D, \tag{2.2}$$

$$\mathbf{u}^D \cdot \mathbf{n} = 0, \quad \text{on } \Gamma_N^D, \tag{2.3}$$

$$p^D = 0, \quad \text{on } \Gamma_D^D. \tag{2.4}$$

Here, $\kappa > 0$ represents the permeability of the porous media, and $\beta > 0$ is the Forchheimer number.

The free-flow and porous-media subproblems are coupled through physically relevant interface conditions, including the mass conservation, the balance of normal forces, and the Beavers–Joseph–Saffman interface condition (cf. [2, 35]). These can be expressed as

$$\mathbf{u}^S \cdot \mathbf{n} = \mathbf{u}^D \cdot \mathbf{n}, \quad \text{on } \Gamma^I, \tag{2.5}$$

$$p^S - p^D = \mu \nabla \mathbf{u}^S \mathbf{n} \cdot \mathbf{n}, \quad \text{on } \Gamma^I, \tag{2.6}$$

$$-\mu(\nabla \mathbf{u}^S \mathbf{n})^t = \alpha \mu \kappa^{-\frac{1}{2}} (\mathbf{u}^S)^t, \quad \text{on } \Gamma^I \tag{2.7}$$

where $\alpha > 0$ is a dimensionless constant dependent on the geometric characteristics of the porous media. Here, for any $\mathbf{v} \in L^2(\Gamma^I)^d$, $(\mathbf{v})^t$ represents its tangent component on Γ^I , namely $(\mathbf{v})^t := \mathbf{v} - (\mathbf{v} \cdot \mathbf{n})\mathbf{n}$. The Beavers–Joseph–Saffman condition indicates that the slip velocity along the interface is proportional to the shear stress.

Throughout this paper, we assume that all the parameters involved above are constants. By introducing an additional variable $\underline{L}^S = \mu \nabla \mathbf{u}^S$, the Navier–Stokes equations can be reformulated as

$$\mu^{-1} \underline{L}^S = \nabla \mathbf{u}^S, \quad \text{in } \Omega^S, \tag{2.8}$$

$$\nabla \cdot (\mathbf{u}^S \otimes \mathbf{u}^S) + \nabla p^S - \nabla \cdot \underline{L}^S = \mathbf{f}^S, \quad \text{in } \Omega^S, \tag{2.9}$$

$$\nabla \cdot \mathbf{u}^S = 0, \quad \text{in } \Omega^S. \tag{2.10}$$

In Section 3, we will present the numerical scheme for (2.1)–(2.10).

2.2. Preliminaries

In this subsection, we introduce definitions and notations that will be used throughout the paper. We begin by recalling standard terminology for Lebesgue and Sobolev spaces. For a measurable set $D \subset \mathbb{R}^d$ (or $D \subset \mathbb{R}^{d-1}$ when considering surfaces) and a real number $p \geq 1$, the L^p -norm on D is defined by

$$\|f\|_{L^p(D)} := \left(\int_D |f|^p dx \right)^{\frac{1}{p}}, \quad \forall f \in L^p(D).$$

The same notation is used for the norms of vector- and tensor-valued functions, provided no confusion arises. When $p = 2$, we denote the L^2 -inner product by $(f_1, f_2)_D = \int_D f_1 f_2 dx$. Moreover, the duality pairing between $L^p(D)$ and its dual $L^q(D)$ (with $1/p + 1/q = 1$) is also written as $(\cdot, \cdot)_D$. For a bounded domain $D \subset \mathbb{R}^d$, a subset $D_0 \subset D$, and a face $F \subset \partial D$, we denote by $f|_{D_0}$ the restriction of a function f (defined on D) to D_0 . If f admits a trace on F , we write $f|_F$ for the trace.

For any integer $p \geq 1$ and real number $s \geq 0$, we denote by $W^{s,p}(D)$ the Sobolev space equipped with the norm $\|\cdot\|_{W^{s,p}(D)}$ and seminorm $|\cdot|_{W^{s,p}(D)}$. When no confusion arises, the same notation is used for the corresponding norms and seminorms on the product spaces $W^{s,p}(D)^d$ and $W^{s,p}(D)^{d \times d}$. In the case $p = 2$, we write $H^s(D) := W^{s,2}(D)$, with norm $\|\cdot\|_{H^s(D)}$ and seminorm $|\cdot|_{H^s(D)}$; this convention extends naturally to vector-valued and tensor-valued functions. Throughout the paper we use 0 , $\mathbf{0}$, and $\underline{\mathbf{0}}$ to denote the null scalar, vector, and second-order tensor, respectively.

We introduce the following function spaces:

$$H_{\Gamma^S}^1(\Omega^S) := \{r^S \in H^1(\Omega^S); r^S = 0 \text{ on } \Gamma^S\},$$

$$\mathbf{H}_{\Gamma_N^D,3}(\text{div}; \Omega^D) := \left\{ \mathbf{v}^D \in \mathbf{H}(\text{div}; \Omega^D) \cap L^3(\Omega^D)^d; \mathbf{v}^D \cdot \mathbf{n} = 0 \text{ on } \Gamma_N^D \right\},$$

where

$$\mathbf{H}(\text{div}; D) := \{ \mathbf{v} \in L^2(D)^d; \nabla \cdot \mathbf{v} \in L^2(D) \}.$$

We recall the following Helmholtz–Leray decomposition for domains with mixed boundary conditions. For further discussion on the role of this decomposition in incompressible flow discretizations, we refer to [29]. For the case of homogeneous Dirichlet boundary conditions, the classical Helmholtz–Hodge decomposition ([19], Thm. III.1.1) can be applied instead.

Lemma 2.1 (Helmholtz–Leray decomposition [33], Lem. 2.2). *For $\mathbf{f}^S \in L^2(\Omega^S)^d$, there exist $\mathbf{f}_0 \in L^2(\Omega^S)^d$ and $\phi \in H^1(\Omega^S)$ such that*

$$\mathbf{f}^S = \mathbf{f}_0 + \nabla \phi,$$

where

$$\nabla \cdot \mathbf{f}_0 = 0 \quad \text{in } \Omega^S, \quad \mathbf{f}_0 \cdot \mathbf{n} = 0 \quad \text{on } \Gamma^S, \quad \text{and } \phi = 0 \quad \text{on } \Gamma^I.$$

Under a suitable small-data assumption, the well-posedness for the coupled Navier–Stokes and Darcy–Forchheimer problems was shown in [7] for the case where the velocity gradient is the symmetric gradient and $\Gamma_D^D = \emptyset$. Denote $\bar{C} := \max\{\widetilde{\mathcal{C}}_{\mathbf{f}}^{\frac{1}{2}}, \widetilde{\mathcal{C}}_{\mathbf{f}}, \widetilde{\mathcal{C}}_{\mathbf{f}}^2\}$, where

$$\widetilde{\mathcal{C}}_{\mathbf{f}}^2 := C \left(\mu^{-1} \|\mathbf{f}_0\|_{L^2(\Omega^S)}^2 + \frac{1}{\sqrt{\beta}} \|\mathbf{f}^D\|_{L^{\frac{3}{2}}(\Omega^D)}^{\frac{3}{2}} + \mu \kappa^{-1} \|g^D\|_{L^2(\Omega^D)}^2 + \beta \|g^D\|_{L^2(\Omega^D)}^{\frac{3}{2}} \right).$$

Here $C > 0$ is derived as a combination of the constants appearing in the Poincaré inequality, the continuous trace inequality and Sobolev inequality, related to Ω^S , Ω^D , Γ^S , Γ_D^D , Γ_N^D , and Γ^I , and \mathbf{f}_0 is the Helmholtz–Leray decomposition of $\mathbf{f}^S = \mathbf{f}_0 + \nabla \phi$ in Lemma 2.1. Under the assumption that $\bar{C} \leq \mu^{\frac{3}{2}}$, with minor modification of the proofs in [7], the well-posedness can be established for (2.1)–(2.10).

3. THE STRONGLY MASS-CONSERVATIVE SCHEME

This section presents the numerical discretization for the coupled Navier–Stokes and Darcy–Forchheimer problem. Unlike several existing approaches [21, 23], our method imposes the interface conditions without introducing any Lagrange multipliers, which is achieved *via* a careful balance of finite element spaces used in each subdomain. Specifically, a staggered DG method developed in [38] will be used for the discretization of the Navier–Stokes equations and standard mixed finite element method will be used for the discretization of Darcy–Forchheimer equations. We begin by describing the mesh settings, then define the finite element spaces, and finally derive the discrete scheme (3.4)–(3.8), which is proved to satisfy strong mass conservation (Lem. 4.10).

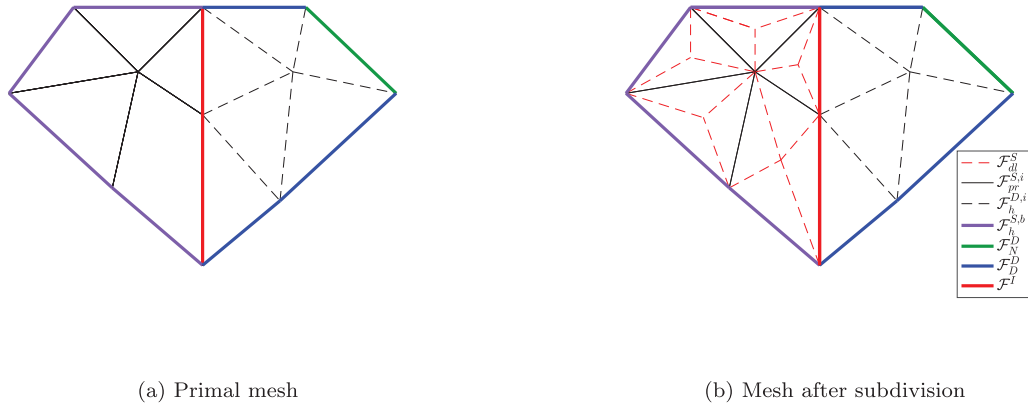


FIGURE 2. Profile of the primal mesh and the mesh after subdivision.

3.1. Mesh settings

The computational domain Ω^S is partitioned into polygonal (for $d = 2$) or polyhedral (for $d = 3$) meshes, and Ω^D is partitioned into triangular ($d = 2$) or tetrahedral ($d = 3$) meshes. We assume that the faces of these two meshes coincide along the interface, and no face simultaneously intersects both Γ_D^D and Γ_N^D . We use \mathcal{T}_0^j to denote the set of primal elements in Ω^j for $j = S, D$. For any measurable set $D \subset \mathbb{R}^d$ or $D \subset \mathbb{R}^{d-1}$, we use h_D to represent its diameter and let $h := \max\{h_\tau : \tau \in \mathcal{T}_0^S \cup \mathcal{T}_0^D\}$. We further assume standard shape-regularity: there exist constants $\rho > 0$ and $C > 0$, such that, for any $\tau_0 \in \mathcal{T}_0^S \cup \mathcal{T}_0^D$, τ_0 is star-shaped with respect to a ball of radius ρh_{τ_0} and satisfies $h_F \geq Ch_{\tau_0}$ for any face $F \subset \partial\tau_0$.

The staggered DG formulation requires the construction of two distinct sets of faces to enforce different continuity conditions. This is accomplished through a suitable subdivision of the primal mesh. In two dimensional case, for each element $\tau \in \mathcal{T}_0^S$, its star-shaped regularity allows us to connect the cell center to all its vertices, thereby subdividing τ into triangles. The set of all these triangles is denoted as \mathcal{T}_h^S . For the domain Ω^D , no such subdivision is required; thus, we simply denote $\mathcal{T}_h^D := \mathcal{T}_0^D$. In three dimensional case, we adopt a two-step subdivision described in [31]. First, each polyhedral element in \mathcal{T}_0^S is decomposed into pyramids by connecting the cell center to the vertices, and then each pyramid is subdivided into tetrahedra by connecting face centers to the corresponding face vertices. The collection of all tetrahedra is denoted by \mathcal{T}_h^S . To guarantee that the meshes match on Γ^I , we apply the same procedure to \mathcal{T}_0^D to obtain a tetrahedral mesh \mathcal{T}_h^D . (If both \mathcal{T}_0^S and \mathcal{T}_0^D are tetrahedral, one may alternatively use the subdivision in [12] and simply set $\mathcal{T}_h^D := \mathcal{T}_0^D$.)

We denote by \mathcal{F}^I the set of faces lying on the interface Γ^I . For $j = S, D$, let \mathcal{F}_h^j be the set of all faces of the mesh \mathcal{T}_h^j , excluding those belonging to \mathcal{F}^I . Let $\mathcal{N}_{\text{center}}$ denote the set of all cell centers of elements in \mathcal{T}_h^0 . A face in \mathcal{T}_h^S is called a *dual face* if it contains at least one vertex in $\mathcal{N}_{\text{center}}$. The set of all such dual faces is denoted by \mathcal{F}_{dl}^S . The set of all *primal faces* in \mathcal{T}_h^S is defined by $\mathcal{F}_{pr}^S := \mathcal{F}_h^S \setminus \mathcal{F}_{dl}^S$.

We define the boundary face sets $\mathcal{F}_h^{S,b} := \{F \in \mathcal{F}_h^S : |F \cap \Gamma^S| > 0\}$, $\mathcal{F}_D^D := \{F \in \mathcal{F}_h^D : |F \cap \Gamma_D^D| > 0\}$ and $\mathcal{F}_N^D := \{F \in \mathcal{F}_h^D : |F \cap \Gamma_N^D| > 0\}$. Then the interior face sets are defined by $\mathcal{F}_{pr}^{S,i} := \mathcal{F}_{pr}^S \setminus \mathcal{F}_h^{S,b}$ and $\mathcal{F}_h^{D,i} := \mathcal{F}_h^D \setminus (\mathcal{F}_D^D \cup \mathcal{F}_N^D)$.

As an illustration, Figure 2 shows a two-dimensional example using a diamond-shaped domain (see Fig. 1), where a thick red line indicates the interface. Figure 2a displays the corresponding primal meshes, while Figure 2b presents the configuration after subdivision. In the latter figure, the solid black lines in Ω^S represent primal faces, and the red dotted lines correspond to dual faces in \mathcal{T}_h^S . Moreover, the black dotted lines represent the interior faces in \mathcal{T}_h^D , while the blue and green solid lines represent Dirichlet and Neumann boundary faces, respectively.

For each face F , we fix a unit normal vector \mathbf{n}_F as follows: If $F \in \mathcal{F}_h^{S,b} \cup \mathcal{F}_D^D \cup \mathcal{F}_N^D$, then \mathbf{n}_F is the unit normal vector on F pointing outside of $\Omega^S \cup \Omega^D$; if $F \in \mathcal{F}^I$, then \mathbf{n}_F represents the unit normal vector pointing from Ω^S to Ω^D ; otherwise, \mathbf{n}_F is chosen as one of the unit normal vectors on F . For any vector $\mathbf{v} \in L^2(F)^d$, its tangent component on F is defined as $(\mathbf{v})^{\mathbf{t}_F} := \mathbf{v} - (\mathbf{v} \cdot \mathbf{n}_F)\mathbf{n}_F$.

We employ the standard DG jump and average operators. For each interior face $F \in \mathcal{F}_{dl}^S \cup \mathcal{F}_{pr}^{S,i} \cup \mathcal{F}_h^{D,i}$ shared by two elements τ_1 and τ_2 , we define the jump and average of a scalar-valued function f over F as

$$[f]_{|F} := (f|_{\tau_1})_{|F} - (f|_{\tau_2})_{|F}, \text{ and } \{f\}_{|F} := \frac{(f|_{\tau_1})_{|F} + (f|_{\tau_2})_{|F}}{2}.$$

On boundary faces $F \in \mathcal{F}_{pr}^{S,b} \cup \mathcal{F}_D^D \cup \mathcal{F}_N^D$, the jump and average reduce to $[f]_{|F} = \{f\}_{|F} = (f)_{|F}$. The above definitions extend naturally to vector-valued functions. When it is clear which face is referring to, we can omit the subscription F of \mathbf{n}_F , $(\cdot)^{\mathbf{t}_F}$, $[\cdot]_{|F}$, and $\{\cdot\}_{|F}$ for brevity. We use ∇_h and $\nabla_h \cdot$ to denote the broken gradient and divergence operators acting cell-wise. For any $k \geq 1$, $\tau \in \mathcal{T}_h^S \cup \mathcal{T}_h^D$, and $F \in \mathcal{F}_{pr}^S \cup \mathcal{F}_{dl}^S \cup \mathcal{F}^I \cup \mathcal{F}_h^D$, we define $P^k(\tau)$ and $P^k(F)$ as the spaces of polynomials of degree up to order k on τ and F , respectively. In the following analysis, constant $C > 0$ represents a generic constant, independent of mesh size h and the parameters, μ , α , β , κ , introduced in the system (2.1)–(2.10).

3.2. Finite element spaces and numerical scheme

We now introduce the finite element spaces for the various unknowns. For the free-fluid domain Ω^S , the locally $\mathbf{H}(\text{div})$ -conforming velocity space is

$$\mathbf{U}_h^S := \left\{ \mathbf{v}_h^S : (\mathbf{v}_h^S)|_{\tau} \in P^k(\tau)^d, \forall \tau \in \mathcal{T}_h^S; [\mathbf{v}_h^S \cdot \mathbf{n}]_{|F} = 0, \text{ on } F \in \mathcal{F}_{dl}^S \right\},$$

equipped with the following norms

$$\begin{aligned} \|\mathbf{v}_h^S\|_{\mathbf{U}_h^S,0}^2 &:= \|\mathbf{v}_h^S\|_{L^2(\Omega^S)}^2 + \sum_{F \in \mathcal{F}_{dl}^S} h_F \|\mathbf{v}_h^S \cdot \mathbf{n}\|_{L^2(F)}^2, \\ \|\mathbf{v}_h^S\|_{\mathbf{U}_h^S,1}^2 &:= \|\nabla_h \mathbf{v}_h^S\|_{L^2(\Omega^S)}^2 + \sum_{F \in \mathcal{F}_{pr}^S} h_F^{-1} \|\llbracket \mathbf{v}_h^S \rrbracket\|_{L^2(F)}^2 + \sum_{F \in \mathcal{F}_{dl}^S} h_F^{-1} \left\| \left[(\mathbf{v}_h^S)^{\mathbf{t}} \right] \right\|_{L^2(F)}^2, \\ \|\mathbf{v}_h^S\|_{0,4,h}^4 &:= \|\mathbf{v}_h^S\|_{L^4(\Omega^S)}^4 + \sum_{\tau \in \mathcal{T}_h^S} \sum_{F \in \partial\tau} h_F \|\mathbf{v}_h^S\|_{L^4(F)}^4. \end{aligned}$$

The norm $\|\cdot\|_{\mathbf{U}_h^S,0}$ will be used for the inf-sup condition of the velocity–pressure coupling, while $\|\cdot\|_{0,4,h}$ is a discrete L^4 -norm that controls the nonlinear terms *via* Hölder’s inequality.

The locally H^1 -conforming pressure space is

$$P_h^S := \left\{ q_h^S : (q_h^S)|_{\tau} \in P^k(\tau), \forall \tau \in \mathcal{T}_h^S; [q_h^S]_{|F} = 0, \text{ on } F \in \mathcal{F}_{pr}^{S,i} \right\}.$$

We define the finite element space for the velocity gradient in Ω^S as

$$\underline{\mathbf{G}}_h^S := \left\{ \underline{\mathbf{G}}_h^S : (\underline{\mathbf{G}}_h^S)|_{\tau} \in P^k(\tau)^{d \times d}, \forall \tau \in \mathcal{T}_h^S; \llbracket \underline{\mathbf{G}}_h^S \mathbf{n} \rrbracket_{|F} = \mathbf{0}, \text{ on } F \in \mathcal{F}_{pr}^{S,i}; \left[(\underline{\mathbf{G}}_h^S \mathbf{n})^{\mathbf{t}} \right]_{|F} = \mathbf{0}, \text{ on } F \in \mathcal{F}_{dl}^S \right\},$$

endowed with the discrete L^2 -norm

$$\|\underline{\mathbf{G}}_h^S\|_{\underline{\mathbf{W}}_h^S,0}^2 := \|\underline{\mathbf{G}}_h^S\|_{L^2(\Omega^S)}^2 + \sum_{F \in \mathcal{F}_{pr}^S \cup \mathcal{F}^I} h_F \|\underline{\mathbf{G}}_h^S \mathbf{n}\|_{L^2(F)}^2 + \sum_{F \in \mathcal{F}_{dl}^S} h_F \left\| (\underline{\mathbf{G}}_h^S \mathbf{n})^{\mathbf{t}} \right\|_{L^2(F)}^2.$$

For the porous medium Ω^D , we adopt the standard Brezzi–Douglas–Marini (BDM) pair [5] in a dual-mixed formulation:

$$\begin{aligned} \mathbf{U}_h^D &:= \left\{ \mathbf{v}_h^D : (\mathbf{v}_h^D)|_\tau \in P^k(\tau)^d, \forall \tau \in \mathcal{T}_h^D; [\mathbf{v}_h^D \cdot \mathbf{n}]_F = 0, \forall F \in \mathcal{F}_h^{D,i} \cup \mathcal{F}_N^D \right\}, \\ P_h^D &:= \left\{ q_h^D : (q_h^D)|_\tau \in P^{k-1}(\tau), \forall \tau \in \mathcal{T}_h^D \right\}. \end{aligned}$$

We now derive the discrete formulation for the coupled problem. Multiplying equation (2.8) by a test function $\underline{\mathbf{G}}_h^S \in \underline{W}_h^S$ and integrating by parts yields

$$\begin{aligned} (\nabla \mathbf{u}^S, \underline{\mathbf{G}}_h^S)_{\Omega^S} &= -(\mathbf{u}^S, \nabla_h \cdot \underline{\mathbf{G}}_h^S)_{\Omega^S} + \sum_{F \in \mathcal{F}_{dl}^S} (\mathbf{u}^S \cdot \mathbf{n}, [\underline{\mathbf{G}}_h^S \mathbf{n} \cdot \mathbf{n}])_F \\ &\quad + \sum_{F \in \mathcal{F}^I} (\mathbf{u}^D \cdot \mathbf{n}, \underline{\mathbf{G}}_h^S \mathbf{n} \cdot \mathbf{n})_F - \sum_{F \in \mathcal{F}^I} \left(\alpha^{-\frac{1}{2}} \mu^{-\frac{1}{2}} \kappa^{\frac{1}{4}} (\underline{\mathbf{L}}^S \mathbf{n})^t, \alpha^{-\frac{1}{2}} \mu^{-\frac{1}{2}} \kappa^{\frac{1}{4}} (\underline{\mathbf{G}}_h^S \mathbf{n})^t \right)_F, \end{aligned}$$

where we have used the decomposition $\mathbf{u}^S = (\mathbf{u}^S \cdot \mathbf{n})\mathbf{n} + (\mathbf{u}^S)^t$, the continuity properties $[\underline{\mathbf{G}}_h^S \mathbf{n}]_F = \mathbf{0}$ on $F \in \mathcal{F}_{pr}^{S,i}$ and $[(\underline{\mathbf{G}}_h^S \mathbf{n})^t]_F = \mathbf{0}$ on $F \in \mathcal{F}_{dl}^S$, the Dirichlet condition $(\mathbf{u}^S)|_{\Gamma^S} = \mathbf{0}$, and the interface conditions (2.5) and (2.7).

For any test function $\mathbf{v}_h^S \in \mathbf{U}_h^S$, integration by parts yields

$$\begin{aligned} (\nabla \cdot \underline{\mathbf{L}}^S, \mathbf{v}_h^S)_{\Omega^S} &= -(\underline{\mathbf{L}}^S, \nabla_h \mathbf{v}_h^S)_{\Omega^S} + \sum_{F \in \mathcal{F}_{pr}^S} (\underline{\mathbf{L}}^S \mathbf{n}, [\mathbf{v}_h^S])_F + \sum_{F \in \mathcal{F}^I} (\underline{\mathbf{L}}^S \mathbf{n}, \mathbf{v}_h^S)_F + \sum_{F \in \mathcal{F}_{dl}^S} \left((\underline{\mathbf{L}}^S \mathbf{n})^t, [(\mathbf{v}_h^S)^t] \right)_F, \\ (\nabla p^S, \mathbf{v}_h^S)_{\Omega^S} &= -(p^S, \nabla_h \cdot \mathbf{v}_h^S)_{\Omega^S} + \sum_{F \in \mathcal{F}_{pr}^S} (p^S, [\mathbf{v}_h^S \cdot \mathbf{n}])_F + \sum_{F \in \mathcal{F}^I} (p^S, \mathbf{v}_h^S \cdot \mathbf{n})_F, \end{aligned}$$

where we have used the fact that $[\mathbf{v}_h^S \cdot \mathbf{n}]_F = 0$ for all $F \in \mathcal{F}_{dl}^S$.

For any test function $q_h^S \in P_h^S$, integration by parts gives

$$-(\nabla \cdot \mathbf{u}^S, q_h^S)_{\Omega^S} = (\mathbf{u}^S, \nabla_h q_h^S)_{\Omega^S} - \sum_{F \in \mathcal{F}_{dl}^S} (\mathbf{u}^S \cdot \mathbf{n}, [q_h^S])_F - \sum_{F \in \mathcal{F}^I} (\mathbf{u}^D \cdot \mathbf{n}, q_h^S)_F,$$

where we have used the Dirichlet condition $(\mathbf{u}^S)|_{\Gamma^S} = \mathbf{0}$, the continuity $[q_h^S]_F = 0$ for all $F \in \mathcal{F}_{pr}^{S,i}$, and the interface condition (2.5).

Similarly, applying integration by parts in the Darcy domain yields

$$(\nabla p^D, \mathbf{v}_h^D)_{\Omega^D} = -(p^D, \nabla \cdot \mathbf{v}_h^D)_{\Omega^D} - \sum_{F \in \mathcal{F}^I} (p^S - \underline{\mathbf{L}}^S \mathbf{n} \cdot \mathbf{n}, \mathbf{v}_h^D \cdot \mathbf{n})_F,$$

which follows from the normal continuity $[\mathbf{v}_h^D \cdot \mathbf{n}]_F = 0$ for all $F \in \mathcal{F}_h^{D,i} \cup \mathcal{F}_N^D$, the Dirichlet condition $(p^D)|_F = 0$ for all $F \in \mathcal{F}_D^D$, and the interface condition (2.6).

Based on the above derivations, we introduce the following bilinear forms to simplify the presentation

$$\begin{aligned}
 a_h(\mathbf{v}_h^D, q_h^D) &= -(\nabla \cdot \mathbf{v}_h^D, q_h^D)_{\Omega^D}, \\
 A_h(\underline{\mathbf{G}}_h^S, \underline{\mathbf{H}}_h^S) &= \left(\mu^{-\frac{1}{2}} \underline{\mathbf{L}}_h^S, \mu^{-\frac{1}{2}} \underline{\mathbf{G}}_h^S \right)_{\Omega^S} + \sum_{F \in \mathcal{F}^I} \left(\alpha^{-\frac{1}{2}} \mu^{-\frac{1}{2}} \kappa^{\frac{1}{4}} (\underline{\mathbf{L}}_h^S \mathbf{n})^t, \alpha^{-\frac{1}{2}} \mu^{-\frac{1}{2}} \kappa^{\frac{1}{4}} (\underline{\mathbf{G}}_h^S \mathbf{n})^t \right)_F, \\
 B_h(\underline{\mathbf{G}}_h^S, \mathbf{v}_h^S) &= (\underline{\mathbf{G}}_h^S, \nabla_h \mathbf{v}_h^S)_{\Omega^S} - \sum_{F \in \mathcal{F}_{pr}^S} (\underline{\mathbf{G}}_h^S \mathbf{n}, [\mathbf{v}_h^S])_F - \sum_{F \in \mathcal{F}^I} (\underline{\mathbf{G}}_h^S \mathbf{n}, \mathbf{v}_h^S)_F - \sum_{F \in \mathcal{F}_{dl}^S} \left((\underline{\mathbf{G}}_h^S \mathbf{n})^t, [(\mathbf{v}_h^S)^t] \right)_F, \\
 B_h^*(\mathbf{v}_h^S, \underline{\mathbf{G}}_h^S) &= -(\mathbf{v}_h^S, \nabla_h \cdot \underline{\mathbf{G}}_h^S)_{\Omega^S} + \sum_{F \in \mathcal{F}_{dl}^S} (\mathbf{v}_h^S \cdot \mathbf{n}, [\underline{\mathbf{G}}_h^S \mathbf{n} \cdot \mathbf{n}])_F, \\
 b_h(\mathbf{v}_h^S, q_h^S) &= (\mathbf{v}_h^S, \nabla_h q_h^S)_{\Omega^S} - \sum_{F \in \mathcal{F}_{dl}^S} (\mathbf{v}_h^S \cdot \mathbf{n}, [q_h^S])_F, \\
 b_h^*(q_h^S, \mathbf{v}_h^S) &= -(q_h^S, \nabla_h \cdot \mathbf{v}_h^S)_{\Omega^S} + \sum_{F \in \mathcal{F}_{pr}^S} (q_h^S, [\mathbf{v}_h^S \cdot \mathbf{n}])_F + \sum_{F \in \mathcal{F}^I} (q_h^S, \mathbf{v}_h^S \cdot \mathbf{n})_F
 \end{aligned} \tag{3.1}$$

and

$$\begin{aligned}
 I_h(\mathbf{v}_h^D, \underline{\mathbf{G}}_h^S) &= \sum_{F \in \mathcal{F}^I} (\mathbf{v}_h^D \cdot \mathbf{n}, \underline{\mathbf{G}}_h^S \mathbf{n} \cdot \mathbf{n})_F, \\
 J_h(\mathbf{v}_h^D, q_h^S) &= \sum_{F \in \mathcal{F}^I} (\mathbf{v}_h^D \cdot \mathbf{n}, q_h^S)_F,
 \end{aligned}$$

for all $\mathbf{v}_h^S \in \mathbf{U}_h^S$, $\mathbf{v}_h^D \in \mathbf{U}_h^D$, $\underline{\mathbf{G}}_h^S \in \underline{W}_h^S$, $\underline{\mathbf{H}}_h^S \in \underline{W}_h^S$, $q_h^S \in P_h^S$, and $q_h^D \in P_h^D$. It is easy to observe the following adjoint properties

$$B_h(\underline{\mathbf{G}}_h^S, \mathbf{v}_h^S) = B_h^*(\mathbf{v}_h^S, \underline{\mathbf{G}}_h^S), \quad \forall (\underline{\mathbf{G}}_h^S, \mathbf{v}_h^S) \in \underline{W}_h^S \times \mathbf{U}_h^S, \tag{3.2}$$

$$b_h(\mathbf{v}_h^S, q_h^S) = b_h^*(q_h^S, \mathbf{v}_h^S), \quad \forall (\mathbf{v}_h^S, q_h^S) \in \mathbf{U}_h^S \times P_h^S. \tag{3.3}$$

Furthermore, we define the trilinear forms

$$\begin{aligned}
 N_h(\mathbf{w}_h^S, \phi_h^S, \mathbf{v}_h^S) &= - \sum_{\tau \in \mathcal{T}_h^S} (\phi_h^S \otimes \mathbf{w}_h^S, \nabla_h \mathbf{v}_h^S)_\tau + \sum_{F \in \mathcal{F}_h^{S,i}} (\{\mathbf{w}_h^S \cdot \mathbf{n}\}, \{\phi_h^S\} \cdot [\mathbf{v}_h^S])_F \\
 &\quad + \sum_{F \in \mathcal{F}_h^S} (|\{\mathbf{w}_h^S \cdot \mathbf{n}\}|, [\phi_h^S] \cdot [\mathbf{v}_h^S])_F + \sum_{F \in \mathcal{F}^I} (\mathbf{w}_h^S \cdot \mathbf{n}, (\phi_h^S \cdot \mathbf{n})(\mathbf{v}_h^S \cdot \mathbf{n}))_F, \\
 D_h(\mathbf{w}_h^S, \underline{\mathbf{H}}_h^S, \mathbf{v}_h^S) &= - \sum_{F \in \mathcal{F}^I} \left(\mathbf{w}_h^S \cdot \mathbf{n}, \alpha^{-1} \mu^{-1} \kappa^{\frac{1}{2}} (\underline{\mathbf{H}}_h^S \mathbf{n})^t \cdot (\mathbf{v}_h^S)^t \right)_F,
 \end{aligned}$$

for $\mathbf{w}_h^S, \phi_h^S, \mathbf{v}_h^S \in \mathbf{U}_h^S$ and $\underline{\mathbf{H}}_h^S \in \underline{W}_h^S$.

Combining the above derivations, the staggered DG method for the coupled Navier–Stokes and Darcy–Forchheimer problems reads as follows: Find $\underline{\mathbf{L}}_h^S \in \underline{W}_h^S$, $\mathbf{u}_h^S \in \mathbf{U}_h^S$, $p_h^S \in P_h^S$, $\mathbf{u}_h^D \in \mathbf{U}_h^D$, and $p_h^D \in P_h^D$, such that for any $\underline{\mathbf{G}}_h^S \in \underline{W}_h^S$, $\mathbf{v}_h^S \in \mathbf{U}_h^S$, $q_h^S \in P_h^S$, $\mathbf{v}_h^D \in \mathbf{U}_h^D$, and $q_h^D \in P_h^D$:

$$A_h(\underline{\mathbf{L}}_h^S, \underline{\mathbf{G}}_h^S) - B_h^*(\mathbf{u}_h^S, \underline{\mathbf{G}}_h^S) - I_h(\mathbf{u}_h^D, \underline{\mathbf{G}}_h^S) = 0, \tag{3.4}$$

$$N_h(\mathbf{u}_h^S, \mathbf{u}_h^S, \mathbf{v}_h^S) + D_h(\mathbf{u}_h^S, \underline{\mathbf{L}}_h^S, \mathbf{v}_h^S) + b_h^*(p_h^S, \mathbf{v}_h^S) + B_h(\underline{\mathbf{L}}_h^S, \mathbf{v}_h^S) = (\mathbf{f}^S, \mathbf{v}_h^S)_{\Omega^S}, \tag{3.5}$$

$$-J_h(\mathbf{u}_h^D, q_h^S) + b_h(\mathbf{u}_h^S, q_h^S) = 0, \tag{3.6}$$

$$((\mu \kappa^{-1} + \beta |\mathbf{u}_h^D|) \mathbf{u}_h^D, \mathbf{v}_h^D)_{\Omega^D} + a_h(\mathbf{v}_h^D, p_h^D) - J_h(\mathbf{v}_h^D, p_h^S) + I_h(\mathbf{v}_h^D, \underline{\mathbf{L}}_h^S) = (\mathbf{f}^D, \mathbf{v}_h^D)_{\Omega^D}, \tag{3.7}$$

$$a_h(\mathbf{u}_h^D, q_h^D) = (g^D, q_h^D)_{\Omega^D}. \tag{3.8}$$

Remark 3.1. To ensure the interface conditions can be naturally incorporated into the formulation without using Lagrange multiplier, we choose to use BDM element for porous media. For simplicity, we only consider triangular meshes in this subdomain; indeed, the current presentation can also be extended to rectangular meshes or cuboid meshes without further subdivision on \mathcal{T}_0^D (cf. [4]).

4. WELL-POSEDNESS AND STABILITY ANALYSIS

In this section, we analyze the well-posedness of the nonlinear scheme (3.4)–(3.8) using a fixed-point argument.

4.1. Preliminary results

We first introduce the Darcy–Forchheimer operator $\mathcal{M} : L^3(\Omega^D)^d \rightarrow L^{\frac{3}{2}}(\Omega^D)^d \subset (L^3(\Omega^D)^d)'$, defined by

$$\mathcal{M}(\mathbf{v}^D) = \mu\kappa^{-1}\mathbf{v}^D + \beta|\mathbf{v}^D|\mathbf{v}^D,$$

where $(L^3(\Omega^D)^d)'$ denotes the dual space of $L^3(\Omega^D)^d$. The operator \mathcal{M} exhibits certain properties that are crucial for subsequent analysis. Specifically, for any $\mathbf{v}^D, \mathbf{w}^D \in L^3(\Omega^D)^d$, the following inequality holds (cf. [26])

$$|\mathcal{M}(\mathbf{v}^D) - \mathcal{M}(\mathbf{w}^D)| \leq |\mu\kappa^{-1}(\mathbf{v}^D - \mathbf{w}^D)| + \beta|\mathbf{v}^D - \mathbf{w}^D|(|\mathbf{v}^D| + |\mathbf{w}^D|). \tag{4.1}$$

Using Lemma 5.1 of [34], we establish the following lemma.

Lemma 4.1 (Monotonicity). *For a fixed $\mathbf{w}^D \in L^3(\Omega^D)^d$, the mapping $\mathbf{v}^D \rightarrow \mathcal{M}(\mathbf{v}^D + \mathbf{w}^D)$ is monotone from $L^3(\Omega^D)^d$ into $L^{\frac{3}{2}}(\Omega^D)^d$ in the following sense: There exists a constant $C_D > 0$, only depending on Ω^D , such that, for any $\mathbf{v}^D, \mathbf{w}^D, \mathbf{r}^D \in L^3(\Omega^D)^d$, the following inequality holds*

$$(\mathcal{M}(\mathbf{v}^D + \mathbf{w}^D) - \mathcal{M}(\mathbf{r}^D + \mathbf{w}^D), \mathbf{v}^D - \mathbf{r}^D)_{\Omega^D} \geq \left\| \mu^{\frac{1}{2}}\kappa^{-\frac{1}{2}}(\mathbf{v}^D - \mathbf{r}^D) \right\|_{L^2(\Omega^D)}^2 + C_D\beta\|\mathbf{v}^D - \mathbf{r}^D\|_{L^3(\Omega^D)}^3.$$

Moreover, the operator \mathcal{M} is hemi-continuous as stated in the next lemma and the proof can be found in Proposition 3 from [26].

Lemma 4.2 (Hemi-continuity). *For fixed $\mathbf{v}^D, \mathbf{w}^D \in L^3(\Omega^D)^d$, the mapping*

$$t \rightarrow \int_{\Omega^D} \mathcal{M}(\mathbf{v}^D + t\mathbf{w}^D) \cdot \mathbf{w}^D \, dx.$$

is continuous from \mathbb{R} to \mathbb{R} .

We next introduce the degrees of freedom for all finite element spaces introduced in Section 3.2.

Lemma 4.3. *The degrees of freedom for \mathbf{U}_h^S are given by (cf. [12], Lem. 2.3)*

(UD1) *For any $F \in \mathcal{F}_{dl}^S$, we have*

$$\Phi_F^{dl}(\mathbf{v}_h^S) := (\mathbf{v}_h^S \cdot \mathbf{n}, p_k)_F, \quad \forall p_k \in P^k(F).$$

(UD2) *For any $\tau \in \mathcal{T}_h^S$, we have*

$$\Phi_\tau^S(\mathbf{v}_h^S) := (\mathbf{v}_h^S, \mathbf{p}_{k-1})_\tau, \quad \forall \mathbf{p}_{k-1} \in P^{k-1}(\tau)^d.$$

Based on these degrees of freedom, we define the projection operator $\Pi_{\mathbf{U}_h^S} : H^1(\Omega^S)^d \rightarrow \mathbf{U}_h^S$ as the unique operator satisfying, for all $\mathbf{v}^S \in H^1(\Omega^S)^d$,

$$\left(\Pi_{\mathbf{U}_h^S} \mathbf{v}^S - \mathbf{v}^S, \mathbf{p}_{k-1} \right)_\tau = 0, \quad \forall \mathbf{p}_{k-1} \in P^{k-1}(\tau)^d, \forall \tau \in \mathcal{T}_h^S, \tag{4.2}$$

$$\left(\left(\mathbf{\Pi}_{\mathcal{U}_h^S} \mathbf{v}^S - \mathbf{v}^S \right) \cdot \mathbf{n}, p_k \right)_F = 0, \quad \forall p_k \in P^k(F), \forall F \in \mathcal{F}_{dl}^S. \quad (4.3)$$

By construction, $\mathbf{\Pi}_{\mathcal{U}_h^S}$ is a polynomial-preserving operator. Consequently, the standard theory for such operators ([1], Cor. 12.13) guarantees the existence of a constant $C > 0$, independent of the mesh size, such that

$$\left\| \mathbf{v}^S - \mathbf{\Pi}_{\mathcal{U}_h^S} \mathbf{v}^S \right\|_{L^2(\tau)} \leq Ch_\tau^m \|\mathbf{v}^S\|_{H^m(\tau)}, \quad \text{and} \quad \left\| \nabla \left(\mathbf{v}^S - \mathbf{\Pi}_{\mathcal{U}_h^S} \mathbf{v}^S \right) \right\|_{L^2(\tau)} \leq Ch_\tau^{m-1} \|\mathbf{v}^S\|_{H^m(\tau)}, \quad (4.4)$$

hold for all $\mathbf{v}^S \in H^\lambda(\tau)^d$, $1 \leq m \leq \min\{k+1, \lambda\}$ and $\tau \in \mathcal{T}_h^S$.

Lemma 4.4. *The projection $\mathbf{\Pi}_{\mathcal{U}_h^S}$ satisfies the following property: There exists a constant $C > 0$, independent of mesh size h and of the parameters α , β , μ , and κ , such that*

$$\left\| \mathbf{\Pi}_{\mathcal{U}_h^S} \mathbf{v}^S \right\|_{\mathcal{U}_{h,1}^S} \leq C \|\mathbf{v}^S\|_{H^1(\Omega^S)}, \quad \forall \mathbf{v}^S \in H_{\Gamma^S}^1(\Omega^S)^d.$$

Proof. An application of the triangle inequality and (4.4) implies

$$\left\| \nabla \mathbf{\Pi}_{\mathcal{U}_h^S} \mathbf{v}^S \right\|_{L^2(\tau)} \leq \|\nabla \mathbf{v}^S\|_{L^2(\tau)} + \left\| \nabla \left(\mathbf{v}^S - \mathbf{\Pi}_{\mathcal{U}_h^S} \mathbf{v}^S \right) \right\|_{L^2(\tau)} \leq C \|\mathbf{v}^S\|_{H^1(\tau)}. \quad (4.5)$$

For $\mathbf{v}^S \in H_{\Gamma^S}^1(\Omega^S)^d$, it holds that

$$[\mathbf{v}^S]_F = \mathbf{0} \quad \forall F \in \mathcal{F}_{dl}^S \cup \mathcal{F}_{pr}^S.$$

Hence, by the continuous trace inequality and (4.4), we have for $F \subset \partial\tau$

$$\begin{aligned} h_F^{-1} \left\| [\mathbf{\Pi}_{\mathcal{U}_h^S} \mathbf{v}^S] \right\|_{L^2(F)}^2 &= h_F^{-1} \left\| [\mathbf{\Pi}_{\mathcal{U}_h^S} \mathbf{v}^S - \mathbf{v}^S] \right\|_{L^2(F)}^2 \\ &\leq C \left(\left\| \nabla \left(\mathbf{\Pi}_{\mathcal{U}_h^S} \mathbf{v}^S - \mathbf{v}^S \right) \right\|_{L^2(\tau)} + h_F^{-2} \left\| \mathbf{\Pi}_{\mathcal{U}_h^S} \mathbf{v}^S - \mathbf{v}^S \right\|_{L^2(\tau)} \right) \leq C \|\mathbf{v}^S\|_{H^1(\tau)}^2. \end{aligned} \quad (4.6)$$

Combining (4.5) and (4.6) gives

$$\left\| \mathbf{\Pi}_{\mathcal{U}_h^S} \mathbf{v}^S \right\|_{\mathcal{U}_{h,1}^S} = \left(\left\| \nabla \mathbf{\Pi}_{\mathcal{U}_h^S} \mathbf{v}^S \right\|_{L^2(\Omega^S)}^2 + \sum_{F \in \mathcal{F}_{dl}^S \cup \mathcal{F}_{pr}^S} h_F^{-1} \left\| [\mathbf{\Pi}_{\mathcal{U}_h^S} \mathbf{v}^S] \right\|_{L^2(F)}^2 \right)^{\frac{1}{2}} \leq C \|\mathbf{v}^S\|_{H^1(\Omega^S)},$$

where the constant $C > 0$ is independent of the mesh size h and of the parameters α , β , μ , and κ . This completes the proof. \square

Lemma 4.5. *The degrees of freedom for P_h^S are given by (cf. [12], Lem. 2.2)*

(VD1) *For any $F \in \mathcal{F}_{pr}^S \cup \mathcal{F}^I$, we have*

$$\phi_F(q_h^S) := (q_h^S, p_k)_F, \quad \forall p_k \in P^k(F).$$

(VD2) *For any $\tau \in \mathcal{T}_h^S$, we have*

$$\phi_\tau(q_h^S) := (q_h^S, p_{k-1})_\tau, \quad \forall p_{k-1} \in P^{k-1}(\tau).$$

Using these degrees of freedom, we define the projection operator $\Pi_{P_h^S} : H^1(\Omega^S) \rightarrow P_h^S$ as the unique linear operator satisfying, for all $q^S \in H^1(\Omega^S)$,

$$\left(\Pi_{P_h^S} q^S - q^S, p_{k-1} \right)_\tau = 0, \quad \forall p_{k-1} \in P^{k-1}(\tau), \forall \tau \in \mathcal{T}_h^S, \quad (4.7)$$

$$\left(\Pi_{P_h^S} q^S - q^S, p_k \right)_F = 0, \quad \forall p_k \in P^k(F), \forall F \in \mathcal{F}_{pr}^S \cup \mathcal{F}^I. \quad (4.8)$$

Lemma 4.6. *The degrees of freedom for \underline{W}_h^S are given by*

(WD1) *For any $F \in \mathcal{F}_{pr}^S \cup \mathcal{F}^I$*

$$\psi_F(\underline{G}_h^S) := (\underline{G}_h^S \mathbf{n}, \mathbf{p}_k)_F, \quad \forall \mathbf{p}_k \in P^k(F)^d.$$

(WD2) *For any $F \in \mathcal{F}_{dl}^S$*

$$\psi_F(\underline{G}_h^S) := \left((\underline{G}_h^S \mathbf{n})^t, \mathbf{p}_k \right)_F, \quad \forall \mathbf{p}_k \in \mathbf{P}_t^k(F),$$

where $\mathbf{P}_t^k(F) := \{\mathbf{q} \in P^k(F)^d : \mathbf{q} \cdot \mathbf{n}_F = 0\}$.

(WD3) *For any $\tau \in \mathcal{T}_h^S$*

$$\psi_\tau(\underline{G}_h^S) := \left(\underline{G}_h^S, \underline{p}_{k-1} \right)_\tau, \quad \forall \underline{p}_{k-1} \in P^{k-1}(\tau)^{d \times d}.$$

Proof. The proof for $d = 2$ and $d = 3$ can be found in Lemma 2.1 of [38] and Lemma 4.2 of [31], respectively. □

Corresponding to these degrees of freedom, we define the projection operator $\underline{\Pi}_{\underline{W}_h^S} : \mathbf{H}(\text{div}; \Omega^S)^d \cap L^p(\Omega^S)^{d \times d} \rightarrow \underline{W}_h^S$ as the unique linear operator satisfying, for all $\underline{G}^S \in \mathbf{H}(\text{div}; \Omega^S)^d \cap L^p(\Omega^S)^{d \times d}$, $p > 2$,

$$\left(\underline{\Pi}_{\underline{W}_h^S} \underline{G}^S - \underline{G}^S, \underline{p}_{k-1} \right)_\tau = 0, \quad \forall \underline{p}_{k-1} \in P^{k-1}(\tau)^{d \times d}, \quad \forall \tau \in \mathcal{T}_h^S, \tag{4.9}$$

$$\left(\left(\underline{\Pi}_{\underline{W}_h^S} \underline{G}^S - \underline{G}^S \right) \mathbf{n}, \mathbf{p}_k \right)_F = 0, \quad \forall \mathbf{p}_k \in P^k(F)^d, \quad \forall F \in \mathcal{F}_{pr}^S \cup \mathcal{F}^I, \tag{4.10}$$

$$\left(\left(\left(\underline{\Pi}_{\underline{W}_h^S} \underline{G}^S - \underline{G}^S \right) \mathbf{n} \right)^t, \mathbf{p}_k \right)_F = 0, \quad \forall \mathbf{p}_k \in \mathbf{P}_t^k(F), \quad \forall F \in \mathcal{F}_{dl}^S. \tag{4.11}$$

Lemma 4.7. *The degrees of freedom for \underline{U}_h^D are given by*

(XD1) *For any $F \in \mathcal{F}_h^{D,i} \cup \mathcal{F}_D^D \cup \mathcal{F}^I$, we have*

$$\eta_F(\mathbf{v}_h^D) := (\mathbf{v}_h^D \cdot \mathbf{n}, p_k)_F, \quad \forall p_k \in P^k(F).$$

(XD2) *For any $\tau \in \mathcal{T}_h^D$, we have*

$$\eta_{\tau,1}(\mathbf{v}_h^D) := (\mathbf{v}_h^D, \nabla p_{k-1})_\tau, \quad \forall p_{k-1} \in P^{k-1}(\tau).$$

(XD3) *For any $\tau \in \mathcal{T}_h^D$, we have*

$$\eta_{\tau,2}(\mathbf{v}_h^D) := (\mathbf{v}_h^D, \mathbf{b}_k)_\tau, \quad \forall \mathbf{b}_k \in \Phi^k(\tau),$$

where $\Phi^k(\tau) = \{\mathbf{b}_k \in P^k(\tau)^d : \nabla \cdot \mathbf{b}_k = 0, (\mathbf{b}_k \cdot \mathbf{n})|_F = 0, \forall F \subset \partial\tau\}$.

Proof. The proof follows from Chapter III.3, Proposition 3.1 of [4]. □

Using the degrees of freedom specified above, we define the BDM projection operator $\mathbf{\Pi}_{\text{BDM}} : \mathbf{H}(\text{div}; \Omega^D) \cap L^p(\Omega^D)^d \rightarrow \underline{U}_h^D$ ($p > 2$), such that, for any $\mathbf{w}^D \in \mathbf{H}(\text{div}; \Omega^D) \cap L^p(\Omega^D)^d$,

$$(\mathbf{w}^D - \mathbf{\Pi}_{\text{BDM}} \mathbf{w}^D, \nabla p_{k-1})_\tau = 0, \quad \forall p_{k-1} \in P^{k-1}(\tau), \quad \forall \tau \in \mathcal{T}_h^D, \tag{4.12}$$

$$\left((\mathbf{w}^D - \mathbf{\Pi}_{\text{BDM}} \mathbf{w}^D) \cdot \mathbf{n}, p_k \right)_F = 0, \quad \forall p_k \in P^k(F)^d, \quad \forall F \in \mathcal{F}_h^D \cup \mathcal{F}^I, \tag{4.13}$$

$$(\mathbf{w}^D - \mathbf{\Pi}_{\text{BDM}} \mathbf{w}^D, \mathbf{b}_k)_\tau = 0, \quad \forall \mathbf{b}_k \in \Phi^k(\tau), \quad \forall \tau \in \mathcal{T}_h^D. \tag{4.14}$$

The following approximation properties hold for any $\mathbf{v}^D \in H^1(\tau)^d$, $\tau \in \mathcal{T}_h^D$

$$\|\mathbf{v}^D - \mathbf{\Pi}_{\text{BDM}}\mathbf{v}^D\|_{L^2(\tau)} \leq Ch_\tau \|\nabla \mathbf{v}^D\|_{L^2(\tau)}, \quad \|\nabla(\mathbf{v}^D - \mathbf{\Pi}_{\text{BDM}}\mathbf{v}^D)\|_{L^2(\tau)} \leq C \|\nabla \mathbf{v}^D\|_{L^2(\tau)}. \quad (4.15)$$

In addition, we denote by $\Pi_{P_h^D} : L^2(\Omega^D) \rightarrow P_h^D$ the standard L^2 -orthogonal projection.

We define the broken polynomial spaces on Ω^j ($j = S, D$) by

$$P^k(\mathcal{T}_h^j) := \left\{ r_h^j : \left(r_h^j \right)_{|\tau} \in P^k(\tau), \forall \tau \in \mathcal{T}_h^j \right\}.$$

They are endowed with the following discrete norms

$$\begin{aligned} \|r_h^S\|_{\text{DG}, \mathcal{T}_h^S} &:= \left(\sum_{\tau \in \mathcal{T}_h^S} \|\nabla r_h^S\|_{L^2(\tau)}^2 + \sum_{F \in \mathcal{F}_{pr}^S \cup \mathcal{F}_{dl}^S} h_F^{-1} \|[r_h^S]\|_{L^2(F)}^2 \right)^{\frac{1}{2}}, \\ \|r_h^D\|_{\text{DG}, \mathcal{T}_h^D} &:= \left(\sum_{\tau \in \mathcal{T}_h^D} \|\nabla r_h^D\|_{L^2(\tau)}^2 + \sum_{F \in \mathcal{F}_N^D \cup \mathcal{F}_h^{D,i}} h_F^{-1} \|[r_h^D]\|_{L^2(F)}^2 \right)^{\frac{1}{2}}. \end{aligned}$$

The following discrete Sobolev embedding result, which follows from Theorem 5.3 of [14] and Section 18.2.3 of [1], will be used repeatedly.

Lemma 4.8 (Discrete Sobolev embedding theorem). *For any $1 \leq p \leq 6$, there exists a constant $C > 0$, depending only on Ω^j , p and k , such that*

$$\|r_h^j\|_{L^p(\Omega^j)} \leq C \|r_h^j\|_{\text{DG}, \mathcal{T}_h^j}, \quad \forall r_h^j \in P^k(\mathcal{T}_h^j), \quad j = S, D.$$

Combining the trace inequality ([14], Lem. 1.52) with Lemma 4.8, we obtain the following estimates, with constants $C_{\mathcal{U}_h^S, 0, 1}, C_{\mathcal{U}_h^S, 4, 1} > 0$ independent of the mesh size h :

$$\|\mathbf{v}_h^S\|_{\mathcal{U}_h^S, 0} \leq C_{\mathcal{U}_h^S, 0, 1} \|\mathbf{v}_h^S\|_{\mathcal{U}_h^S, 1}, \quad (4.16)$$

$$\|\mathbf{v}_h^S\|_{0, 4, h} \leq C_{\mathcal{U}_h^S, 4, 1} \|\mathbf{v}_h^S\|_{\mathcal{U}_h^S, 1}. \quad (4.17)$$

Moreover, by an argument analogous to that of Lemma 4.4, there exists a constant $C > 0$, independent of h , α , β , μ , and κ , such that

$$\|\mathbf{\Pi}_{\text{BDM}}\mathbf{v}^D\|_{\text{DG}, \mathcal{T}_h^D} \leq C \|\mathbf{v}^D\|_{H^1(\Omega^D)}. \quad (4.18)$$

The next lemma shows that N_h and D_h are consistent with the continuous convective term when the exact solution is sufficiently regular.

Lemma 4.9 (Consistency). *Assume that $\mathbf{u}^S \in H_{\Gamma^S}^1(\Omega^S)^d$ with $\nabla \cdot \mathbf{u}^S = 0$. Let $\underline{L}^S \in L^p(\Omega^S)^{d \times d} \cap \mathbf{H}(\text{div}; \Omega^S)^d$, $p > 2$. In addition, the interface condition (2.7) holds. Then, for every $\mathbf{v}_h^S \in \mathcal{U}_h^S$,*

$$N_h(\mathbf{u}^S, \mathbf{u}^S, \mathbf{v}_h^S) + D_h(\mathbf{u}^S, \underline{L}^S, \mathbf{v}_h^S) = (\mathbf{u}^S \otimes \mathbf{u}^S, \nabla_h \mathbf{v}_h^S)_{\Omega^S}.$$

The following lemma establishes the strong mass conservation property, which plays a crucial role in the subsequent analysis.

Lemma 4.10 (Mass conservation). *Assume that $\mathbf{z}_h^S \in \mathbf{U}_h^S$ and $\mathbf{z}_h^D \in \mathbf{U}_h^D$ satisfy*

$$-J_h(\mathbf{z}_h^D, q_h^S) + b_h(\mathbf{z}_h^S, q_h^S) = 0, \quad \forall q_h^S \in P_h^S. \tag{4.19}$$

Then, \mathbf{z}_h^S and \mathbf{z}_h^D satisfy the strong mass conservation in the following sense:

$$\begin{aligned} \mathbf{z}_h^S &\in \mathbf{H}(\text{div}; \Omega^S), \text{ and } \nabla \cdot \mathbf{z}_h^S = 0, \text{ in } \Omega^S, \\ \mathbf{z}_h^S \cdot \mathbf{n} &= \mathbf{z}_h^D \cdot \mathbf{n}, \text{ on } \Gamma^I, \text{ and } \mathbf{z}_h^S \cdot \mathbf{n} = 0, \text{ on } \Gamma^S. \end{aligned}$$

Proof. A proof for the two-dimensional case is provided in Lemma 3.1 of [37]. For the three-dimensional setting, we follow an analogous argument. The degrees of freedom for the space \mathbf{U}_h^S guarantee the existence of a function $q_h^S \in \mathbf{U}_h^S$ satisfying

$$\begin{aligned} (q^S, p^{k-1})_\tau &= (\nabla \cdot \mathbf{z}_h^S, p^{k-1})_\tau, & \forall p^{k-1} \in P^k(\tau)^d, \quad \forall \tau \in \mathcal{T}_h^S, \\ (q_h^S, p^k)_F &= -([\mathbf{z}_h^S \cdot \mathbf{n}], p^k)_F, & \forall p^k \in P^k(F), \quad \forall F \in \mathcal{F}_{dl}^S, \\ (q_h^S, p^k)_F &= -(\mathbf{z}_h^S \cdot \mathbf{n} - \mathbf{z}_h^D \cdot \mathbf{n}, p^k)_F, & \forall p^k \in P^k(F), \quad \forall F \in \mathcal{F}^I. \end{aligned}$$

Substituting the definition of q_h^S into (4.19) yields

$$0 = -J_h(\mathbf{z}_h^D, q_h^S) + b_h(\mathbf{z}_h^S, q_h^S) = \|\nabla_h \cdot \mathbf{z}_h^S\|_{L^2(\Omega^S)}^2 + \sum_{F \in \mathcal{F}_{pr}^S} \|[\mathbf{z}_h^S \cdot \mathbf{n}]\|_{L^2(F)}^2 + \sum_{F \in \mathcal{F}^I} \|(\mathbf{z}_h^S - \mathbf{z}_h^D) \cdot \mathbf{n}\|_{L^2(F)}^2.$$

Consequently, $[\mathbf{z}_h^S \cdot \mathbf{n}]|_F = 0$ for every face $F \in \mathcal{F}_{pr}^S$, which implies $\mathbf{z}_h^S \in \mathbf{H}(\text{div}; \Omega^S)$. Moreover, we have $(\mathbf{z}_h^S \cdot \mathbf{n})|_F = (\mathbf{z}_h^D \cdot \mathbf{n})|_F$ for any $F \in \mathcal{F}^I$ and $\nabla \cdot \mathbf{z}_h^S = 0$. This completes the proof. \square

Remark 4.1. As a direct consequence of the strong mass-conservation, the velocity–pressure coupling term vanishes in the error analysis. This property leads to the pressure robustness of the proposed scheme, in the sense that the velocity error is independent of the pressure. For a detailed illustration, we refer the reader to [37].

Lemma 4.11 (Velocity invariance). *For any $\mathbf{v}_h^S \in \mathbf{U}_h^S$ and $\mathbf{f}^S \in L^2(\Omega^S)^d$, let $\mathbf{f}^S = \mathbf{f}_0 + \nabla\phi$ be the Helmholtz–Leray decomposition given in Lemma 2.1. Then the following identity holds:*

$$(\mathbf{f}^S, \mathbf{v}_h^S)_{\Omega^S} = (\mathbf{f}_0, \mathbf{v}_h^S)_{\Omega^S} + b_h^*(\Pi_{P_h^S} \phi, \mathbf{v}_h^S).$$

Proof. By the Helmholtz–Leray decomposition stated in Lemma 2.1 and integration by parts, we obtain

$$\begin{aligned} (\mathbf{f}^S, \mathbf{v}_h^S)_{\Omega^S} &= (\mathbf{f}_0, \mathbf{v}_h^S)_{\Omega^S} + (\nabla\phi, \mathbf{v}_h^S)_{\Omega^S} \\ &= (\mathbf{f}_0, \mathbf{v}_h^S)_{\Omega^S} + \sum_{F \in \mathcal{F}_{pr}^S} (\phi, [\mathbf{v}_h^S \cdot \mathbf{n}])_F + \sum_{F \in \mathcal{F}^I} (\phi, \mathbf{v}_h^S \cdot \mathbf{n})_F - \sum_{\tau \in \mathcal{T}_h^S} (\phi, \nabla \cdot \mathbf{v}_h^S)_\tau \\ &= (\mathbf{f}_0, \mathbf{v}_h^S)_{\Omega^S} + b_h^*(\phi, \mathbf{v}_h^S) \\ &= (\mathbf{f}_0, \mathbf{v}_h^S)_{\Omega^S} + b_h^*(\Pi_{P_h^S} \phi, \mathbf{v}_h^S), \end{aligned}$$

where the last equality follows from (4.7) and (4.8). \square

Remark 4.2. An immediate consequence of Lemmas 4.10 and 4.11 is the independence of the fluid velocity field from the irrotational part of the body force \mathbf{f}^S .

Lemma 4.12 (Boundedness). *There exists a constant $C_{N_h} > 0$, independent of h , with the following property. For any $\mathbf{r}_h^S, \mathbf{z}_h^S, \mathbf{v}_h^S \in \mathbf{U}_h^S$, and $\underline{H}_h^S \in \underline{W}_h^S$ satisfying $\mathbf{r}_h^S \in \mathbf{H}(\text{div}; \Omega^S)$ and $\nabla \cdot \mathbf{r}_h^S = 0$, we have*

$$\begin{aligned} & |N_h(\mathbf{r}_h^S, \mathbf{z}_h^S, \mathbf{v}_h^S) + D_h(\mathbf{r}_h^S, \underline{H}_h^S, \mathbf{v}_h^S)| \\ & \leq C_{N_h} \|\mathbf{r}_h^S\|_{0,4,h} \left(\|\mathbf{z}_h^S\|_{\mathbf{U}_h^S,1}^2 + \sum_{F \in \mathcal{F}^I} h_F^{-1} \left\| (z_h^S)^t + \alpha^{-1} \mu^{-1} \kappa^{\frac{1}{2}} (\underline{H}_h^S \mathbf{n})^t \right\|_{L^2(F)}^2 \right)^{\frac{1}{2}} \|\mathbf{v}_h^S\|_{0,4,h}. \end{aligned}$$

Proof. The proof is postponed in Section 6.1. \square

Before proceeding with the detailed proofs, we present several auxiliary estimates that will be used in the subsequent analysis. The proofs of these results are postponed to Section 6.2.

Lemma 4.13. *The following statements hold:*

- (1) *There exists a constant $C_{\underline{W}_h^S, \mathbf{U}_h^S} > 0$, independent of the mesh size h and of the parameters $\alpha, \beta, \mu, \kappa$, such that for any $\underline{H}_h^S \in \underline{W}_h^S$, $\mathbf{z}_h^S \in \mathbf{U}_h^S$ and $\mathbf{z}_h^D \in \mathbf{U}_h^D$ satisfying*

$$A_h(\underline{H}_h^S, \underline{G}_h^S) - B_h^*(\mathbf{z}_h^S, \underline{G}_h^S) - I_h(\mathbf{z}_h^D, \underline{G}_h^S) = 0, \quad \forall \underline{G}_h^S \in \underline{W}_h^S, \quad (4.20)$$

the following inequalities hold:

$$\left(\|\mathbf{z}_h^S\|_{\mathbf{U}_h^S,1}^2 + \sum_{F \in \mathcal{F}^I} h_F^{-1} \left\| (z_h^S)^t + \alpha^{-1} \mu^{-1} \kappa^{\frac{1}{2}} (\underline{H}_h^S \mathbf{n})^t \right\|_{L^2(F)}^2 \right)^{\frac{1}{2}} \leq \mu^{-\frac{1}{2}} C_{\underline{W}_h^S, \mathbf{U}_h^S} \left\| \mu^{-\frac{1}{2}} \underline{H}_h^S \right\|_{L^2(\Omega^S)}, \quad (4.21)$$

$$\begin{aligned} & \left(\left\| \mu^{-\frac{1}{2}} \underline{H}_h^S \right\|_{L^2(\Omega^S)}^2 + \sum_{F \in \mathcal{F}^I} \left\| \alpha^{-\frac{1}{2}} \mu^{-\frac{1}{2}} \kappa^{\frac{1}{4}} (\underline{H}_h^S \mathbf{n})^t \right\|_{L^2(F)}^2 \right)^{\frac{1}{2}} \\ & \leq \mu^{\frac{1}{2}} C_{\alpha, \kappa} \left(\|\mathbf{z}_h^S\|_{\mathbf{U}_h^S,1}^2 + \sum_{F \in \mathcal{F}^I} \|(z_h^S)^t\|_{L^2(F)}^2 + \sum_{F \in \mathcal{F}^I} h_F^{-1} \|\mathbf{z}_h^S \cdot \mathbf{n} - \mathbf{z}_h^D \cdot \mathbf{n}\|_{L^2(F)}^2 \right)^{\frac{1}{2}}, \end{aligned} \quad (4.22)$$

where $C_{\alpha, \kappa} := \max\{1, \alpha^{\frac{1}{2}} \kappa^{-\frac{1}{4}}\}$.

- (2) *There exists a constant $C_{\mathbf{U}_h^D, P_h^D} > 0$, independent of $h, \alpha, \mu, \kappa, \beta$, such that for any $\mathbf{z}_h^D \in \mathbf{U}_h^D$, $r_h^D \in P_h^D$, $r_h^S \in P_h^S$ and $\underline{H}_h^S \in \underline{W}_h^S$ satisfying*

$$(\mathcal{M}(\mathbf{z}_h^D), \mathbf{v}_h^D)_{\Omega^D} + a_h(\mathbf{v}_h^D, r_h^D) - J_h(\mathbf{v}_h^D, r_h^S) + I_h(\mathbf{v}_h^D, \underline{H}_h^S) = 0, \quad \forall \mathbf{v}_h^D \in \mathbf{U}_h^D, \quad (4.23)$$

the following estimate holds:

$$\|r_h^D\|_{L^2(\Omega^D)}^2 \leq C_{\mathbf{U}_h^D, P_h^D} \left(\mu^{\frac{1}{2}} \kappa^{-\frac{1}{2}} \left\| \mu^{\frac{1}{2}} \kappa^{-\frac{1}{2}} \mathbf{z}_h^D \right\|_{L^2(\Omega^D)} + \beta \|\mathbf{z}_h^D\|_{L^3(\Omega^D)}^2 \right). \quad (4.24)$$

4.2. The fixed-point operator

To facilitate the subsequent analysis, we introduce the divergence-free subspace

$$\mathbf{U}_{h,\text{div}}^S := \{\mathbf{v}_h^S \in \mathbf{U}_h^S \cap \mathbf{H}(\text{div}; \Omega^S) : \nabla \cdot \mathbf{v}_h^S = 0 \text{ in } \Omega^S\}.$$

The solution operator $T : \mathbf{U}_{h,\text{div}}^S \rightarrow \mathbf{U}_{h,\text{div}}^S$ is defined by $T(\mathbf{w}_h^S) := \mathbf{u}_h^S$, where \mathbf{u}_h^S is the velocity component obtained from solving the following nonlinear problem: For a given $\mathbf{w}_h^S \in \mathbf{U}_{h,\text{div}}^S$, find $(\underline{L}_h^S, \mathbf{u}_h^S, p_h^S, \mathbf{u}_h^D, p_h^D) \in \underline{W}_h^S \times \mathbf{U}_h^S \times P_h^S \times \mathbf{U}_h^D \times P_h^D$ such that, for any $(\underline{G}_h^S, \mathbf{v}_h^S, q_h^S, \mathbf{v}_h^D, q_h^D) \in \underline{W}_h^S \times \mathbf{U}_h^S \times P_h^S \times \mathbf{U}_h^D \times P_h^D$:

$$A_h(\underline{L}_h^S, \underline{G}_h^S) - B_h^*(\mathbf{u}_h^S, \underline{G}_h^S) - I_h(\mathbf{u}_h^D, \underline{G}_h^S) = 0, \quad (4.25)$$

$$N_h(\mathbf{w}_h^S, \mathbf{u}_h^S, \mathbf{v}_h^S) + D_h(\mathbf{w}_h^S, \underline{\mathbf{L}}_h^S, \mathbf{v}_h^S) + b_h^*(p_h^S, \mathbf{v}_h^S) + B_h(\underline{\mathbf{L}}_h^S, \mathbf{v}_h^S) = (\mathbf{f}^S, \mathbf{v}_h^S)_{\Omega^S}, \tag{4.26}$$

$$-J_h(\mathbf{u}_h^D, q_h^S) + b_h(\mathbf{u}_h^S, q_h^S) = 0, \tag{4.27}$$

$$(\mathcal{M}(\mathbf{u}_h^D), \mathbf{v}_h^D)_{\Omega^D} + a_h(\mathbf{v}_h^D, p_h^D) - J_h(\mathbf{v}_h^D, p_h^S) + I_h(\mathbf{v}_h^D, \underline{\mathbf{L}}_h^S) = (\mathbf{f}^D, \mathbf{v}_h^D)_{\Omega^D}, \tag{4.28}$$

$$a_h(\mathbf{u}_h^D, q_h^D) = (g^D, q_h^D)_{\Omega^D}. \tag{4.29}$$

To establish the well-posedness of the nonlinear scheme (3.4)–(3.8), we employ a Picard iteration: starting from an initial guess we define the sequence $\{\mathbf{u}_{h,m}^S\}_{m=0}^\infty$ by

$$\mathbf{u}_{h,m+1}^S := T(\mathbf{u}_{h,m}^S), \quad m = 0, 1, 2, \dots$$

The well-posedness of the original nonlinear system follows from the existence and uniqueness of a fixed point of T , or equivalently, the convergence of this iterative sequence.

We recall the classical Browder–Minty fixed point theorem (see, e.g., [32]).

Theorem 4.1 (Browder–Minty fixed point theorem). *Let X be a real, separable, reflexive Banach space equipped with norm $\|\cdot\|_X$ and let X' denote its dual. Suppose that the operator $\mathcal{A} : X \times X \rightarrow \mathbb{R}$ satisfies the following conditions:*

(1) *Monotonicity: for all $x, y \in X$,*

$$\mathcal{A}(x, x - y) - \mathcal{A}(y, x - y) \geq 0.$$

(2) *Hemi-continuity: for all $x, y \in X$, the map*

$$\begin{aligned} \mathbb{R} &\rightarrow \mathbb{R}, \\ t &\rightarrow \mathcal{A}(x + ty, y), \end{aligned}$$

is continuous.

(3) *Coercivity:*

$$\lim_{\|x\|_X \rightarrow +\infty} \frac{\mathcal{A}(x, x)}{\|x\|_X} = +\infty.$$

Then, the operator $X \rightarrow X'$ defined by $x \rightarrow \mathcal{A}(x, \cdot)$ is surjective.

To facilitate the subsequent analysis, we define the product spaces $\mathbf{U}_h := \mathbf{U}_h^S \times \mathbf{U}_h^D$ and $P_h := P_h^S \times P_h^D$, equipped with the norms

$$\begin{aligned} \|\mathbf{v}_h\|_{\mathbf{U}_h} &:= \left(\|\mathbf{v}_h^S\|_{\mathbf{U}_{h,1}^S}^2 + \sum_{F \in \mathcal{F}^I} \left(\|(\mathbf{v}_h^S)^t\|_{L^2(F)}^2 + h_F^{-1} \|\mathbf{v}_h^S \cdot \mathbf{n} - \mathbf{v}_h^D \cdot \mathbf{n}\|_{L^2(F)}^2 \right) \right)^{\frac{1}{2}} + \|\mathbf{v}_h^D\|_{L^3(\Omega^D)}, \\ \|q_h\|_{P_h}^2 &:= \|q_h^S\|_{L^2(\Omega^S)}^2 + \|q_h^D\|_{L^2(\Omega^D)}^2. \end{aligned} \tag{4.30}$$

Since $A_h(\cdot, \cdot)$ is an inner product on \underline{W}_h^S , the Riesz representation theorem guarantees that for any $\mathbf{v}_h = (\mathbf{v}_h^S, \mathbf{v}_h^D) \in \mathbf{U}_h$ there exists a unique $\underline{\mathbf{L}}_{\mathbf{v}_h} \in \underline{W}_h^S$ such that

$$A_h(\underline{\mathbf{L}}_{\mathbf{v}_h}, \underline{\mathbf{G}}_h^S) = B_h^*(\mathbf{v}_h^S, \underline{\mathbf{G}}_h^S) + I_h(\mathbf{v}_h^D, \underline{\mathbf{G}}_h^S), \quad \forall \underline{\mathbf{G}}_h^S \in \underline{W}_h^S. \tag{4.31}$$

This defines a linear mapping $\underline{L}_{(\cdot)} : \mathbf{U}_h \rightarrow \underline{W}_h^S$. We now introduce the following bilinear forms, which will simplify the presentation:

$$Q_h(\mathbf{u}_h, \mathbf{v}_h) = N_h(\mathbf{w}_h^S, \mathbf{u}_h^S, \mathbf{v}_h^S) + D_h(\mathbf{w}_h^S, \underline{\mathbf{L}}_{\mathbf{u}_h}, \mathbf{v}_h) + I_h(\mathbf{v}_h^D, \underline{\mathbf{L}}_{\mathbf{u}_h}) + B_h(\underline{\mathbf{L}}_{\mathbf{u}_h}, \mathbf{v}_h^S) + (\mathcal{M}(\mathbf{u}_h^D), \mathbf{v}_h^D)_{\Omega^D}, \tag{4.32}$$

$$\begin{aligned} R_h(\mathbf{u}_h, q_h) &= a_h(\mathbf{u}_h^D, q_h^D) - J_h(\mathbf{u}_h^D, q_h^S) + b_h(\mathbf{u}_h^S, q_h^S), \\ R_h^*(p_h, \mathbf{v}_h) &= a_h(\mathbf{v}_h^D, p_h^D) - J_h(\mathbf{v}_h^D, p_h^S) + b_h^*(p_h^S, \mathbf{v}_h^S) \end{aligned} \quad (4.33)$$

for $\mathbf{u}_h = (\mathbf{u}_h^S, \mathbf{u}_h^D) \in \mathbf{U}_h$, $\mathbf{v}_h = (\mathbf{v}_h^S, \mathbf{v}_h^D) \in \mathbf{U}_h$, $q_h = (q_h^S, q_h^D) \in P_h$, and $p_h = (p_h^S, p_h^D) \in P_h$.

For given $\mathbf{w}_h^S \in \mathbf{U}_h^S$, if $(\underline{L}_h^S, \mathbf{u}_h^S, p_h^S, \mathbf{u}_h^D, p_h^D)$ solves the system (4.25)–(4.29), then the pair (\mathbf{u}_h, p_h) with $\mathbf{u}_h := (\mathbf{u}_h^S, \mathbf{u}_h^D) \in \mathbf{U}_h$ and $p_h := (p_h^S, p_h^D) \in P_h$ satisfies the reduced problem

$$Q_h(\mathbf{u}_h, \mathbf{v}_h) + R_h^*(p_h, \mathbf{v}_h) = (\mathbf{f}^S, \mathbf{v}_h^S)_{\Omega^S} + (\mathbf{f}^D, \mathbf{v}_h^D)_{\Omega^D}, \quad \forall \mathbf{v}_h \in \mathbf{U}_h, \quad (4.34)$$

$$R_h(\mathbf{u}_h, q_h) = (g^D, q_h^D)_{\Omega^D}, \quad \forall q_h \in P_h. \quad (4.35)$$

Conversely, if (\mathbf{u}_h, p_h) satisfies (4.34) and (4.35), then by construction $(\underline{L}_{\mathbf{u}_h}, \mathbf{u}_h^S, p_h^S, \mathbf{u}_h^D, p_h^D)$ is a solution of (4.25)–(4.29). Hence, it suffices to establish the well-posedness of the reduced system (4.34) and (4.35).

Lemma 4.14. *There exists a constant $C_R > 0$, independent of mesh size h , such that the following inf-sup condition holds:*

$$\inf_{0 \neq q_h \in P_h} \sup_{0 \neq \mathbf{v}_h \in \mathbf{U}_h} \frac{R_h(\mathbf{v}_h, q_h)}{\|\mathbf{v}_h\|_{\mathbf{U}_h} \|q_h\|_{P_h}} \geq C_R. \quad (4.36)$$

Proof. For any $q_h = (q_h^S, q_h^D) \in P_h \subseteq L^2(\Omega^S \cup \Omega^D)$, there exists a function $\mathbf{v} \in H^1(\Omega^S \cup \Omega^D)^d$ such that (cf. [17], Lem. 53.9)

$$\begin{aligned} \nabla \cdot \mathbf{v} &= -q_h^S && \text{in } \Omega^S, \\ \nabla \cdot \mathbf{v} &= -q_h^D && \text{in } \Omega^D, \\ (\mathbf{v})|_{\Gamma^S \cup \Gamma_N^D} &= \mathbf{0}, \end{aligned}$$

with the stability estimate

$$\|\mathbf{v}^S\|_{H^1(\Omega^S)} + \|\mathbf{v}^D\|_{H^1(\Omega^D)} \leq C \|q_h\|_{P_h}, \quad (4.37)$$

where $\mathbf{v}^S := \mathbf{v}|_{\Omega^S}$ and $\mathbf{v}^D := \mathbf{v}|_{\Omega^D}$. Define the discrete pair $\mathbf{v}_h := (\mathbf{v}_h^S, \mathbf{v}_h^D)$ by

$$\mathbf{v}_h^S = \Pi_{\mathbf{U}_h^S} \mathbf{v}^S, \quad \mathbf{v}_h^D = \Pi_{\text{BDM}} \mathbf{v}^D.$$

Using (4.2), (4.3), (4.13) and integration by parts, we obtain

$$\begin{aligned} b_h(\mathbf{v}_h^S, q_h^S) - J_h(\mathbf{v}_h^D, q_h^S) &= b_h(\mathbf{v}^S, q_h^S) - J_h(\mathbf{v}^D, q_h^S) \\ &= -(\nabla \cdot \mathbf{v}^S, q_h^S)_{\Omega^S} + \sum_{F \in \mathcal{F}^I} (\mathbf{v}^S \cdot \mathbf{n} - \mathbf{v}^D \cdot \mathbf{n}, q_h^S)_F \\ &= \|q_h^S\|_{L^2(\Omega^S)}^2. \end{aligned}$$

The definition of the BDM projection yields

$$a_h(\mathbf{v}_h^D, q_h^D) = -(\nabla \cdot \mathbf{v}^D, q_h^D)_{\Omega^D} = \|q_h^D\|_{L^2(\Omega^D)}^2.$$

Hence, the definition of $R_h(\cdot, \cdot)$ (cf. (4.33)) gives

$$R_h(\mathbf{v}_h, q_h) = \|q_h\|_{P_h}^2. \quad (4.38)$$

It remains to bound $\|\mathbf{v}_h\|_{\mathbf{U}_h}$. We first note the following discrete trace inequality (see, e.g., Thm. 4.4 from [25] for $d = 2$ and Prop. 5 from [26] for the extension to $d = 3$): there exists a constant $C > 0$, independent of h , such that

$$\sum_{F \in \mathcal{F}^I} \|\mathbf{v}_h^S\|_{L^2(F)}^2 \leq C \|\mathbf{v}_h^S\|_{\mathbf{U}_h^S, 1}^2, \quad \forall \mathbf{v}_h^S \in \mathbf{U}_h^S. \quad (4.39)$$

Combining (4.39) with Lemma 4.4 and (4.37) yields

$$\|\mathbf{v}_h^S\|_{\mathbf{U}_h^S,1} + \|(\mathbf{v}_h^S)^\dagger\|_{L^2(\mathcal{F}^I)} \leq C \|\mathbf{v}_h^S\|_{\mathbf{U}_h^S,1} \leq C \|\mathbf{v}^S\|_{H^1(\Omega^S)} \leq C \|q_h\|_{P_h}. \tag{4.40}$$

Next, since $(\mathbf{v}^S \cdot \mathbf{n})|_F = (\mathbf{v}^D \cdot \mathbf{n})|_F$ for any $F \in \mathcal{F}^I$, the continuous trace inequality, (4.4), (4.15) and (4.37) give

$$\begin{aligned} & \sum_{F \in \mathcal{F}^I} h_F^{-1} \|\mathbf{v}_h^S \cdot \mathbf{n} - \mathbf{v}_h^D \cdot \mathbf{n}\|_{L^2(F)}^2 \\ & \leq \sum_{F \in \mathcal{F}^I} h_F^{-1} \left(\|\mathbf{v}^S \cdot \mathbf{n} - \mathbf{v}_h^S \cdot \mathbf{n}\|_{L^2(F)}^2 + \|\mathbf{v}^D \cdot \mathbf{n} - \mathbf{v}_h^D \cdot \mathbf{n}\|_{L^2(F)}^2 \right) \\ & \leq C \left(\|\mathbf{v}^S\|_{H^1(\Omega^S)}^2 + \|\mathbf{v}^D\|_{H^1(\Omega^D)}^2 \right) \leq C \|q_h\|_{P_h}^2. \end{aligned} \tag{4.41}$$

The discrete Sobolev embedding (Lem. 4.8), (4.18), and (4.37) imply

$$\|\mathbf{v}_h^D\|_{L^3(\Omega^D)} \leq C \|\mathbf{v}_h^D\|_{\text{DG},\mathcal{T}_h^D} \leq C \|\mathbf{v}^D\|_{H^1(\Omega^D)} \leq C \|q_h\|_{P_h}. \tag{4.42}$$

Combining (4.40)–(4.42) gives

$$\|\mathbf{v}_h\|_{\mathbf{U}_h} \leq C \|q_h\|_{P_h}. \tag{4.43}$$

Finally, (4.38) and (4.43) yield

$$\sup_{\mathbf{0} \neq \mathbf{v}_h \in \mathbf{U}_h} \frac{R_h(\mathbf{v}_h, q_h)}{\|\mathbf{v}_h\|_{\mathbf{U}_h}} \geq \frac{R_h(\mathbf{v}_h, q_h)}{\|\mathbf{v}_h\|_{\mathbf{U}_h}} \geq C^{-1} \|q_h\|_{P_h}.$$

This establishes the uniform inf–sup condition. □

Next, we define the kernel space of R_h as

$$\mathbf{U}_h^0 := \{\mathbf{v}_h \in \mathbf{U}_h : R_h(\mathbf{v}_h, q_h) = 0, \forall q_h \in P_h\}.$$

This enables us to introduce $\mathbf{U}_h^* \subset \mathbf{U}_h$ by decomposing $\mathbf{U}_h := \mathbf{U}_h^0 \oplus \mathbf{U}_h^*$.

Lemma 4.15. *Assume that the given data $\mathbf{w}_h^S \in \mathbf{U}_{h,\text{div}}^S$ satisfies the small-data assumption*

$$2\mu^{-1} \left(C_{\underline{W}_h^S, \mathbf{U}_h^S} C_{\mathbf{U}_h^S, 4,1} \right)^2 C_{N_h} \|\mathbf{w}_h^S\|_{\mathbf{U}_h^S,1} \leq 1, \tag{4.44}$$

then, the nonlinear form $Q_h(\cdot, \cdot)$ defined in (4.32) satisfies the following conditions.

- (1) Q_h is strictly monotone: there exists a constant $C > 0$, independent of mesh size h , such that, for any $\mathbf{v}_j = (\mathbf{v}_j^S, \mathbf{v}_j^D) \in \mathbf{U}_h^0$, $j = 1, 2$, and $\mathbf{r}_h = (\mathbf{r}_h^S, \mathbf{r}_h^D) \in \mathbf{U}_h$,

$$\begin{aligned} & Q_h(\mathbf{v}_1 + \mathbf{r}_h, \mathbf{v}_1 - \mathbf{v}_2) - Q_h(\mathbf{v}_2 + \mathbf{r}_h, \mathbf{v}_1 - \mathbf{v}_2) \\ & \geq C \left(\beta \|\mathbf{v}_1^D - \mathbf{v}_2^D\|_{L^3(\Omega^D)}^3 + \mu \left(\|\mathbf{v}_1^S - \mathbf{v}_2^S\|_{\mathbf{U}_h^S,1}^2 + \sum_{F \in \mathcal{F}^I} \|(\mathbf{v}_1^S - \mathbf{v}_2^S)^\dagger\|_{L^2(F)}^2 \right) \right). \end{aligned} \tag{4.45}$$

- (2) Q_h is hemi-continuous, which is, for any fixed $\mathbf{r}_h \in \mathbf{U}_h$ and $\mathbf{v}_1, \mathbf{v}_2 \in \mathbf{U}_h^0$, the mapping

$$\begin{aligned} & K : \mathbb{R} \rightarrow \mathbb{R}, \\ & t \rightarrow K(t) = Q_h(\mathbf{r}_h + \mathbf{v}_1 + t\mathbf{v}_2, \mathbf{v}_2). \end{aligned}$$

is continuous.

- (3) Q_h is coercive: for any given $\mathbf{v}_0 = (\mathbf{v}_0^S, \mathbf{v}_0^D) \in \mathbf{U}_h$, $Q_h(\mathbf{v}_0 + \cdot, \cdot)$ defined in (4.32) is coercive in the following sense: For any $\mathbf{v}_h = (\mathbf{v}_h^S, \mathbf{v}_h^D) \in \mathbf{U}_h^0$,

$$\lim_{\|\mathbf{v}_h\|_{\mathbf{U}_h} \rightarrow +\infty} \frac{1}{\|\mathbf{v}_h\|_{\mathbf{U}_h}} Q_h(\mathbf{v}_0 + \mathbf{v}_h, \mathbf{v}_h) = +\infty.$$

Proof. We prove the three assertions separately.

- (1) Let $\mathbf{v}_j = (\mathbf{v}_j^S, \mathbf{v}_j^D) \in \mathbf{U}_h^0$ ($j = 1, 2$) and $\mathbf{r}_h = (\mathbf{r}_h^S, \mathbf{r}_h^D) \in \mathbf{U}_h$ be arbitrary. By the linearity of the mapping $\underline{L}_{(\cdot)}$, we have

$$\underline{L}_{\mathbf{v}_1 + \mathbf{r}_h} - \underline{L}_{\mathbf{v}_2 + \mathbf{r}_h} = \underline{L}_{\mathbf{v}_1 - \mathbf{v}_2}.$$

Setting $\underline{G}_h^S = \underline{L}_{\mathbf{v}_1 - \mathbf{v}_2}$ in (4.31), and using the adjoint property (3.2), we obtain

$$\begin{aligned} A_h(\underline{L}_{\mathbf{v}_1 - \mathbf{v}_2}, \underline{L}_{\mathbf{v}_1 - \mathbf{v}_2}) &= B_h(\underline{L}_{\mathbf{v}_1 + \mathbf{r}_h}, \mathbf{v}_1^S - \mathbf{v}_2^S) - B_h(\underline{L}_{\mathbf{v}_2 + \mathbf{r}_h}, \mathbf{v}_1^S - \mathbf{v}_2^S) \\ &\quad + I_h(\mathbf{v}_1^D - \mathbf{v}_2^D, \underline{L}_{\mathbf{v}_1 + \mathbf{r}_h}) - I_h(\mathbf{v}_1^D - \mathbf{v}_2^D, \underline{L}_{\mathbf{v}_2 + \mathbf{r}_h}). \end{aligned} \quad (4.46)$$

As such, we obtain from the definition of Q_h in (4.32) and the identity (4.46) that

$$\begin{aligned} &Q_h(\mathbf{v}_1 + \mathbf{r}_h, \mathbf{v}_1 - \mathbf{v}_2) - Q_h(\mathbf{v}_2 + \mathbf{r}_h, \mathbf{v}_1 - \mathbf{v}_2) \\ &= N_h(\mathbf{w}_h^S, \mathbf{v}_1^S + \mathbf{r}_h, \mathbf{v}_1^S - \mathbf{v}_2^S) + D_h(\mathbf{w}_h^S, \underline{L}_{\mathbf{v}_1 + \mathbf{r}_h}, \mathbf{v}_1 - \mathbf{v}_2) + I_h(\mathbf{v}_1^D - \mathbf{v}_2^D, \underline{L}_{\mathbf{v}_1 + \mathbf{r}_h}) \\ &\quad + B_h(\underline{L}_{\mathbf{v}_1 + \mathbf{r}_h}, \mathbf{v}_1^S - \mathbf{v}_2^S) + (\mathcal{M}(\mathbf{v}_1^D + \mathbf{r}_h^D), \mathbf{v}_1^D - \mathbf{v}_2^D)_{\Omega^D} \\ &\quad - \left(N_h(\mathbf{w}_h^S, \mathbf{v}_2^S + \mathbf{r}_h, \mathbf{v}_1^S - \mathbf{v}_2^S) + D_h(\mathbf{w}_h^S, \underline{L}_{\mathbf{v}_2 + \mathbf{r}_h}, \mathbf{v}_1 - \mathbf{v}_2) \right. \\ &\quad \left. + I_h(\mathbf{v}_1^D - \mathbf{v}_2^D, \underline{L}_{\mathbf{v}_2 + \mathbf{r}_h}) + B_h(\underline{L}_{\mathbf{v}_2 + \mathbf{r}_h}, \mathbf{v}_1^S - \mathbf{v}_2^S) + (\mathcal{M}(\mathbf{v}_2^D + \mathbf{r}_h^D), \mathbf{v}_1^D - \mathbf{v}_2^D)_{\Omega^D} \right) \\ &= (\mathcal{M}(\mathbf{v}_1^D + \mathbf{r}_h^D) - \mathcal{M}(\mathbf{v}_2^D + \mathbf{r}_h^D), \mathbf{v}_1^D - \mathbf{v}_2^D)_{\Omega^D} + A_h(\underline{L}_{\mathbf{v}_1 - \mathbf{v}_2}, \underline{L}_{\mathbf{v}_1 - \mathbf{v}_2}) \\ &\quad + N_h(\mathbf{w}_h^S, \mathbf{v}_1^S - \mathbf{v}_2^S, \mathbf{v}_1^S - \mathbf{v}_2^S) + D_h(\mathbf{w}_h^S, \underline{L}_{\mathbf{v}_1 - \mathbf{v}_2}, \mathbf{v}_1^S - \mathbf{v}_2^S). \end{aligned} \quad (4.47)$$

Lemma 4.1 implies

$$(\mathcal{M}(\mathbf{v}_1^D + \mathbf{r}_h^D) - \mathcal{M}(\mathbf{v}_2^D + \mathbf{r}_h^D), \mathbf{v}_1^D - \mathbf{v}_2^D)_{\Omega^D} \geq C_D \beta \|\mathbf{v}_1^D - \mathbf{v}_2^D\|_{L^3(\Omega^D)}^3. \quad (4.48)$$

The small-data assumption (4.44) and the discrete Sobolev inequality (4.17) yield

$$\mu^{-1} C_{\mathbf{U}_h^S, 4, 1} C_{N_h} (C_{\underline{W}_h^S, \mathbf{U}_h^S})^2 \|\mathbf{w}_h^S\|_{0, 4, h} \leq \frac{1}{2}.$$

Applying Lemma 4.12 and (4.21) gives

$$\begin{aligned} &N_h(\mathbf{w}_h^S, \mathbf{v}_1^S - \mathbf{v}_2^S, \mathbf{v}_1^S - \mathbf{v}_2^S) + D_h(\mathbf{w}_h^S, \underline{L}_{\mathbf{v}_1 - \mathbf{v}_2}, \mathbf{v}_1^S - \mathbf{v}_2^S) \\ &\geq -\mu^{-1} C_{\mathbf{U}_h^S, 4, 1} C_{N_h} (C_{\underline{W}_h^S, \mathbf{U}_h^S})^2 \|\mathbf{w}_h^S\|_{0, 4, h} \left\| \mu^{-\frac{1}{2}} \underline{L}_{\mathbf{v}_1 - \mathbf{v}_2} \right\|_{L^2(\Omega^S)}^2 \geq -\frac{1}{2} \left\| \mu^{\frac{1}{2}} \underline{L}_{\mathbf{v}_1 - \mathbf{v}_2} \right\|_{L^2(\Omega^S)}^2. \end{aligned} \quad (4.49)$$

Combining (4.49) with the definition of A_h (cf. (3.1)) gives

$$\begin{aligned} &A_h(\underline{L}_{\mathbf{v}_1 - \mathbf{v}_2}, \underline{L}_{\mathbf{v}_1 - \mathbf{v}_2}) + N_h(\mathbf{w}_h^S, \mathbf{v}_1^S - \mathbf{v}_2^S, \mathbf{v}_1^S - \mathbf{v}_2^S) \\ &\quad + D_h(\mathbf{w}_h^S, \underline{L}_{\mathbf{v}_1 - \mathbf{v}_2}, \mathbf{v}_1^S - \mathbf{v}_2^S) \geq \frac{1}{2} \left\| \mu^{-\frac{1}{2}} \underline{L}_{\mathbf{v}_1 - \mathbf{v}_2} \right\|_{L^2(\Omega^S)}^2. \end{aligned} \quad (4.50)$$

By the linearity of $\underline{L}_{(\cdot)}$, B_h , and I_h , equation (4.46) can be reformulated as

$$A(\underline{L}_{\mathbf{v}_1 - \mathbf{v}_2}, \underline{L}_{\mathbf{v}_1 - \mathbf{v}_2}) = B_h(\underline{L}_{\mathbf{v}_1 - \mathbf{v}_2}, \mathbf{v}_1 - \mathbf{v}_2) + I_h(\mathbf{v}_1^D - \mathbf{v}_2^D, \underline{L}_{\mathbf{v}_1 - \mathbf{v}_2}).$$

Using (4.21), we have

$$\left\| \mu^{-\frac{1}{2}} \underline{L} \mathbf{v}_1 - \mathbf{v}_2 \right\|_{L^2(\Omega^S)} \geq \frac{1}{C_{\underline{W}_h^S, \underline{U}_h^S}} \mu^{\frac{1}{2}} \|\mathbf{v}_1^S - \mathbf{v}_2^S\|_{\underline{U}_h^S, 1}.$$

This and (4.39) yield

$$\left\| \mu^{-\frac{1}{2}} \underline{L} \mathbf{v}_1 - \mathbf{v}_2 \right\|_{L^2(\Omega^S)}^2 \geq C \mu \left(\|\mathbf{v}_1^S - \mathbf{v}_2^S\|_{\underline{U}_h^S, 1}^2 + \sum_{F \in \mathcal{F}^I} \|(\mathbf{v}_1^S - \mathbf{v}_2^S)^\mathbf{t}\|_{L^2(F)}^2 \right),$$

which combined with (4.47), (4.48) and (4.50) gives

$$\begin{aligned} & Q_h(\mathbf{v}_1 + \mathbf{r}_h, \mathbf{v}_1 - \mathbf{v}_2) - Q_h(\mathbf{v}_2 + \mathbf{r}_h, \mathbf{v}_1 - \mathbf{v}_2) \\ & \geq C \left(\beta \|\mathbf{v}_1^D - \mathbf{v}_2^D\|_{L^3(\Omega^D)}^3 + \mu \left(\|\mathbf{v}_1^S - \mathbf{v}_2^S\|_{\underline{U}_h^S, 1}^2 + \sum_{F \in \mathcal{F}^I} \|(\mathbf{v}_1^S - \mathbf{v}_2^S)^\mathbf{t}\|_{L^2(F)}^2 \right) \right). \end{aligned}$$

(2) The hemi-continuity of $Q_h(\cdot, \cdot)$ follows directly from Lemma 4.2.

(3) For a fixed $\mathbf{v}_0 = (\mathbf{v}_0^S, \mathbf{v}_0^D) \in \underline{U}_h$ and any $\mathbf{v}_h \in \underline{U}_h^0$. We let

$$Q_h(\mathbf{v}_0 + \mathbf{v}_h, \mathbf{v}_h) = Q_1 + Q_2,$$

where

$$Q_1 := Q_h(\mathbf{v}_0 + \mathbf{v}_h, \mathbf{v}_h) - Q_h(\mathbf{v}_0, \mathbf{v}_h), \quad \text{and} \quad Q_2 := Q_h(\mathbf{v}_0, \mathbf{v}_h).$$

Applying (4.45) with $\mathbf{v}_1 = \mathbf{v}_h$, $\mathbf{v}_2 = \mathbf{0}$, and $\mathbf{r}_h = \mathbf{v}_0$, we obtain

$$Q_1 \geq C \left(\beta \|\mathbf{v}_h\|_{L^3(\Omega^D)}^3 + \mu \left(\|\mathbf{v}_h^S\|_{\underline{U}_h^S, 1}^2 + \sum_{F \in \mathcal{F}^I} \|(\mathbf{v}_h^S)^\mathbf{t}\|_{L^2(F)}^2 \right) \right). \tag{4.51}$$

Moreover, since $\mathbf{v}_h \in \underline{U}_h^0$, it holds that

$$R_h(\mathbf{v}_h, q_h) = 0, \quad \forall q_h := (q_h^S, q_h^D) \in P_h. \tag{4.52}$$

Setting $q_h^D = 0$ in (4.52) and applying the definition of $R_h(\cdot, \cdot)$ given in (4.33) yields

$$-J_h(\mathbf{v}_h^D, q_h^S) + b_h(\mathbf{v}_h^S, q_h^S) = 0,$$

which combined with Lemma 4.10 implies

$$\sum_{F \in \mathcal{F}^I} h_F^{-1} \|(\mathbf{v}_h^S - \mathbf{v}_h^D) \cdot \mathbf{n}\|_{L^2(F)}^2 = 0.$$

Plugging this into (4.30) gives

$$\|\mathbf{v}_h\|_{\underline{U}_h} = \left(\|\mathbf{v}_h^S\|_{\underline{U}_h^S, 1}^2 + \sum_{F \in \mathcal{F}^I} \|(\mathbf{v}_h^S)^\mathbf{t}\|_{L^2(F)}^2 \right)^{\frac{1}{2}} + \|\mathbf{v}_h^D\|_{L^3(\Omega^D)},$$

which coupled with (4.51) yields

$$\frac{Q_1}{\|\mathbf{v}_h\|_{\underline{U}_h}} \geq C \frac{\left(\beta \|\mathbf{v}_h\|_{L^3(\Omega^D)}^3 + \mu \left(\|\mathbf{v}_h^S\|_{\underline{U}_h^S, 1}^2 + \sum_{F \in \mathcal{F}^I} \|(\mathbf{v}_h^S)^\mathbf{t}\|_{L^2(F)}^2 \right) \right)}{\|\mathbf{v}_h^D\|_{L^3(\Omega^D)} + \left(\|\mathbf{v}_h^S\|_{\underline{U}_h^S, 1}^2 + \sum_{F \in \mathcal{F}^I} \|(\mathbf{v}_h^S)^\mathbf{t}\|_{L^2(F)}^2 \right)^{\frac{1}{2}}}.$$

It is easy to check that, for any $C_1, C_2 > 0$ and $a, b > 0$,

$$\lim_{a+b \rightarrow +\infty} \frac{C_1 a^2 + C_2 b^3}{a+b} = +\infty.$$

By setting $C_1 = C\mu$, $C_2 = C\beta$ and $a = (\|\mathbf{v}_h^S\|_{\mathcal{U}_h^S}^2 + \sum_{F \in \mathcal{F}^I} \|(\mathbf{v}_h^S)^t\|_{L^2(F)}^2)^{\frac{1}{2}}$ and $b = \|\mathbf{v}_h^D\|_{L^3(\Omega^D)}$, we have

$$\lim_{\|\mathbf{v}_h\|_{\mathcal{U}_h} \rightarrow +\infty} \frac{Q_1}{\|\mathbf{v}_h\|_{\mathcal{U}_h}} = +\infty. \quad (4.53)$$

We now turn to the analysis for Q_2 . It follows from (4.32) and (4.31) that

$$\begin{aligned} Q_2 := Q_h(\mathbf{v}_0, \mathbf{v}_h) &= N_h(\mathbf{w}_h^S, \mathbf{v}_0^S, \mathbf{v}_h^S) + D_h(\mathbf{w}_h^S, \underline{L}_{\mathbf{v}_0}, \mathbf{v}_h^S) \\ &\quad + I_h(\mathbf{v}_h^D, \underline{L}_{\mathbf{v}_0}) + B_h(\underline{L}_{\mathbf{v}_0}, \mathbf{v}_h) + (\mathcal{M}(\mathbf{v}_0^D), \mathbf{v}_h^D)_{\Omega^D} \\ &= N_h(\mathbf{w}_h^S, \mathbf{v}_0^S, \mathbf{v}_h^S) + D_h(\mathbf{w}_h^S, \underline{L}_{\mathbf{v}_0}, \mathbf{v}_h^S) + A_h(\underline{L}_{\mathbf{v}_h}, \underline{L}_{\mathbf{v}_0}) + (\mathcal{M}(\mathbf{v}_0^D), \mathbf{v}_h^D)_{\Omega^D}. \end{aligned} \quad (4.54)$$

Lemma 4.12, inequality (4.21) in Lemma 4.13, and the small-data assumption (4.44) yield

$$\begin{aligned} &N_h(\mathbf{w}_h^S, \mathbf{v}_0^S, \mathbf{v}_h^S) + D_h(\mathbf{w}_h^S, \underline{L}_{\mathbf{v}_0}, \mathbf{v}_h^S) \\ &\geq -\mu^{-1} C_{\mathcal{U}_h^S, 4, 1} C_{N_h} (C_{\underline{W}_h^S, \mathcal{U}_h^S})^2 \|\mathbf{w}_h^S\|_{0, 4, h} \left\| \mu^{-\frac{1}{2}} \underline{L}_{\mathbf{v}_0} \right\|_{L^2(\Omega^S)} \left\| \mu^{-\frac{1}{2}} \underline{L}_{\mathbf{v}_h} \right\|_{L^2(\Omega^S)} \\ &\geq -\frac{1}{2} \left\| -\mu^{\frac{1}{2}} \underline{L}_{\mathbf{v}_0} \right\|_{L^2(\Omega^S)} \left\| \mu^{-\frac{1}{2}} \underline{L}_{\mathbf{v}_h} \right\|_{L^2(\Omega^S)} \\ &\geq -\frac{\mu (C_{\alpha, \mu})^2}{2} \|\mathbf{v}_0\|_{\mathcal{U}_h} \|\mathbf{v}_h\|_{\mathcal{U}_h}. \end{aligned} \quad (4.55)$$

The Cauchy–Schwarz inequality and inequality (4.22) in Lemma 4.13 give

$$\begin{aligned} A_h(\underline{L}_{\mathbf{v}_h}, \underline{L}_{\mathbf{v}_0}) &\geq -\left(\left\| \mu^{-\frac{1}{2}} \underline{L}_{\mathbf{v}_0} \right\|_{L^2(\Omega^S)} \right. \\ &\quad \left. + \sum_{F \in \mathcal{F}^I} \left\| \alpha^{-\frac{1}{2}} \mu^{-\frac{1}{2}} \kappa^{\frac{1}{4}} \underline{L}_{\mathbf{v}_0} \right\|_{L^2(F)} \right) \left(\left\| \mu^{-\frac{1}{2}} \underline{L}_{\mathbf{v}_h} \right\|_{L^2(\Omega^S)} + \sum_{F \in \mathcal{F}^I} \left\| \alpha^{-\frac{1}{2}} \mu^{-\frac{1}{2}} \kappa^{\frac{1}{4}} \underline{L}_{\mathbf{v}_h} \right\|_{L^2(F)} \right) \\ &\geq -\mu (C_{\alpha, \kappa})^2 \|\mathbf{v}_0\|_{\mathcal{U}_h} \|\mathbf{v}_h\|_{\mathcal{U}_h}. \end{aligned} \quad (4.56)$$

Using Hölder’s inequality, we obtain that

$$\|\mathbf{v}_h^D\|_{L^2(\Omega^D)} \leq |\Omega^D|^{\frac{1}{6}} \|\mathbf{v}_h^D\|_{L^3(\Omega^D)},$$

which combined with the definition of \mathcal{M} yields

$$(\mathcal{M}(\mathbf{v}_0^D), \mathbf{v}_h)_{\Omega^D} \geq -\left(\mu \kappa^{-1} |\Omega^D|^{\frac{1}{6}} \|\mathbf{v}_0^D\|_{L^2(\Omega^D)} + \beta \|\mathbf{v}_0^D\|_{L^3(\Omega^D)}^2 \right) \|\mathbf{v}_h^D\|_{L^3(\Omega^D)}. \quad (4.57)$$

Combining (4.54)–(4.57) yields

$$\frac{Q_2}{\|\mathbf{v}_h\|_{\mathcal{U}_h}} \geq -\left(\mu \kappa^{-1} |\Omega^D|^{\frac{1}{6}} \|\mathbf{v}_0^D\|_{L^2(\Omega^D)} + \beta \|\mathbf{v}_0^D\|_{L^3(\Omega^D)}^2 \right) - \frac{3\mu (C_{\alpha, \mu})^2}{2} \|\mathbf{v}_0\|_{\mathcal{U}_h}. \quad (4.58)$$

Since \mathbf{v}_0^D is fixed, the right-hand side of (4.58) is a constant independent of \mathbf{v}_h .

Combining (4.53) and (4.58) yields

$$\lim_{\|\mathbf{v}_h\|_{\mathcal{U}_h} \rightarrow +\infty} \frac{Q_h(\mathbf{v}_0 + \mathbf{v}_h, \mathbf{v}_h)}{\|\mathbf{v}_h\|_{\mathcal{U}_h}} = \lim_{\|\mathbf{v}_h\|_{\mathcal{U}_h} \rightarrow +\infty} \frac{Q_1 + Q_2}{\|\mathbf{v}_h\|_{\mathcal{U}_h}} = +\infty,$$

which completes the proof. \square

Theorem 4.2 (Well-posedness of T). *Assume that $\mathbf{w}_h^S \in \mathbf{U}_{h,\text{div}}^S$ satisfies the small-data condition (4.44). Then (4.25)–(4.29) admits a unique solution $(\underline{L}_h^S, \mathbf{u}_h^S, p_h^S, \mathbf{u}_h^D, p_h^D) \in \underline{W}_h^S \times \mathbf{U}_h^S \times P_h^S \times \mathbf{U}_h^D \times P_h^D$. In addition, the following estimate holds*

$$\frac{1}{4} \left\| \mu^{-\frac{1}{2}} \underline{L}_h^S \right\|_{L^2(\Omega^S)}^2 + \frac{1}{4} \left\| \mu^{\frac{1}{2}} \kappa^{-\frac{1}{2}} \mathbf{u}_h^D \right\|_{L^2(\Omega^D)}^2 + \frac{\beta}{27} \left\| \mathbf{u}_h^D \right\|_{L^3(\Omega^D)}^3 \leq (\widehat{C}_f)^2, \quad (4.59)$$

where

$$\begin{aligned} (\widehat{C}_f)^2 := & \left(C_{\mathbf{U}_h^S, 0,1} C_{\underline{W}_h^S, \mathbf{U}_h^S} \right)^2 \mu^{-1} \|\mathbf{f}_0\|_{L^2(\Omega^S)}^2 \\ & + \frac{2}{5} \beta \left(C_{\mathbf{U}_h^D, P_h^D} \right)^{\frac{3}{2}} \|g^D\|_{L^2(\Omega^D)}^{\frac{3}{2}} + \frac{1}{2} \left(C_{\mathbf{U}_h^D, P_h^D} \right)^2 \mu \kappa^{-1} \|g^D\|_{L^2(\Omega^D)}^2 + \frac{2}{\sqrt{\beta}} \|\mathbf{f}^D\|_{L^{\frac{3}{2}}(\Omega^D)}^{\frac{3}{2}}. \end{aligned} \quad (4.60)$$

Proof. The proof of existence follows the classical construction in mixed finite element method (cf. [20], Thm. 2.1), which is based on the Babuška–Nečas–Brezzi theorem and the subjectivity of coercive term. For completeness, we briefly outline the main steps.

By the classical Babuška–Nečas–Brezzi (BNB) theorem (cf. [20], Lem. 2.1), the inf–sup condition stated in Lemma 4.14 ensures the existence of $\mathbf{u}_f \in \mathbf{U}_h^*$ such that

$$R_h(\mathbf{u}_f, q_h) = (g^D, q_h^D)_{\Omega^D}, \quad \forall q_h = (q_h^S, q_h^D) \in P_h.$$

Under the small-data assumption (4.44), Lemma 4.15 guarantees that the nonlinear operator $Q_h(\mathbf{v}_f + \cdot, \cdot)$ is strictly monotone, hemi-continuous, and coercive on \mathbf{U}_h^0 . As a consequence, the Browder–Minty theorem (Thm. 4.1) ensures that the operator $Q_h(\mathbf{u}_f + \cdot, \cdot)$ is surjective from \mathbf{U}_h^0 onto its dual space. Hence, there exists $\mathbf{u}_h^0 \in \mathbf{U}_h^0$ satisfying

$$Q_h(\mathbf{u}_f + \mathbf{u}_h^0, \mathbf{v}_h^0) = (\mathbf{f}^S, \mathbf{v}_h^0)_{\Omega^S} + (\mathbf{f}^D, \mathbf{v}_h^0)_{\Omega^D}, \quad \forall \mathbf{v}_h^0 = (\mathbf{v}_h^S, \mathbf{v}_h^D) \in \mathbf{U}_h^0.$$

We then define $\mathbf{u}_h = \mathbf{u}_f + \mathbf{u}_h^0$. To recover the discrete pressure, we introduce the linear functional $\mathcal{B} : \mathbf{U}_h \rightarrow \mathbb{R}$ by

$$\mathcal{B}(\mathbf{v}_h) := (\mathbf{f}^S, \mathbf{v}_h^S)_{\Omega^S} + (\mathbf{f}^D, \mathbf{v}_h^D)_{\Omega^D} - Q_h(\mathbf{u}_h, \mathbf{v}_h), \quad \forall \mathbf{v}_h = (\mathbf{v}_h^S, \mathbf{v}_h^D) \in \mathbf{U}_h. \quad (4.61)$$

By construction, \mathcal{B} vanishes on \mathbf{U}_h^0 , namely, $\mathcal{B}(\mathbf{v}_h^0) = 0$, $\forall \mathbf{v}_h^0 \in \mathbf{U}_h^0$. Therefore, an application of the BNB theorem (cf. [20], Lem. 2.1) yields the existence of $p_h \in P_h$ such that

$$R_h^*(p_h, \mathbf{v}_h) = R_h(\mathbf{v}_h, p_h) = \mathcal{B}(\mathbf{v}_h), \quad \forall \mathbf{v}_h \in \mathbf{U}_h.$$

Therefore, the pair $(\mathbf{u}_h, p_h) \in \mathbf{U}_h \times P_h$ satisfies the reduced system (4.34) and (4.35), which is equivalent to the original discrete system (4.25)–(4.29).

Now, we focus on the uniqueness. Assume that $(\underline{L}_j^S, \mathbf{u}_j^S, p_j^S, \mathbf{u}_j^D, p_j^D) \in \underline{W}_h^S \times \mathbf{U}_h^S \times P_h^S \times \mathbf{U}_h^D \times P_h^D$, $j = 1, 2$, are the solutions of (4.25)–(4.29). Then, the following equations hold

$$A_h(\underline{L}_1^S - \underline{L}_2^S, \underline{G}_h^S) - B_h^*(\mathbf{u}_1^S - \mathbf{u}_2^S, \underline{G}_h^S) - I_h(\mathbf{u}_1^D - \mathbf{u}_2^D, \underline{G}_h^S) = 0, \quad (4.62)$$

$$N_h(\mathbf{w}_h^S, \mathbf{u}_1^S - \mathbf{u}_2^S, \mathbf{v}_h^S) + D_h(\mathbf{w}_h^S, \underline{L}_1^S - \underline{L}_2^S, \mathbf{v}_h^S) + b_h^*(p_1^S - p_2^S, \mathbf{v}_h^S) + B_h(\underline{L}_1^S - \underline{L}_2^S, \mathbf{v}_h^S) = 0, \quad (4.63)$$

$$-J_h(\mathbf{u}_1^D - \mathbf{u}_2^D, q_h^S) + b_h(\mathbf{u}_1^S - \mathbf{u}_2^S, q_h^S) = 0, \quad (4.64)$$

$$(\mathcal{M}(\mathbf{u}_1^D) - \mathcal{M}(\mathbf{u}_2^D), \mathbf{v}_h^D)_{\Omega^D} + a_h(\mathbf{v}_h^D, p_1^D - p_2^D) - J_h(\mathbf{v}_h^D, p_1^S - p_2^S) + I_h(\mathbf{v}_h^D, \underline{L}_1^S - \underline{L}_2^S) = 0, \quad (4.65)$$

$$a_h(\mathbf{u}_1^D - \mathbf{u}_2^D, q_h^D) = 0, \quad (4.66)$$

for any test functions $\underline{G}_h^S \in \underline{W}_h^S$, $\mathbf{v}_h^S \in \mathbf{U}_h^S$, $q_h^S \in P_h^S$, $\mathbf{v}_h^D \in \mathbf{U}_h^D$, and $q_h^D \in P_h^D$.

Taking $\underline{G}_h^S = \underline{L}_1^S - \underline{L}_2^S$, $\mathbf{v}_h^S = \mathbf{u}_1^S - \mathbf{u}_2^S$, $q_h^S = p_1^S - p_2^S$, $\mathbf{v}_h^D = \mathbf{u}_1^D - \mathbf{u}_2^D$, $q_h^D = p_1^D - p_2^D$ in (4.62)–(4.66) and summing up the resulting equations yield

$$\begin{aligned} & A_h(\underline{L}_1^S - \underline{L}_2^S, \underline{L}_1^S - \underline{L}_2^S) + (\mathcal{M}(\mathbf{u}_1^D) - \mathcal{M}(\mathbf{u}_2^D), \mathbf{u}_1^D - \mathbf{u}_2^D)_{\Omega^D} \\ & + N_h(\mathbf{w}_h^S, \mathbf{u}_1^S - \mathbf{u}_2^S, \mathbf{u}_1^S - \mathbf{u}_2^S) + D_h(\mathbf{w}_h^S, \underline{L}_1^S - \underline{L}_2^S, \mathbf{u}_1^S - \mathbf{u}_2^S) = 0. \end{aligned} \quad (4.67)$$

By Lemma 4.1 and the definition of the operator A_h (cf. (3.1)), we have

$$\begin{aligned} & A_h(\underline{L}_1^S - \underline{L}_2^S, \underline{L}_1^S - \underline{L}_2^S) + (\mathcal{M}(\mathbf{u}_1^D) - \mathcal{M}(\mathbf{u}_2^D), \mathbf{u}_1^D - \mathbf{u}_2^D)_{\Omega^D} \\ & \geq \left\| \mu^{-\frac{1}{2}} (\underline{L}_1^S - \underline{L}_2^S) \right\|_{L^2(\Omega^S)}^2 + \left\| \mu^{\frac{1}{2}} \kappa^{-\frac{1}{2}} (\mathbf{u}_1^D - \mathbf{u}_2^D) \right\|_{L^2(\Omega^D)}^2. \end{aligned} \quad (4.68)$$

It follows from (4.62) and inequality (4.21) in Lemma 4.13 that

$$\begin{aligned} & \left(\left\| \mathbf{u}_1^S - \mathbf{u}_2^S \right\|_{\mathbf{U}_{h,1}^S}^2 + \sum_{F \in \mathcal{F}^I} h_F^{-1} \left\| (\mathbf{u}_1^S - \mathbf{u}_2^S)^t + \alpha^{-1} \mu^{-1} \kappa^{\frac{1}{2}} ((\underline{L}_1^S - \underline{L}_2^S) \mathbf{n})^t \right\|_{L^2(F)}^2 \right)^{\frac{1}{2}} \\ & \leq \mu^{-\frac{1}{2}} C_{\underline{W}_h^S, \mathbf{U}_h^S} \left\| \mu^{-\frac{1}{2}} (\underline{L}_1^S - \underline{L}_2^S) \right\|_{L^2(\Omega^S)}. \end{aligned} \quad (4.69)$$

Combining (4.69) with Lemma 4.12, the discrete Sobolev embedding (4.17), and the small-data assumption (4.44), we obtain

$$\begin{aligned} & N_h(\mathbf{w}_h^S, \mathbf{u}_1^S - \mathbf{u}_2^S, \mathbf{u}_1^S - \mathbf{u}_2^S) + D_h(\mathbf{w}_h^S, \underline{L}_1^S - \underline{L}_2^S, \mathbf{u}_1^S - \mathbf{u}_2^S) \\ & \geq -\mu^{-1} (C_{\mathbf{U}_h^S, 4,1} C_{\underline{W}_h^S, \mathbf{U}_h^S})^2 C_{N_h} \|\mathbf{w}_h^S\|_{\mathbf{U}_h^S,1} \left\| \mu^{-\frac{1}{2}} (\underline{L}_1^S - \underline{L}_2^S) \right\|_{L^2(\Omega^S)}^2 \\ & \geq -\frac{1}{2} \left\| \mu^{-\frac{1}{2}} (\underline{L}_1^S - \underline{L}_2^S) \right\|_{L^2(\Omega^S)}^2. \end{aligned} \quad (4.70)$$

Substituting (4.68) and (4.70) into (4.67) gives

$$\frac{1}{2} \left\| \mu^{-\frac{1}{2}} (\underline{L}_1^S - \underline{L}_2^S) \right\|_{L^2(\Omega^S)}^2 + \left\| \mu^{\frac{1}{2}} \kappa^{-\frac{1}{2}} (\mathbf{u}_1^D - \mathbf{u}_2^D) \right\|_{L^2(\Omega^D)}^2 \leq 0.$$

Hence, $\mathbf{u}_1^D = \mathbf{u}_2^D$, and $\underline{L}_1^S = \underline{L}_2^S$. Moreover, (4.69) and the discrete Poincaré inequality (cf. [3], Thm. 5.1) yield $\mathbf{u}_1^S = \mathbf{u}_2^S$. Substituting these identities into (4.63) and (4.65), we obtain

$$a_h(\mathbf{v}_h^D, p_1^D - p_2^D) - J_h(\mathbf{v}_h^D, p_1^S - p_2^S) = 0 \quad \text{and} \quad b_h^*(p_1^S - p_2^S, \mathbf{v}_h^S) = 0, \quad \forall \mathbf{v}_h^S \in \mathbf{U}_h^S, \mathbf{v}_h^D \in \mathbf{U}_h^D.$$

An application of Lemma 4.14 gives $p_1^S = p_2^S$ and $p_1^D = p_2^D$. Thus, the unique solvability of (4.25)–(4.29) is established.

It remains to prove (4.59). Taking $\mathbf{v}_h^S = \mathbf{u}_h^S$, $\mathbf{v}_h^D = \mathbf{u}_h^D$, $\underline{G}_h^S = \underline{L}_h^S$, $q_h^S = p_h^S$, $q_h^D = p_h^D$ in (4.25)–(4.29) and summing up the resulting equations, we obtain the following identity

$$\begin{aligned} & A_h(\underline{L}_h^S, \underline{L}_h^S) + (\mathcal{M}(\mathbf{u}_h^D), \mathbf{u}_h^D)_{\Omega^D} + N_h(\mathbf{w}_h^S, \mathbf{u}_h^S, \mathbf{u}_h^S) + D_h(\mathbf{w}_h^S, \underline{L}_h^S, \mathbf{u}_h^S) \\ & = (\mathbf{f}^S, \mathbf{u}_h^S)_{\Omega^S} + (\mathbf{f}^D, \mathbf{u}_h^D)_{\Omega^D} - (g^D, p_h^D)_{\Omega^D}. \end{aligned} \quad (4.71)$$

Proceeding analogously to that of (4.70), we obtain

$$N_h(\mathbf{w}_h^S, \mathbf{u}_h^S, \mathbf{u}_h^S) + D_h(\mathbf{w}_h^S, \underline{L}_h^S, \mathbf{u}_h^S) \geq -\frac{1}{2} \left\| \mu^{-\frac{1}{2}} \underline{L}_h^S \right\|_{L^2(\Omega^S)}^2.$$

Substituting this result and the definition of \mathcal{M} into (4.71) yields

$$\frac{1}{2} \left\| \mu^{-\frac{1}{2}} \underline{L}_h^S \right\|_{L^2(\Omega^S)}^2 + \left\| \mu^{\frac{1}{2}} \kappa^{-\frac{1}{2}} \mathbf{u}_h^D \right\|_{L^2(\Omega^D)}^2 + \beta \left\| \mathbf{u}_h^D \right\|_{L^3(\Omega^D)}^3 \leq (\mathbf{f}^S, \mathbf{u}_h^S)_{\Omega^S} + (\mathbf{f}^D, \mathbf{u}_h^D)_{\Omega^D} - (g^D, p_h^D)_{\Omega^D}.$$

Applying Lemma 4.11 with $\mathbf{v}_h^S = \mathbf{u}_h^S$, Lemma 4.10, inequality (4.21) in Lemma 4.13, and the discrete Sobolev embedding (4.16), we obtain

$$\begin{aligned} (\mathbf{f}^S, \mathbf{u}_h^S)_{\Omega^S} &= (\mathbf{f}_0, \mathbf{u}_h^S)_{\Omega^S} \leq \|\mathbf{f}_0\|_{L^2(\Omega^S)} \|\mathbf{u}_h^S\|_{L^2(\Omega^S)} \\ &\leq \frac{\mu}{4 \left(C_{U_h^S, 0, 1} C_{W_h^S, U_h^S} \right)^2} \|\mathbf{u}_h^S\|_{L^2(\Omega^S)}^2 + \left(C_{U_h^S, 0, 1} C_{W_h^S, U_h^S} \right)^2 \mu^{-1} \|\mathbf{f}_0\|_{L^2(\Omega^S)}^2 \\ &\leq \frac{1}{4} \left\| \mu^{-\frac{1}{2}} \underline{L}_h^S \right\|_{L^2(\Omega^S)}^2 + \left(C_{U_h^S, 0, 1} C_{W_h^S, U_h^S} \right)^2 \mu^{-1} \|\mathbf{f}_0\|_{L^2(\Omega^S)}^2. \end{aligned}$$

Also, inequality (4.24) in Lemma 4.13 and Young’s inequality reveal that

$$\begin{aligned} (g^D, p_h^D)_{\Omega^D} &\leq \|g^D\|_{L^2(\Omega^D)} \|p_h^D\|_{L^2(\Omega^D)} \\ &\leq \|g^D\|_{L^2(\Omega^D)} C_{U_h^D, P_h^D} \left(\mu^{\frac{1}{2}} \kappa^{-\frac{1}{2}} \|\mu^{\frac{1}{2}} \kappa^{-\frac{1}{2}} \mathbf{u}_h^D\|_{L^2(\Omega^D)} + \beta \|\mathbf{u}_h^D\|_{L^3(\Omega^D)}^2 \right) \\ &\leq \frac{1}{2} \left\| \mu^{\frac{1}{2}} \kappa^{-\frac{1}{2}} \mathbf{u}_h^D \right\|_{L^2(\Omega^D)}^2 + \frac{25\beta}{27} \|\mathbf{u}_h^D\|_{L^3(\Omega^D)}^3 \\ &\quad + \frac{1}{2} \left(C_{U_h^D, P_h^D} \right)^2 \mu \kappa^{-1} \|g^D\|_{L^2(\Omega^D)}^2 + \frac{2}{5} \beta \left(C_{U_h^D, P_h^D} \right)^{\frac{3}{2}} \|g^D\|_{L^2(\Omega^D)}^{\frac{3}{2}}. \end{aligned}$$

An application of Hölder inequality yields

$$(\mathbf{f}^D, \mathbf{u}_h^D)_{\Omega^D} \leq \frac{2}{\sqrt{\beta}} \|\mathbf{f}^D\|_{L^{\frac{3}{2}}(\Omega^D)}^{\frac{3}{2}} + \frac{1}{27} \beta \|\mathbf{u}_h^D\|_{L^3(\Omega^D)}^3.$$

Combining the aforementioned estimates, we finally obtain that

$$\begin{aligned} &\frac{1}{4} \left\| \mu^{-\frac{1}{2}} \underline{L}_h^S \right\|_{L^2(\Omega^S)}^2 + \frac{1}{4} \left\| \mu^{\frac{1}{2}} \kappa^{-\frac{1}{2}} \mathbf{u}_h^D \right\|_{L^2(\Omega^D)}^2 + \frac{\beta}{27} \|\mathbf{u}_h^D\|_{L^3(\Omega^D)}^3 \\ &\leq \left(C_{U_h^S, 0, 1} C_{W_h^S, U_h^S} \right)^2 \mu^{-1} \|\mathbf{f}_0\|_{L^2(\Omega^S)}^2 + \frac{1}{2} \left(C_{U_h^D, P_h^D} \right)^2 \mu \kappa^{-1} \|g^D\|_{L^2(\Omega^D)}^2 \\ &\quad + \frac{2}{5} \beta \left(C_{U_h^D, P_h^D} \right)^{\frac{3}{2}} \|g^D\|_{L^2(\Omega^D)}^{\frac{3}{2}} + \frac{2}{\sqrt{\beta}} \|\mathbf{f}^D\|_{L^{\frac{3}{2}}(\Omega^D)}^{\frac{3}{2}}. \end{aligned}$$

Therefore, the proof is completed. □

Remark 4.3. The stability analysis in Theorem 4.2 together with (4.21) in Lemma 4.13 yields

$$\left(\|\mathbf{u}_h^S\|_{U_{h,1}^S}^2 + \sum_{F \in \mathcal{F}^I} h_F^{-1} \left\| (\mathbf{u}_h^S)^t + \alpha^{-1} \mu^{-1} \kappa^{\frac{1}{2}} (\underline{L}_h^S \mathbf{n})^t \right\|_{L^2(F)}^2 \right)^{\frac{1}{2}} \leq 2\mu^{-\frac{1}{2}} C_{W_h^S, U_h^S} \widehat{C}_f. \tag{4.72}$$

4.3. Well-posedness of the fixed-point

The final step is to establish the well-posedness of the nonlinear system (3.4)–(3.8), building upon the results for the iterative scheme (4.25)–(4.29). The stability estimate (4.72) provides the key insight: a suitable small-data assumption on the source term directly implies condition (4.44), which ensures the generation of a bounded Picard sequence $\{\mathbf{u}_{h,m}^S\}_{m=1}^\infty$. The well-posedness of the nonlinear system then follows by proving that T is a contraction mapping under this small-data assumption.

We begin by introducing the continuous property of $N_h + D_h$.

Lemma 4.16. *Assume that $\mathbf{w}_1^S, \mathbf{w}_2^S \in \mathbf{U}_{h,\text{div}}^S$ with $\nabla \cdot \mathbf{w}_1^S = \nabla \cdot \mathbf{w}_2^S = 0$. Then for any $\mathbf{v}_h^S \in \mathbf{U}_h^S$, $\underline{\mathbf{G}}_h^S \in \underline{W}_h^S$, and $\mathbf{r}_h^S \in \mathbf{U}_h^S$, the following estimate holds:*

$$\begin{aligned} & |N_h(\mathbf{w}_1^S, \mathbf{v}_h^S, \mathbf{r}_h^S) - N_h(\mathbf{w}_2^S, \mathbf{v}_h^S, \mathbf{r}_h^S) + D_h(\mathbf{w}_1^S - \mathbf{w}_2^S, \underline{\mathbf{G}}_h^S, \mathbf{r}_h^S)| \\ & \leq C_{N_h} \|\mathbf{w}_1^S - \mathbf{w}_2^S\|_{0,4,h} \left(\|\mathbf{v}_h^S\|_{\mathbf{U}_{h,1}^S}^2 + \sum_{F \in \mathcal{F}^I} h_F^{-1} \left\| (\mathbf{v}_h^S)^{\mathbf{t}} + \alpha^{-1} \mu^{-1} \kappa^{\frac{1}{2}} (\underline{\mathbf{G}}_h^S \mathbf{n})^{\mathbf{t}} \right\|_{L^2(F)}^2 \right)^{\frac{1}{2}} \|\mathbf{r}_h^S\|_{0,4,h}, \end{aligned}$$

where the constant C_{N_h} is given in Lemma 4.12.

Proof. Note that for every face $F \in \mathcal{F}_h^{S,b}$, the following inequality holds:

$$\left(|\mathbf{w}_1^S \cdot \mathbf{n}| - |\mathbf{w}_2^S \cdot \mathbf{n}|, |\mathbf{v}_h^S \cdot \mathbf{r}_h^S| \right)_F \leq \left(|(\mathbf{w}_1^S - \mathbf{w}_2^S) \cdot \mathbf{n}|, |\mathbf{v}_h^S \cdot \mathbf{r}_h^S| \right)_F.$$

Using this observation, the desired result follows by the same argument employed in the proof of Lemma 4.12. We omit the details for brevity. \square

Now, we are ready to prove Theorem 4.3, namely, the unique solvability of the nonlinear system (4.25)–(4.29).

Theorem 4.3 (Existence and uniqueness of the discrete system). *Assume the source term satisfies the following small-data condition:*

$$4\mu^{-\frac{3}{2}} C_{N_h} \left(C_{\underline{W}_h^S, \mathbf{U}_h^S} \right)^3 \left(C_{\mathbf{U}_h^S, 4,1} \right)^2 \widehat{C}_{\mathbf{f}} < 1, \quad (4.73)$$

where $\widehat{C}_{\mathbf{f}}$ is defined in (4.60). Then the nonlinear discrete problem (3.4)–(3.8) admits a unique solution.

Proof. We define the subset of $\mathbf{U}_{h,\text{div}}^S$ satisfying the small-data condition (4.44) as

$$\mathbf{U}_{h,\text{small}}^S := \left\{ \mathbf{v}_h^S \in \mathbf{U}_{h,\text{div}}^S : 2\mu^{-1} \left(C_{\underline{W}_h^S, \mathbf{U}_h^S} C_{\mathbf{U}_h^S, 4,1} \right)^2 C_{N_h} \|\mathbf{v}_h^S\|_{\mathbf{U}_{h,1}^S} \leq 1 \right\}.$$

For any given $\mathbf{w}_h^S \in \mathbf{U}_{h,\text{small}}^S$, Theorem 4.2 guarantees the existence and uniqueness of $T(\mathbf{w}_h^S)$. Furthermore, the stability estimate (4.72) implies that $T(\mathbf{w}_h^S) \in \mathbf{U}_{h,\text{small}}^S$. Consequently, it remains to show that under condition (4.73), the mapping T is a contraction on $\mathbf{U}_{h,\text{small}}^S$ with respect to the $\|\cdot\|_{\mathbf{U}_{h,1}^S}$ -norm.

Let $\mathbf{w}_j^S \in \mathbf{U}_{h,\text{small}}^S$, $j = 1, 2$. Then the system (4.25)–(4.29) admits unique solutions $(\underline{\mathbf{L}}_j^S, \mathbf{u}_j^S, p_j^S, \mathbf{u}_j^D, p_j^D) \in \underline{W}_h^S \times \mathbf{U}_h^S \times P_h^S \times \mathbf{U}_h^D \times P_h^D$. Subtracting the two systems and testing with $\underline{\mathbf{G}}_h^S = \underline{\mathbf{L}}_1^S - \underline{\mathbf{L}}_2^S$, $\mathbf{v}_h^S = \mathbf{u}_1^S - \mathbf{u}_2^S$, $q_h^S = p_1^S - p_2^S$, $\mathbf{v}_h^D = \mathbf{u}_1^D - \mathbf{u}_2^D$, and $q_h^D = p_1^D - p_2^D$, and summing up the resulting equations, we obtain

$$\begin{aligned} & A_h(\underline{\mathbf{L}}_1^S - \underline{\mathbf{L}}_2^S, \underline{\mathbf{L}}_1^S - \underline{\mathbf{L}}_2^S) + (\mathcal{M}(\mathbf{u}_1^D) - \mathcal{M}(\mathbf{u}_2^D), \mathbf{u}_1^D - \mathbf{u}_2^D)_{\Omega^D} + N_h(\mathbf{w}_1^S, \mathbf{u}_1^S, \mathbf{u}_1^S - \mathbf{u}_2^S) \\ & - N_h(\mathbf{w}_2^S, \mathbf{u}_2^S, \mathbf{u}_1^S - \mathbf{u}_2^S) + D_h(\mathbf{w}_1^S, \underline{\mathbf{L}}_1^S, \mathbf{u}_1^S - \mathbf{u}_2^S) - D_h(\mathbf{w}_2^S, \underline{\mathbf{L}}_2^S, \mathbf{u}_1^S - \mathbf{u}_2^S) = 0. \end{aligned} \quad (4.74)$$

Using the algebraic identity

$$\begin{aligned} & N_h(\mathbf{w}_1^S, \mathbf{u}_1^S, \mathbf{u}_1^S - \mathbf{u}_2^S) - N_h(\mathbf{w}_2^S, \mathbf{u}_2^S, \mathbf{u}_1^S - \mathbf{u}_2^S) \\ & + D_h(\mathbf{w}_1^S, \underline{\mathbf{L}}_1^S, \mathbf{u}_1^S - \mathbf{u}_2^S) - D_h(\mathbf{w}_2^S, \underline{\mathbf{L}}_2^S, \mathbf{u}_1^S - \mathbf{u}_2^S) =: G_1 + G_2, \end{aligned}$$

where

$$\begin{aligned} G_1 &= N_h(\mathbf{w}_1^S, \mathbf{u}_1^S - \mathbf{u}_2^S, \mathbf{u}_1^S - \mathbf{u}_2^S) + D_h(\mathbf{w}_1^S, \underline{\mathbf{L}}_1^S - \underline{\mathbf{L}}_2^S, \mathbf{u}_1^S - \mathbf{u}_2^S), \\ G_2 &= N_h(\mathbf{w}_1^S, \mathbf{u}_2^S, \mathbf{u}_1^S - \mathbf{u}_2^S) - N_h(\mathbf{w}_2^S, \mathbf{u}_2^S, \mathbf{u}_1^S - \mathbf{u}_2^S) + D_h(\mathbf{w}_1^S - \mathbf{w}_2^S, \underline{\mathbf{L}}_2^S, \mathbf{u}_1^S - \mathbf{u}_2^S), \end{aligned}$$

we can rewrite (4.74) as

$$A_h(\underline{L}_1^S - \underline{L}_2^S, \underline{L}_1^S - \underline{L}_2^S) + (\mathcal{M}(\mathbf{u}_1^D) - \mathcal{M}(\mathbf{u}_2^D), \mathbf{u}_1^D - \mathbf{u}_2^D)_{\Omega^D} + G_1 = -G_2. \tag{4.75}$$

By the definition of $A_h(\cdot, \cdot)$ (cf. (3.1)) the monotonicity of \mathcal{M} (Lem. 4.1), we have

$$A_h(\underline{L}_1^S - \underline{L}_2^S, \underline{L}_1^S - \underline{L}_2^S) \geq \left\| \mu^{-\frac{1}{2}}(\underline{L}_1^S - \underline{L}_2^S) \right\|_{L^2(\Omega^S)}^2, \text{ and } (\mathcal{M}(\mathbf{u}_1^D) - \mathcal{M}(\mathbf{u}_2^D), \mathbf{u}_1^D - \mathbf{u}_2^D)_{\Omega^D} \geq 0.$$

Since (4.25) is linear and $\mathbf{w}_1^S \in \mathbf{U}_{h,\text{small}}^S$, an argument analogous to that used in (4.49) yields

$$G_1 \geq -\frac{1}{2} \left\| \mu^{-\frac{1}{2}}(\underline{L}_1^S - \underline{L}_2^S) \right\|_{L^2(\Omega^S)}^2.$$

Combining the above estimates with inequality (4.21) in Lemma 4.13 gives

$$\begin{aligned} & A_h(\underline{L}_1^S - \underline{L}_2^S, \underline{L}_1^S - \underline{L}_2^S) + (\mathcal{M}(\mathbf{u}_1^D) - \mathcal{M}(\mathbf{u}_2^D), \mathbf{u}_1^D - \mathbf{u}_2^D)_{\Omega^D} + G_1 \\ & \geq \left(1 - \frac{1}{2}\right) \left\| \mu^{-\frac{1}{2}}(\underline{L}_1^S - \underline{L}_2^S) \right\|_{L^2(\Omega^S)}^2 \geq \frac{1}{2} \mu^{\frac{1}{2}} \left(C_{\underline{W}_h^S, \mathbf{U}_h^S}\right)^{-1} \left\| \mu^{-\frac{1}{2}}(\underline{L}_1^S - \underline{L}_2^S) \right\|_{L^2(\Omega^S)} \|\mathbf{u}_1^S - \mathbf{u}_2^S\|_{\mathbf{U}_h^S, 1}. \end{aligned} \tag{4.76}$$

Moreover, Lemma 4.16 and the stability result (4.72) imply

$$\begin{aligned} -G_2 & \leq C_{N_h} \|\mathbf{w}_1^S - \mathbf{w}_2^S\|_{0,4,h} \left(\|\mathbf{u}_1^S\|_{\mathbf{U}_h^S, 1}^2 + \sum_{F \in \mathcal{F}^I} h_F^{-1} \left\| (\mathbf{u}_1^S)^t + \alpha^{-1} \mu^{-1} \kappa^{\frac{1}{2}} (\underline{L}_1^S \mathbf{n})^t \right\|_{L^2(F)}^2 \right)^{\frac{1}{2}} \|\mathbf{u}_1^S - \mathbf{u}_2^S\|_{0,4,h} \\ & \leq 2\mu^{-1} C_{N_h} \left(C_{\mathbf{U}_h^S, 4,1}\right)^2 \left(C_{\underline{W}_h^S, \mathbf{U}_h^S}\right)^2 \widehat{C}_{\mathbf{f}} \|\mathbf{w}_1^S - \mathbf{w}_2^S\|_{\mathbf{U}_h^S, 1} \left\| \mu^{-\frac{1}{2}}(\underline{L}_1^S - \underline{L}_2^S) \right\|_{L^2(\Omega^S)}. \end{aligned} \tag{4.77}$$

Substituting (4.76) and (4.77) into (4.75) yields

$$\begin{aligned} & \frac{1}{2} \mu^{\frac{1}{2}} \left(C_{\underline{W}_h^S, \mathbf{U}_h^S}\right)^{-1} \left\| \mu^{-\frac{1}{2}}(\underline{L}_1^S - \underline{L}_2^S) \right\|_{L^2(\Omega^S)} \|\mathbf{u}_1^S - \mathbf{u}_2^S\|_{\mathbf{U}_h^S, 1} \\ & \leq 2\mu^{-1} C_{N_h} \left(C_{\mathbf{U}_h^S, 4,1}\right)^2 \left(C_{\underline{W}_h^S, \mathbf{U}_h^S}\right)^2 \widehat{C}_{\mathbf{f}} \|\mathbf{w}_1^S - \mathbf{w}_2^S\|_{\mathbf{U}_h^S, 1} \left\| \mu^{-\frac{1}{2}}(\underline{L}_1^S - \underline{L}_2^S) \right\|_{L^2(\Omega^S)}. \end{aligned}$$

Assuming $\underline{L}_1^S \neq \underline{L}_2^S$ and recalling that $\mathbf{u}_j^S = T(\mathbf{w}_j^S)$ for $j = 1, 2$, we obtain the following estimate for T :

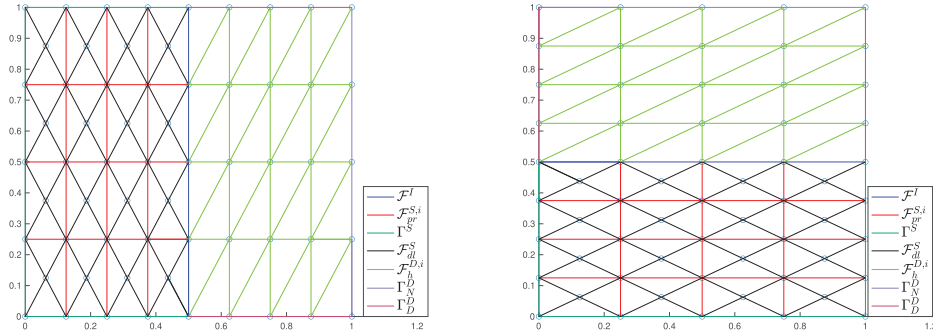
$$\|T(\mathbf{w}_1^S) - T(\mathbf{w}_2^S)\|_{\mathbf{U}_h^S, 1} \leq 4\mu^{-\frac{3}{2}} C_{N_h} \left(C_{\mathbf{U}_h^S, 4,1}\right)^2 \left(C_{\underline{W}_h^S, \mathbf{U}_h^S}\right)^3 \widehat{C}_{\mathbf{f}} \|\mathbf{w}_1^S - \mathbf{w}_2^S\|_{\mathbf{U}_h^S, 1}. \tag{4.78}$$

Under assumption (4.73), the coefficient on the right-hand side of (4.78) is strictly less than 1, which shows that T is a contraction. If $\underline{L}_1^S = \underline{L}_2^S$, (4.21) in conjunction with the discrete Poincaré inequality implies $\mathbf{u}_1^S = \mathbf{u}_2^S$, and (4.78) still holds. The existence and uniqueness of a fixed point for (4.25)–(4.29) then follow from the classical Banach fixed-point theorem (cf. [13]).

We denote by \mathbf{u}_h^S the unique fixed point of the operator T . By taking the given data $\mathbf{w}_h^S = \mathbf{u}_h^S$ in (4.25)–(4.29), Theorem 4.2 ensures the unique existence of

$$(\underline{L}_h^S, p_h^S, \mathbf{u}_h^D, p_h^D) \in \underline{W}_h^S \times P_h^S \times \mathbf{U}_h^D \times P_h^D,$$

which, together with \mathbf{u}_h^S , satisfies (4.25)–(4.29). Consequently, this solution also constitutes a solution of the nonlinear system (3.4)–(3.8). Moreover, the uniqueness of the fixed point \mathbf{u}_h^S implies the uniqueness of the corresponding solution to (3.4)–(3.8). \square


 FIGURE 3. Sample meshes for Examples 5.1, 5.3 (left) and 5.2 (right) when $h = \frac{1}{4}$.

5. NUMERICAL EXPERIMENTS

This section presents a series of numerical experiments aimed at verifying the theoretical results established in the previous sections. Due to the difficulty of constructing manufactured solutions that satisfy all interface conditions exactly, we adopt the approach proposed in Example 4.2 of [36], in which the formulation is modified to accommodate non-homogeneous interface conditions. For notational convenience, we define

$$\underline{e}_{\underline{L}^S} := \underline{L}^S - \underline{L}_h^S, \quad \mathbf{e}_{\mathbf{u}^S} := \mathbf{u}^S - \mathbf{u}_h^S, \quad e_{p^S} := p^S - p_h^S, \quad \mathbf{e}_{\mathbf{u}^D} := \mathbf{u}^D - \mathbf{u}_h^D, \quad \text{and} \quad e_{p^D} := p^D - p_h^D.$$

Here, $(\underline{L}^S, \mathbf{u}^S, p^S, \mathbf{u}^D, p^D)$ and $(\underline{L}_h^S, \mathbf{u}_h^S, p_h^S, \mathbf{u}_h^D, p_h^D)$ denote the solutions of the continuous system (2.1)–(2.10) and the discrete system (3.4)–(3.8), respectively.

Examples 5.1–5.3 are based on smooth analytical solutions. In particular, Examples 5.1 and 5.2 examine the performance of the scheme under standard and small-viscosity regimes, respectively. Example 5.3 investigates the performance of the proposed scheme in the presence of large irrotational body force. These tests are intended to assess the numerical performance of the proposed method. In particular, Examples 5.2 and 5.3 are designed to verify its pressure-robustness. Finally, Example 5.4 considers a solution with limited regularity in order to assess the convergence behavior of the scheme in a more challenging setting. All these numerical results provide further evidence of the robustness and accuracy of the proposed method across a range of representative scenarios.

5.1. Example 1: Smooth solutions

In this example, we adopt domain $\Omega^D = [\frac{1}{2}, 1] \times [0, 1]$, and $\Omega^S = [0, \frac{1}{2}] \times [0, 1]$. The boundary is $\Gamma_D^D = \{1\} \times [0, 1]$, and $\Gamma_N^D = [\frac{1}{2}, 1] \times \{0, 1\}$. The left panel of Figure 3 illustrates a sample mesh after the subdivision when $h = \frac{1}{4}$, where h represents the largest edge length of the rectangular element in \mathcal{T}_0^S . The exact solution is given by

$$\begin{aligned} \mathbf{u}^S(x, y) &= \begin{pmatrix} -x^2((y-1)y^2 + (y-1)^2y)(x - \frac{1}{2})^2 \\ y^2((x - \frac{1}{2})x^2 + (x - \frac{1}{2})^2x)(y-1)^2 \end{pmatrix}, \\ \mathbf{u}^D(x, y) &= \begin{pmatrix} \frac{1}{4}y(y-1)(-8x + 12x^2 + 1) \\ \frac{1}{4}x(2x-1)^2(2y-1) \end{pmatrix}, \\ p^S(x, y) &= x \left(x - \frac{1}{2}\right)^2 \left(y - \frac{1}{2}\right), \\ p^D(x, y) &= -xy \left(x - \frac{1}{2}\right)^2 (y-1). \end{aligned}$$

TABLE 1. Convergence history in free fluid domain of Example 1.

μ	k	Mesh	$\ \mathbf{e}_{\mathbf{u}^S}\ _{L^2(\Omega^S)}$		$\ \mathbf{e}_{L^S}\ _{L^2(\Omega^S)}$		$\ e_{p^S}\ _{L^2(\Omega^S)}$			
		h^{-1}	Error	Rate	Error	Rate	Error	Rate		
1	1	2	2.8790e-04	NA	2.4820e-03	NA	3.7745e-03	NA		
		4	5.5724e-05	2.3692	7.0256e-04	1.8208	1.0808e-03	1.8042		
		8	1.3497e-05	2.0456	1.8108e-04	1.9560	2.7492e-04	1.9750		
		16	3.3465e-06	2.0119	4.5658e-05	1.9877	6.8866e-05	1.9972		
		32	8.3468e-07	2.0034	1.1452e-05	1.9952	1.7210e-05	2.0006		
		64	2.0854e-07	2.0009	2.8673e-06	1.9979	4.3001e-06	2.0008		
	2	2	2.2565e-05	NA	3.9470e-04	NA	2.6485e-04	NA		
		4	3.5406e-06	2.6721	6.0329e-05	2.7098	2.8898e-05	3.1962		
		8	4.4045e-07	3.0069	7.7808e-06	2.9548	3.1910e-06	3.1789		
		16	5.4681e-08	3.0099	9.8724e-07	2.9785	3.6415e-07	3.1314		
		32	6.8192e-09	3.0034	1.2446e-07	2.9877	4.2907e-08	3.0853		
		64	8.5183e-10	3.0010	1.5629e-08	2.9934	5.1808e-09	3.0500		
		2×10^{-3}	1	1	1.0557e-03	NA	1.1364e-05	NA	2.2247e-03	NA
				2	2.7995e-03	-1.4070	5.2159e-05	-2.1984	7.3002e-04	1.6076
4	4.4247e-04			2.6615	8.9452e-06	2.5437	1.7441e-04	2.0654		
8	8.0478e-05			2.4589	1.6044e-06	2.4790	4.1166e-05	2.0830		
16	1.6054e-05			2.3257	3.2013e-07	2.3253	1.0025e-05	2.0379		
32	3.5849e-06			2.1629	7.1786e-08	2.1569	2.4847e-06	2.0125		
2	1		3.4838e-03	NA	6.8226e-05	NA	6.4334e-04	NA		
	2		1.1538e-04	4.9162	2.8937e-06	4.5593	7.3492e-05	3.1299		
	4		1.1063e-05	3.3825	2.2260e-07	3.7004	8.7625e-06	3.0682		
	8		6.5826e-07	4.0710	1.7389e-08	3.6782	1.0757e-06	3.0260		
		16	6.0306e-08	3.4483	2.0077e-09	3.1145	1.3407e-07	3.0043		
		32	6.9820e-09	3.1106	2.4980e-10	3.0067	1.6750e-08	3.0007		

When the viscosity parameter μ is very small, the small-data assumption (4.73) may no longer be satisfied. In our numerical experiments, we first consider the case $\mu = 10^{-4}$. For this choice, the fixed-point iteration fails to converge when starting from the initial guess $\mathbf{u}_{h,0}^S = \mathbf{0}$. For $\mu = 2 \times 10^{-3}$, the fixed-point residual decreases monotonically with respect to the iteration count, exhibiting a clear contraction behavior. However, the convergence rate is relatively slow. Overall, these results indicate that although the fixed-point iteration remains convergent for moderately small viscosity values, its convergence rate deteriorates as μ decreases. This behavior is consistent with the theoretical small-data condition, in which the contraction constant depends explicitly on the inverse of the viscosity parameter. The convergence history against the mesh size for $\mu = 1$ and $\mu = 2 \times 10^{-3}$ is reported in Tables 1 and 2. It is worth noting that, for both standard and small viscosity values, the proposed scheme exhibits stable and robust convergence behavior.

5.2. Example 2: Vortex with small viscosity and low velocity

In this example, which is modified from [15], we examine the behavior of our scheme when viscosity is small and velocity is low. To ensure the well-posedness of the problem, the velocity is kept low, which is more suitable for the Darcy–Forchheimer problem. We let $\Omega^S = [0, 1] \times [0, \frac{1}{2}]$, $\Omega^D = [0, 1] \times [\frac{1}{2}, 1]$, $\Gamma_D^D = [0, 1] \times 1$, and $\Gamma_N^D = \{0, 1\} \times [0, 1]$. The sample mesh when $h = \frac{1}{4}$ is displayed in the right panel of Figure 3, where h denotes the largest edge length of the cubic element in \mathcal{T}_0^S . The exact solution is defined by

TABLE 2. Convergence history in porous media of Example 1.

μ	k	Mesh	$\ \mathbf{e}_{\mathbf{u}^D}\ _{L^2(\Omega^D)}$		$\ e_{p^D}\ _{L^2(\Omega^D)}$			
		h^{-1}	Error	Rate	Error	Rate		
1	1	2	2.5051e-02	NA	3.7906e-03	NA		
		4	6.5290e-03	1.9399	1.1855e-03	1.6769		
		8	1.6517e-03	1.9829	3.1117e-04	1.9298		
		16	4.1408e-04	1.9960	7.8695e-05	1.9834		
		32	1.0356e-04	1.9994	1.9730e-05	1.9959		
		64	2.5890e-05	2.0001	4.9360e-06	1.9990		
	2	2	2.6001e-03	NA	3.6711e-03	NA		
		4	3.3358e-04	2.9625	9.3140e-04	1.9787		
		8	4.2147e-05	2.9846	2.3410e-04	1.9922		
		16	5.2916e-06	2.9936	5.8608e-05	1.9980		
		32	6.6273e-07	2.9972	1.4657e-05	1.9995		
		64	8.2915e-08	2.9987	3.6646e-06	1.9999		
		2×10^{-3}	1	1	8.7484e-02	NA	2.6319e-04	NA
				2	2.5289e-02	1.7905	9.4364e-04	-1.8421
4	8.1215e-03			1.6387	2.8283e-04	1.7383		
8	2.3466e-03			1.7912	6.9665e-05	2.0215		
16	6.3174e-04			1.8932	1.7140e-05	2.0230		
32	1.6528e-04			1.9345	4.2588e-06	2.0089		
2	1		2.2536e-02	NA	1.2959e-02	NA		
	2		4.2484e-03	2.4072	3.5517e-03	1.8674		
	4		6.6163e-04	2.6828	9.2476e-04	1.9413		
	8		7.3891e-05	3.1625	2.3367e-04	1.9846		
	16		8.0263e-06	3.2026	5.8580e-05	1.9960		
	32		9.5476e-07	3.0715	1.4655e-05	1.9990		

$$\mathbf{u}^S(x, y) = \mu \begin{pmatrix} 16y \sin(\pi x)^2 (y^2 - \frac{1}{4}) \\ -8\pi \cos(\pi x) \sin(\pi x) (y^2 - \frac{1}{4})^2 \end{pmatrix},$$

$$\mathbf{u}^D(x, y) = \mu \begin{pmatrix} \cos(2\pi y) \sin(2\pi x) \\ -\cos(2\pi x) \sin(2\pi y) \end{pmatrix},$$

$$p^j(x, y) = \sin(2\pi x) \sin(2\pi y), \quad j = S, D.$$

The convergence histories with respect to the mesh size h for $\mu = 1$ and $\mu = 10^{-4}$ are summarized in Tables 3 and 4, respectively. As expected, the pressure errors remain essentially unchanged for decreasing viscosity. In contrast, the L^2 -errors of \mathbf{u}^S , \underline{L}^S , and \mathbf{u}^D are significantly reduced as μ decreases. In this example, the velocity is selected with an explicit scaling proportional to μ . As a consequence, both the velocity and its interpolation error naturally decay as μ becomes small. If the discrete velocity were sensitive to pressure effects, existing analyses (see, e.g., Thm. 6.2 of [25] for coupled Navier-Stokes and Darcy systems) indicate that the error bound for velocity depends on negative powers of μ multiplied by the pressure error. In the small-viscosity regime, such pressure-related terms would dominate and lead to an increase of the velocity errors as $\mu \rightarrow 0$. The absence of this behavior in the numerical results therefore provides clear numerical evidence of the pressure-robust behavior of the proposed scheme.

TABLE 3. Convergence history in free fluid domain of Example 2.

μ	k	Mesh h^{-1}	$\ \mathbf{e}_{\mathbf{u}^S}\ _{L^2(\Omega^S)}$		$\ \mathbf{e}_{L^S}\ _{L^2(\Omega^S)}$		$\ e_{p^S}\ _{L^2(\Omega^S)}$			
			Error	Rate	Error	Rate	Error	Rate		
1	1	2	1.3385e-01	NA	1.6587e+00	NA	1.2478e+00	NA		
		4	7.1335e-02	0.9079	7.8893e-01	1.0721	2.8858e-01	2.1124		
		8	1.7646e-02	2.0153	2.0821e-01	1.9218	8.9112e-02	1.6953		
		16	4.2686e-03	2.0475	5.3050e-02	1.9727	2.1226e-02	2.0698		
		32	1.0545e-03	2.0172	1.3367e-02	1.9886	4.9822e-03	2.0910		
		64	2.6281e-04	2.0045	3.3562e-03	1.9938	1.1916e-03	2.0639		
	2	2	6.2498e-02	NA	7.1319e-01	NA	1.6271e-01	NA		
		4	1.0409e-02	2.5859	1.5720e-01	2.1817	8.4829e-02	0.9396		
		8	1.4462e-03	2.8475	1.9645e-02	3.0003	9.1249e-03	3.2167		
		16	1.8116e-04	2.9969	2.5194e-03	2.9630	1.0861e-03	3.0707		
		32	2.2652e-05	2.9996	3.1893e-04	2.9818	1.3195e-04	3.0410		
		64	2.8322e-06	2.9996	4.0113e-05	2.9911	1.6255e-05	3.0210		
		10^{-4}	1	4	1.4697e-07	NA	1.3077e-10	NA	1.9525e-01	NA
				8	1.0733e-08	3.7754	1.6086e-11	3.0232	4.6091e-02	2.0828
16	3.5065e-09			1.6140	2.8994e-12	2.4720	1.1954e-02	1.9469		
32	9.9670e-10			1.8148	7.1699e-13	2.0158	3.0161e-03	1.9868		
64	2.5843e-10			1.9474	1.8387e-13	1.9632	7.5575e-04	1.9967		
128	6.5091e-11			1.9892	4.6280e-14	1.9903	1.8905e-04	1.9992		
2	2		1.9023e-07	NA	1.8759e-10	NA	5.2274e-02	NA		
	4		1.6357e-08	3.5398	1.4122e-11	3.7316	2.0695e-02	1.3368		
	8		1.3967e-09	3.5499	1.5903e-12	3.1506	3.3442e-03	2.6296		
	16		1.5139e-10	3.2057	1.4907e-13	3.4153	4.2767e-04	2.9671		
		32	9.5740e-12	3.9830	1.2795e-14	3.5423	5.3765e-05	2.9918		
		64	5.1676e-13	4.2116	1.0482e-15	3.6096	6.7302e-06	2.9979		

5.3. Example 3: Large irrotational body force

This example is inspired by Benchmark 3.3 of [30] and [6]. We use this example to demonstrate the robustness of our method for large irrotational body force. The domain is selected as $\Omega^S = [0, \frac{1}{2}] \times [0, 1]$, and $\Omega^D = [\frac{1}{2}, 1] \times [0, 1]$, where the boundary conditions are imposed on $\Gamma_D^D = \{1\} \times [0, 1]$, $\Gamma_N^D = [\frac{1}{2}, 1] \times \{0, 1\}$. The sample mesh can refer to the left panel of Figure 3. The parameters are selected as $\mu = \beta = \kappa = \alpha = 1$. The source terms are selected corresponding to the solutions given by

$$\mathbf{u}^D(x, y) = \mathbf{u}^S(x, y) = \begin{pmatrix} y \\ -x \end{pmatrix},$$

$$p^S(x, y) = p^D(x, y) = \lambda x^3 + \frac{x^2 + y^2}{2}.$$

In this case, the body force $\mathbf{f}^S = \begin{pmatrix} 3\lambda x^2 \\ 0 \end{pmatrix}$ is irrotational. In our numerical tests, we consider two cases: $\lambda = 1$ and $\lambda = 10^6$. The corresponding results are summarized in Tables 5 and 6 for $\lambda = 1$ and $\lambda = 10^6$, respectively. A comparison of the results for these two values of λ shows that the pressure error grows proportionally to λ , while the velocity error remains essentially unchanged. This behavior clearly demonstrates the robustness of the proposed scheme in the presence of large irrotational body force.

TABLE 4. Convergence history in porous media of Example 2.

μ	k	Mesh	$\ \mathbf{e}_{\mathbf{u}^D}\ _{L^2(\Omega^D)}$		$\ e_{p^D}\ _{L^2(\Omega^D)}$			
		h^{-1}	Error	Rate	Error	Rate		
1	1	2	1.8939e-01	NA	4.0425e-01	NA		
		4	3.4780e-01	-0.8769	1.3676e-01	1.5636		
		8	1.2689e-01	1.4547	3.0482e-02	2.1657		
		16	3.3664e-02	1.9143	7.8238e-03	1.9620		
		32	8.5374e-03	1.9793	1.9726e-03	1.9878		
		64	2.1446e-03	1.9931	4.9434e-04	1.9965		
	2	2	3.4243e-01	NA	2.6456e-01	NA		
		4	9.4358e-02	1.8596	3.2988e-01	-0.3183		
		8	1.6876e-02	2.4832	9.1193e-02	1.8550		
		16	2.3463e-03	2.8465	2.4749e-02	1.8816		
		32	3.1828e-04	2.8820	6.3138e-03	1.9708		
		64	4.2845e-05	2.8931	1.5865e-03	1.9927		
		10^{-4}	1	4	3.4748e-05	NA	1.3271e-01	1.3541
				8	1.2670e-05	1.4555	3.1266e-02	2.0857
16	3.3649e-06			1.9128	8.0694e-03	1.9541		
32	8.5350e-07			1.9791	2.0335e-03	1.9885		
64	2.1430e-07			1.9937	5.0940e-04	1.9971		
128	5.3533e-08			2.0012	1.2741e-04	1.9993		
2	2		3.4231e-05	NA	2.6161e-01	NA		
	4		9.3874e-06	1.8665	3.2885e-01	-0.3300		
	8		1.6871e-06	2.4762	9.1168e-02	1.8508		
	16		2.3455e-07	2.8466	2.4744e-02	1.8814		
	32		3.1768e-08	2.8843	6.3138e-03	1.9705		
	64		4.2183e-09	2.9128	1.5865e-03	1.9926		

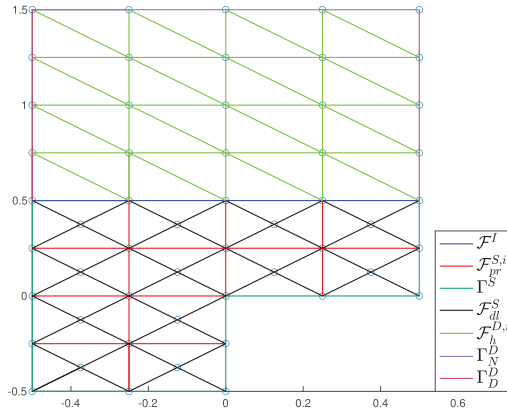


FIGURE 4. Sample mesh for Example 4 when $h = \frac{1}{4}$.

TABLE 5. Convergence history in free fluid domain of Example 3.

λ	k	Mesh h^{-1}	$\ e_{\mathbf{u}^S}\ _{L^2(\Omega^S)}$		$\ e_{\mathbf{L}^S}\ _{L^2(\Omega^S)}$		$\ e_{p^S}\ _{L^2(\Omega^S)}$	
			Error	Rate	Error	Rate	Error	Rate
1	1	1	1.0589e-04	NA	5.8611e-04	NA	4.4541e-02	NA
		2	2.8805e-05	1.8781	2.6496e-04	1.1454	1.0543e-02	2.0789
		4	5.8214e-06	2.3069	5.5384e-05	2.2582	2.6104e-03	2.0139
		8	1.4458e-06	2.0095	1.3395e-05	2.0478	6.5149e-04	2.0024
		16	3.6208e-07	1.9975	3.3373e-06	2.0049	1.6281e-04	2.0005
		32	9.0575e-08	1.9991	8.3406e-07	2.0005	4.0700e-05	2.0001
		64	2.2648e-08	1.9998	2.0851e-07	2.0000	1.0175e-05	2.0000
		128	5.6625e-09	1.9998	5.2130e-08	1.9999	2.5437e-06	2.0000
	2	1	2.4729e-05	NA	1.9456e-04	NA	1.4536e-03	NA
		2	2.4300e-06	3.3472	1.8672e-05	3.3813	1.3702e-04	3.4072
		4	1.1454e-07	4.4070	9.4232e-07	4.3085	1.6424e-05	3.0605
		8	6.8938e-09	4.0544	5.2470e-08	4.1667	2.0388e-06	3.0100
		16	4.2894e-10	4.0064	3.0597e-09	4.1000	2.5444e-07	3.0023
		32	2.7313e-11	3.9731	1.8597e-10	4.0403	3.1793e-08	3.0006
64		2.2911e-12	3.5755	1.4769e-11	3.6544	3.9737e-09	3.0001	
10^6		1	1	1.0589e-04	NA	5.8611e-04	NA	1.3266e+04
	2		2.8805e-05	1.8781	2.6496e-04	1.1454	3.6387e+03	1.8662
	4		5.8214e-06	2.3069	5.5384e-05	2.2582	9.2873e+02	1.9701
	8		1.4458e-06	2.0095	1.3395e-05	2.0478	2.3336e+02	1.9927
	16		3.6207e-07	1.9976	3.3372e-06	2.0050	5.8412e+01	1.9982
	32		9.0562e-08	1.9993	8.3393e-07	2.0006	1.4608e+01	1.9995
	64		2.2635e-08	2.0004	2.0837e-07	2.0007	3.6522e+00	1.9999
	2		1	2.4729e-05	NA	1.9456e-04	NA	1.0417e+03
		2	2.4300e-06	3.3472	1.8672e-05	3.3813	1.3021e+02	3.0000
		4	1.1455e-07	4.4070	9.4237e-07	4.3084	1.6276e+01	3.0000
		8	6.8953e-09	4.0542	5.2509e-08	4.1657	2.0345e+00	3.0000
		16	4.3003e-10	4.0031	3.0986e-09	4.0829	2.5431e-01	3.0000
		32	3.0848e-11	3.8012	2.6034e-10	3.5731	3.1789e-02	3.0000

5.4. Example 4: Singular solution

In this numerical example, we simulate the behavior of our scheme in the case when the regularity of solution doesn't fulfill the assumption given in the convergence analysis. We consider L-shaped domain $\Omega^S = [-0.5, 0.5] \times [-0.5, 0.5] - [0, 0.5] \times [-0.5, 0.5]$ and $\Omega^D = [-0.5, 0.5] \times [0.5, 1.5]$, the boundary is separated by $\Gamma_D^D = \{(x, y) : y = 1.5\}$ and $\Gamma_N^D = \{(x, y) : x \in \{-\frac{1}{2}, \frac{1}{2}\}, y \geq 0\}$, as shown in Figure 4. The analytic solution is given by polar system (r, θ) by [36]

$$p^S(r, \theta) = p^D(r, \theta) = -\frac{r^{\gamma-1}}{1-\gamma}((1+\gamma)^2\psi'(\theta) + \psi'''(\theta)),$$

$$\mathbf{u}^S(r, \theta) = \mathbf{u}^D(r, \theta) = r^\gamma \begin{pmatrix} (1+\gamma)\sin(\theta)\psi(\theta) + \cos(\theta)\psi'(\theta) \\ -(1+\gamma)\cos(\theta)\psi(\theta) + \sin(\theta)\psi'(\theta) \end{pmatrix},$$

where

$$\psi(\phi) = \sin((1+\gamma)\phi)\cos(\gamma\omega)/(1+\gamma) - \cos((1+\gamma)\phi) - \sin((1-\gamma)\phi)\cos(\gamma\omega)/(1-\gamma) + \cos((1-\gamma)\phi).$$

We take $\gamma \approx 0.54448373678246$ and $\omega = 3\pi/2$, where $\mathbf{u}^j \in H^{1+\gamma}(\Omega^j)^2$ and $p^j \in H^\gamma(\Omega^j)$, where $j = S, D$. For the equation parameters, we select $\alpha = \mu = \beta = \kappa = 1$. The convergence history against the mesh size

TABLE 6. Convergence history in porous media of Example 3.

λ	k	Mesh	$\ \mathbf{e}_{\mathbf{u}^D}\ _{L^2(\Omega^D)}$		$\ e_{p^D}\ _{L^2(\Omega^D)}$	
		h^{-1}	Error	Rate	Error	Rate
1	1	1	1.1192e-02	NA	4.7326e-02	NA
		2	2.8948e-03	1.9509	1.2602e-02	1.9090
		4	7.1996e-04	2.0075	3.1918e-03	1.9812
		8	1.7970e-04	2.0023	8.0012e-04	1.9961
		16	4.4906e-05	2.0006	2.0016e-04	1.9991
		32	1.1226e-05	2.0001	5.0048e-05	1.9998
		64	2.8070e-06	1.9997	1.2512e-05	1.9999
		128	7.0246e-07	1.9986	3.1281e-06	2.0000
	2	1	6.4717e-04	NA	1.4048e-01	NA
		2	9.4344e-05	2.7781	3.5427e-02	1.9875
		4	1.2844e-05	2.8768	8.8740e-03	1.9972
		8	1.6739e-06	2.9398	2.2194e-03	1.9994
		16	2.1410e-07	2.9668	5.5492e-04	1.9998
		32	2.7207e-08	2.9763	1.3873e-04	2.0000
64		4.2419e-09	2.6812	3.4684e-05	2.0000	
10^6	1	1	1.1192e-02	NA	2.2170e+04	NA
		2	2.8948e-03	1.9509	5.6050e+03	1.9838
		4	7.1996e-04	2.0075	1.4051e+03	1.9960
		8	1.7970e-04	2.0023	3.5152e+02	1.9990
		16	4.4906e-05	2.0006	8.7896e+01	1.9998
		32	1.1226e-05	2.0001	2.1975e+01	1.9999
		64	2.8070e-06	1.9997	5.4938e+00	2.0000
		2	1	6.4717e-04	NA	6.8939e+04
	2		9.4345e-05	2.7781	1.7463e+04	1.9810
	4		1.2844e-05	2.8769	4.3800e+03	1.9953
	8		1.6721e-06	2.9413	1.0959e+03	1.9988
	16		2.1025e-07	2.9915	2.7403e+02	1.9997
	32		2.3695e-08	3.1494	6.8511e+01	1.9999

can be referred to Tables 7 and 8, which is consistent with the results given in [27]. The convergence rate of pressure and velocity gradient is approximately $\mathcal{O}(h^\gamma)$, while the convergence rate of velocity is approximately $\mathcal{O}(h^{\min\{k+1, 2\gamma\}})$.

6. PROOFS

This section gives the proofs for Lemmas 4.12 and 4.13.

6.1. Proof of Lemma 4.12

For an arbitrary element $\tau \in \mathcal{T}_h^S$, integration by parts together with the condition $\nabla \cdot \mathbf{r}_h^S = 0$ yields

$$(\mathbf{z}_h^S \otimes \mathbf{r}_h^S, \nabla \mathbf{v}_h^S)_\tau = -(\mathbf{r}_h^S \nabla \mathbf{z}_h^S, \mathbf{v}_h^S)_\tau + \sum_{F \in \partial\tau} (\mathbf{r}_h^S \cdot \mathbf{n}, \mathbf{z}_h^S \cdot \mathbf{v}_h^S)_F. \tag{6.1}$$

Since $\mathbf{r}_h^S \in \mathbf{H}(\text{div}; \Omega^S)$ and $(\mathbf{r}_h^S)|_\tau \in H^1(\tau)^d$ for every $\tau \in \mathcal{T}_h^S$, the normal component $\mathbf{r}_h^S \cdot \mathbf{n}$ is continuous across interior faces in \mathcal{T}_h^S , i.e., $[\mathbf{r}_h^S \cdot \mathbf{n}]|_F = 0$ for all $F \in \mathcal{F}_h^{S,i}$. Consequently, on each interior face the average

TABLE 7. Convergence history in free fluid domain of Example 4.

k	Mesh	$\ \mathbf{e}_{\mathbf{u}^S}\ _{L^2(\Omega^S)}$		$\ \mathbf{e}_{L^S}\ _{L^2(\Omega^S)}$		$\ \mathbf{e}_{p^S}\ _{L^2(\Omega^S)}$	
	h^{-1}	Error	Rate	Error	Rate	Error	Rate
1	1	1.2329e-01	NA	1.6093e+00	NA	1.7952e+00	NA
	2	4.5819e-02	1.4281	1.1882e+00	0.4376	1.1182e+00	0.6830
	4	1.7320e-02	1.4035	8.4748e-01	0.4875	7.2913e-01	0.6168
	8	6.8695e-03	1.3341	5.9126e-01	0.5194	4.8548e-01	0.5867
	16	2.8576e-03	1.2654	4.0838e-01	0.5338	3.2756e-01	0.5676
	32	1.2381e-03	1.2067	2.8087e-01	0.5400	2.2275e-01	0.5563
	64	5.5323e-04	1.1621	1.9283e-01	0.5425	1.5211e-01	0.5503

TABLE 8. Convergence history in porous media of Example 4.

k	Mesh	$\ \mathbf{e}_{\mathbf{u}^D}\ _{L^2(\Omega^D)}$		$\ \mathbf{e}_{p^D}\ _{L^2(\Omega^D)}$	
	h^{-1}	Error	Rate	Error	Rate
1	1	2.2905e-01	NA	3.7207e-02	NA
	2	7.9220e-02	1.5318	9.0887e-03	2.0334
	4	2.7650e-02	1.5186	2.5303e-03	1.8447
	8	9.7383e-03	1.5055	8.8805e-04	1.5106
	16	3.4536e-03	1.4956	3.8795e-04	1.1948
	32	1.2333e-03	1.4856	1.8349e-04	1.0802
	64	4.4443e-04	1.4724	8.7702e-05	1.0650

coincides with the trace: $\{\mathbf{r}_h^S \cdot \mathbf{n}\}_F = (\mathbf{r}_h^S \cdot \mathbf{n})|_F$. Summing (6.1) over all elements $\tau \in \mathcal{T}_h^S$, we obtain

$$\begin{aligned}
 N_h(\mathbf{r}_h^S, \mathbf{z}_h^S, \mathbf{v}_h^S) + D_h(\mathbf{r}_h^S, \underline{H}_h^S, \mathbf{v}_h^S) &= \sum_{\tau \in \mathcal{T}_h^S} (\mathbf{r}_h^S \nabla \mathbf{z}_h^S, \mathbf{v}_h^S)_\tau - \sum_{F \in \mathcal{F}_h^S} (\mathbf{r}_h^S \cdot \mathbf{n}, [\mathbf{z}_h^S] \cdot \{\mathbf{v}_h^S\})_F \\
 &\quad + \sum_{F \in \mathcal{F}_h^{S,i}} (|\mathbf{r}_h^S \cdot \mathbf{n}|, [\mathbf{z}_h^S] \cdot [\mathbf{v}_h^S])_F + \sum_{F \in \mathcal{F}_h^{S,b}} (|\mathbf{r}_h^S \cdot \mathbf{n}| - \mathbf{r}_h^S \cdot \mathbf{n}, \mathbf{z}_h^S \cdot \mathbf{v}_h^S)_F \\
 &\quad - \sum_{F \in \mathcal{F}^I} (\mathbf{r}_h^S \cdot \mathbf{n}, ((\mathbf{z}_h^S)^t + \alpha^{-1} \mu^{-1} \kappa^{\frac{1}{2}} (\underline{H}_h^S \mathbf{n})^t) \cdot (\mathbf{v}_h^S)^t)_F =: \sum_{j=1}^5 I_j.
 \end{aligned}$$

We now estimate each term separately. Hölder’s inequality gives

$$I_1 \leq \sum_{\tau \in \mathcal{T}_h^S} \|\mathbf{r}_h^S\|_{L^4(\tau)} \|\nabla \mathbf{z}_h^S\|_{L^2(\tau)} \|\mathbf{v}_h^S\|_{L^4(\tau)} \leq \|\mathbf{r}_h^S\|_{L^4(\Omega^S)} \|\nabla_h \mathbf{z}_h^S\|_{L^2(\Omega^S)} \|\mathbf{v}_h^S\|_{L^4(\Omega^S)}$$

and

$$\begin{aligned}
 I_2 &\leq \sum_{F \in \mathcal{F}_h^S} h_F^{\frac{1}{4}} \|\mathbf{r}_h^S \cdot \mathbf{n}\|_{L^4(F)} h_F^{-\frac{1}{2}} \|[\mathbf{z}_h^S]\|_{L^2(F)} h_F^{\frac{1}{4}} \|\{\mathbf{v}_h^S\}\|_{L^4(F)} \\
 &\leq \left(\sum_{\tau \in \mathcal{T}_h^S} \sum_{F \in \partial\tau} h_F \|\mathbf{r}_h^S\|_{L^4(F)}^4 \right)^{\frac{1}{4}} \left(\sum_{F \in \mathcal{F}_h^S} h_F^{-1} \|[\mathbf{z}_h^S]\|_{L^2(F)}^2 \right)^{\frac{1}{2}} \left(\sum_{\tau \in \mathcal{T}_h^S} \sum_{F \in \partial\tau} h_F \|\mathbf{v}_h^S\|_{L^4(F)}^4 \right)^{\frac{1}{4}}.
 \end{aligned}$$

Proceeding in a similar fashion, we obtain

$$\begin{aligned}
 I_3 + I_4 &\leq 2 \left(\sum_{\tau \in \mathcal{T}_h^S} \sum_{F \in \partial\tau} h_F \|\mathbf{r}_h^S\|_{L^4(F)}^4 \right)^{\frac{1}{4}} \left(\sum_{F \in \mathcal{F}_h^S} h_F^{-1} \|[\mathbf{z}_h^S]\|_{L^2(F)}^2 \right)^{\frac{1}{2}} \left(\sum_{\tau \in \mathcal{T}_h^S} \sum_{F \in \partial\tau} h_F \|\mathbf{v}_h^S\|_{L^4(F)}^4 \right)^{\frac{1}{4}} \\
 I_5 &\leq \left(\sum_{F \in \mathcal{F}^I} h_F \|\mathbf{r}_h^S\|_{L^4(F)}^4 \right)^{\frac{1}{4}} \left(\sum_{F \in \mathcal{F}^I} h_F^{-1} \|(\mathbf{z}_h^S)^t + \alpha^{-1} \mu^{-1} \kappa^{\frac{1}{2}} (\underline{H}_h^S \mathbf{n})^t\|_{L^2(F)}^2 \right)^{\frac{1}{2}} \left(\sum_{F \in \mathcal{F}^I} h_F \|\mathbf{v}_h^S\|_{L^4(F)}^4 \right)^{\frac{1}{4}}.
 \end{aligned}$$

Combining the above estimates completes the proof.

6.2. Proof of Lemma 4.13

(1) Proof of (4.21). In view of Lemma 4.6, there exists a unique $\underline{G}_h^S \in \underline{W}_h^S$ satisfying

$$\begin{aligned}
 (\underline{G}_h^S \mathbf{n}, \mathbf{p}_k)_F &= -h_F^{-1} ([\mathbf{z}_h^S], \mathbf{p}_k)_F, & \forall F \in \mathcal{F}_{pr}^S, \forall \mathbf{p}^k \in P^k(F)^d, \\
 ((\underline{G}_h^S \mathbf{n})^t, \mathbf{p}_k)_F &= -h_F^{-1} ([(\mathbf{z}_h^S)^t], \mathbf{p}_k)_F, & \forall F \in \mathcal{F}_{dl}^S, \forall \mathbf{p}_k \in \mathbf{P}_t^k(F), \\
 ((\underline{G}_h^S \mathbf{n})^t, \mathbf{p}_k)_F &= -h_F^{-1} ((\mathbf{z}_h^S)^t + \alpha^{-1} \mu^{-1} \kappa^{\frac{1}{2}} (\underline{H}_h^S \mathbf{n})^t, \mathbf{p}_k)_F, & \forall F \in \mathcal{F}^I, \forall \mathbf{p}_k \in \mathbf{P}_t^k(F), \\
 (\underline{G}_h^S \mathbf{n} \cdot \mathbf{n}, p_k)_F &= 0, & \forall F \in \mathcal{F}^I, \forall p_k \in P^k(F), \\
 (\underline{G}_h^S, \underline{p}_{k-1})_\tau &= (\nabla \mathbf{z}_h^S, \underline{p}_{k-1})_\tau, & \forall \tau \in \mathcal{T}_h^S, \forall \underline{p}_{k-1} \in P^{k-1}(\tau)^{d \times d},
 \end{aligned}$$

where for any $F \in \mathcal{F}^I$, we use the decomposition $P^k(F)^d = \mathbf{P}_t^k(F) \oplus P^k(F)\mathbf{n}$.

A scaling argument implies the existence of a constant $C_{\underline{W}_h^S, \underline{U}_h^S} > 0$, independent of the mesh size h and the parameters α , β , μ , and κ , such that

$$\|\underline{G}_h^S\|_{L^2(\Omega^S)} \leq C_{\underline{W}_h^S, \underline{U}_h^S} \left(\|\mathbf{z}_h^S\|_{\underline{U}_h^S, 1}^2 + \sum_{F \in \mathcal{F}^I} h_F^{-1} \left\| (\mathbf{u}^S)^t + \alpha^{-1} \mu^{-1} \kappa^{\frac{1}{2}} (\underline{H}_h^S \mathbf{n})^t \right\|_{L^2(F)}^2 \right)^{\frac{1}{2}}. \quad (6.2)$$

Since $\underline{G}_h^S \mathbf{n} \cdot \mathbf{n}|_F = 0$ for any $F \in \mathcal{F}^I$, we obtain $I_h(\mathbf{z}_h^D, \underline{G}_h^S) = 0$. This, together with the adjoint property (3.2), yields

$$\begin{aligned}
 \left(\mu^{-\frac{1}{2}} \underline{H}_h^S, \mu^{-\frac{1}{2}} \underline{G}_h^S \right)_{\Omega^S} &= B_h(\underline{G}_h^S, \mathbf{z}_h^S) - \sum_{F \in \mathcal{F}^I} \left(\alpha^{-1} \mu^{-1} \kappa^{\frac{1}{2}} (\underline{H}_h^S \mathbf{n})^t, (\underline{G}_h^S \mathbf{n})^t \right)_F \\
 &= \|\mathbf{z}_h^S\|_{\underline{U}_h^S, 1}^2 + \sum_{F \in \mathcal{F}^I} h_F^{-1} \left\| (\mathbf{z}_h^S)^t + \alpha^{-1} \mu^{-1} \kappa^{\frac{1}{2}} (\underline{H}_h^S \mathbf{n})^t \right\|_{L^2(F)}^2.
 \end{aligned}$$

Combining this identity, (6.2) and the Cauchy–Schwarz inequality gives (4.21).

To prove (4.22), setting $\underline{G}_h^S = \underline{H}_h^S$ in (4.20) yields

$$A_h(\underline{H}_h^S, \underline{H}_h^S) - B_h^*(\mathbf{z}_h^S, \underline{H}_h^S) - I_h(\mathbf{z}_h^D, \underline{H}_h^S) = 0. \quad (6.3)$$

The definition of $A_h(\cdot, \cdot)$ (cf. (3.1)) gives

$$A_h(\underline{H}_h^S, \underline{H}_h^S) = \left\| \mu^{-\frac{1}{2}} \underline{H}_h^S \right\|_{L^2(\Omega^S)}^2 + \left\| \alpha^{-\frac{1}{2}} \mu^{-\frac{1}{2}} \kappa^{\frac{1}{4}} (\underline{H}_h^S \mathbf{n})^t \right\|_{L^2(\Gamma^I)}^2. \quad (6.4)$$

Integration by parts and the Cauchy–Schwarz inequality imply

$$\begin{aligned}
 B_h^*(\mathbf{z}_h^S, \underline{\mathbf{H}}_h^S) + I_h(\mathbf{z}_h^D, \underline{\mathbf{H}}_h^S) &= (\nabla_h \mathbf{z}_h^S, \underline{\mathbf{H}}_h^S)_{\Omega^S} - \sum_{F \in \mathcal{F}_{pr}^S} ([\mathbf{z}_h^S], \underline{\mathbf{H}}_h^S \mathbf{n})_F - \sum_{F \in \mathcal{F}_{dt}^S} ([(\mathbf{z}_h^S)^t], (\underline{\mathbf{H}}_h^S \mathbf{n})^t)_F \\
 &\quad - \sum_{F \in \mathcal{F}^I} ((\mathbf{z}_h^S)^t, (\underline{\mathbf{H}}_h^S \mathbf{n})^t)_F - \sum_{F \in \mathcal{F}^I} (\mathbf{z}_h^S \cdot \mathbf{n} - \mathbf{z}_h^D \cdot \mathbf{n}, \underline{\mathbf{H}}_h^S \mathbf{n} \cdot \mathbf{n})_F \\
 &\leq \left(\|\mathbf{z}_h^S\|_{\underline{U}_h^S, 1}^2 + \sum_{F \in \mathcal{F}^I} \|(\mathbf{z}_h^S)^t\|_{L^2(F)}^2 + \sum_{F \in \mathcal{F}^I} h_F^{-1} \|\mathbf{z}_h^S \cdot \mathbf{n} - \mathbf{z}_h^D \cdot \mathbf{n}\|_{L^2(F)}^2 \right)^{\frac{1}{2}} \\
 &\quad \times \left(\|\underline{\mathbf{H}}_h^S\|_{\underline{W}_h^S, 0}^2 + \|(\underline{\mathbf{H}}_h^S \mathbf{n})^t\|_{L^2(\Gamma^I)}^2 \right)^{\frac{1}{2}}, \tag{6.5}
 \end{aligned}$$

Moreover,

$$\begin{aligned}
 &\left(\|\underline{\mathbf{H}}_h^S\|_{\underline{W}_h^S, 0}^2 + \|(\underline{\mathbf{H}}_h^S \mathbf{n})^t\|_{L^2(\Gamma^I)}^2 \right)^{\frac{1}{2}} \\
 &\leq \mu^{\frac{1}{2}} C_{\alpha, \kappa} \left(\|\mu^{-\frac{1}{2}} \underline{\mathbf{H}}_h^S\|_{L^2(\Omega^S)}^2 + \|\alpha^{-\frac{1}{2}} \mu^{-\frac{1}{2}} \kappa^{\frac{1}{4}} (\underline{\mathbf{H}}_h^S \mathbf{n})^t\|_{L^2(\Gamma^I)}^2 \right)^{\frac{1}{2}}, \tag{6.6}
 \end{aligned}$$

with $C_{\alpha, \kappa} = \max\{1, \alpha^{\frac{1}{2}} \kappa^{-\frac{1}{4}}\}$. Combining (6.3)–(6.6), we obtain (4.22).

- (2) Proof of (4.24). Since $r_h^D \in L^2(\Omega^D)$, according to Lemma 53.9 from [17], there exists $\mathbf{v}^D \in H^1(\Omega^D)^d$ satisfying that

$$\mathbf{v}^D = \mathbf{0} \text{ on } \Gamma^I \cup \Gamma_N^D, \quad \nabla \cdot \mathbf{v}^D = -r_h^D \text{ in } \Omega^D, \quad \text{and } \|\mathbf{v}^D\|_{H^1(\Omega^D)} \leq C \|r_h^D\|_{L^2(\Omega^D)}. \tag{6.7}$$

Using the commutative property of the BDM projection,

$$\nabla \cdot \mathbf{\Pi}_{\text{BDM}} \mathbf{v}^D = \mathbf{\Pi}_{P_h^D} (\nabla \cdot \mathbf{v}^D), \tag{6.8}$$

we obtain

$$\begin{aligned}
 a_h(\mathbf{\Pi}_{\text{BDM}} \mathbf{v}^D, r_h^D) &= -(\nabla \cdot \mathbf{\Pi}_{\text{BDM}} \mathbf{v}^D, r_h^D)_{\Omega^D} \\
 &= -(\mathbf{\Pi}_{P_h^D} (\nabla \cdot \mathbf{v}^D), r_h^D)_{\Omega^D} \\
 &= -(\mathbf{\Pi}_{P_h^D} (-r_h^D), r_h^D)_{\Omega^D} = \|r_h^D\|_{L^2(\Omega^D)}^2, \\
 J_h(\mathbf{\Pi}_{\text{BDM}} \mathbf{v}^D, r_h^S) &= I_h(\mathbf{\Pi}_{\text{BDM}} \mathbf{v}^D, \underline{\mathbf{H}}_h^S) = 0.
 \end{aligned}$$

Set $\mathbf{v}_h^D = \mathbf{\Pi}_{\text{BDM}} \mathbf{v}^D$. Using the discrete Sobolev embedding (Lem. 4.8), the continuous trace inequality ([14, Lem. 1.52]), the homogeneous boundary condition of \mathbf{v}^D , (4.18) and (6.7), we have the following result for any $1 < p \leq 6$:

$$\|\mathbf{\Pi}_{\text{BDM}} \mathbf{v}^D\|_{L^p(\Omega^D)} \leq C \|\mathbf{\Pi}_{\text{BDM}} \mathbf{v}^D\|_{\text{DG}, \mathcal{T}_h^D} \leq C \|\mathbf{v}^D\|_{H^1(\Omega^D)} \leq C \|r_h^D\|_{L^2(\Omega^D)}.$$

Now, taking $\mathbf{v}_h^D = \mathbf{\Pi}_{\text{BDM}} \mathbf{v}^D$ in (4.23) and applying Lemma 4.8 yields

$$\begin{aligned}
 \|r_h^D\|_{L^2(\Omega^D)}^2 &= a_h(\mathbf{\Pi}_{\text{BDM}} \mathbf{v}^D, r_h^D) \\
 &= -(\mathcal{M}(\mathbf{z}_h^D), \mathbf{\Pi}_{\text{BDM}} \mathbf{v}^D)_{\Omega^D} \\
 &\leq \left\| \mu^{\frac{1}{2}} \kappa^{-\frac{1}{2}} \mathbf{z}_h^D \right\|_{L^2(\Omega^D)} \left\| \mu^{\frac{1}{2}} \kappa^{-\frac{1}{2}} \mathbf{\Pi}_{\text{BDM}} \mathbf{v}^D \right\|_{L^2(\Omega^D)} + \beta \|\mathbf{z}_h^D\|_{L^3(\Omega^D)}^2 \|\mathbf{\Pi}_{\text{BDM}} \mathbf{v}^D\|_{L^3(\Omega^D)} \\
 &\leq C \left(\mu^{\frac{1}{2}} \kappa^{-\frac{1}{2}} \left\| \mu^{\frac{1}{2}} \kappa^{-\frac{1}{2}} \mathbf{z}_h^D \right\|_{L^2(\Omega^D)} + \beta \|\mathbf{z}_h^D\|_{L^3(\Omega^D)}^2 \right) \|\mathbf{v}^D\|_{H^1(\Omega^D)} \\
 &\leq C_{U_h^D, P_h^D} \left(\mu^{\frac{1}{2}} \kappa^{-\frac{1}{2}} \left\| \mu^{\frac{1}{2}} \kappa^{-\frac{1}{2}} \mathbf{z}_h^D \right\|_{L^2(\Omega^D)} + \beta \|\mathbf{z}_h^D\|_{L^3(\Omega^D)}^2 \right) \|r_h^D\|_{L^2(\Omega^D)},
 \end{aligned}$$

where in the second equality we have used that $\mathbf{\Pi}_{\text{BDM}}\mathbf{v}^D \cdot \mathbf{n} = 0$ on Γ^I , which follows from $\mathbf{v}^D \cdot \mathbf{n} = 0$ on Γ^I . Dividing both sides by $\|r_h^D\|_{L^2(\Omega^D)}$ implies (4.24).

ACKNOWLEDGMENTS

The authors would like to express their sincere thanks to the anonymous referees, whose invaluable comments led to an improved version of the paper.

FUNDING

The research of Lina Zhao is partially supported by the Research Grants Council of the Hong Kong Special Administrative Region, China (Project No. CityU 21309522, CityU 11302424) and Young Scientists fund, NSFC (Project No. 12401543).

REFERENCES

- [1] A. Ern and J.L. Guermond, *Finite Elements I*. Vol. 1084. Springer (2021).
- [2] G.S. Beavers and D.D. Joseph, Boundary conditions at a naturally permeable wall. *J. Fluid. Mech.* **30** (1967) 197–207.
- [3] S.C. Brenner, Poincaré–Friedrichs inequalities for piecewise H^1 functions. *SIAM J. Numer. Anal.* **41** (2003) 306–324.
- [4] F. Brezzi and M. Fortin, *Mixed and Hybrid Finite Element Methods*. Vol. 15. Springer Science & Business Media (2012).
- [5] F. Brezzi, J. Douglas and L.D. Marini, Two families of mixed finite elements for second order elliptic problems. *Numer. Math.* **47** (1985) 217–235.
- [6] D. Castanon Quiroz and D.A. Di Pietro, A hybrid high-order method for the incompressible Navier–Stokes problem robust for large irrotational body forces. *Comput. Math. Appl.* **79** (2020) 2655–2677.
- [7] S. Caucao, M. Discacciati, G.N. Gatica and R. Oyarzúa, A conforming mixed finite element method for the Navier–Stokes/Darcy–Forchheimer coupled problem. *ESAIM-Math. Model. Numer. Anal.* **54** (2020) 1689–1723.
- [8] A. Cesmelioglu and S. Rhebergen, A hybridizable discontinuous Galerkin method for the coupled Navier–Stokes and Darcy problem. *J. Comput. Appl. Math.* **422** (2023) 114923.
- [9] A. Cesmelioglu, S. Rhebergen and G.N. Wells, An embedded–hybridized discontinuous Galerkin method for the coupled Stokes–Darcy system. *J. Comput. Appl. Math.* **367** (2020) 112476.
- [10] A. Cesmelioglu, J.J. Lee and S. Rhebergen, A strongly conservative hybridizable discontinuous Galerkin method for the coupled time-dependent Navier–Stokes and Darcy problem. *ESAIM-Math. Model. Numer. Anal.* **58** (2024) 273–302.
- [11] N. Chaabane, V. Girault, C. Puelz and B. Riviere, Convergence of IPDG for coupled time-dependent Navier–Stokes and Darcy equations. *J. Comput. Appl. Math.* **324** (2017) 25–48.
- [12] E.T. Chung and B. Engquist, Optimal discontinuous Galerkin methods for the acoustic wave equation in higher dimensions. *SIAM J. Numer. Anal.* **47** (2009) 3820–3848.
- [13] P.G. Ciarlet, *Linear and Nonlinear Functional Analysis with Applications*. SIAM (2025).
- [14] D.A. Di Pietro and A. Ern, *Mathematical Aspects of Discontinuous Galerkin Methods*. Vol. 69. Springer Science & Business Media (2011).
- [15] M. Discacciati and R. Oyarzúa, A conforming mixed finite element method for the Navier–Stokes/Darcy coupled problem. *Numer. Math.* **135** (2017) 571–606.
- [16] M. Discacciati, A. Quarteroni and A. Valli, Robin–Robin domain decomposition methods for the Stokes–Darcy coupling. *SIAM J. Numer. Anal.* **45** (2007) 1246–1268.
- [17] A. Ern and J.-L. Guermond, *Finite Elements II*. Springer (2021).
- [18] P.H. Forchheimer, Wasserbewegung durch boden. *z. vereines dtsch. Ingenieur* **45** (1901) 1792–1788.
- [19] G. Galdi, *An Introduction to the Mathematical Theory of the Navier–Stokes Equations: Steady-State Problems*. Springer Science & Business Media (2011).
- [20] G.N. Gatica, *A simple introduction to the mixed finite element method, in Theory and Applications*. Springer Briefs in Mathematics. Springer, London (2014).
- [21] G.N. Gatica, S. Meddahi and R. Oyarzúa, A conforming mixed finite-element method for the coupling of fluid flow with porous media flow. *IMA J. Numer. Anal.* **29** (2009) 86–108.

- [22] G.N. Gatica, G.C. Hsiao and S. Meddahi, A coupled mixed finite element method for the interaction problem between an electromagnetic field and an elastic body. *SIAM J. Numer. Anal.* **48** (2010) 1338–1368.
- [23] G.N. Gatica, R. Oyarzúa and F.-J. Sayas, Convergence of a family of Galerkin discretizations for the Stokes–Darcy coupled problem. *Numer. Meth. Part Differ. Equ.* **27** (2011) 721–748.
- [24] G.N. Gatica, R. Oyarzúa and N. Valenzuela, A five-field augmented fully-mixed finite element method for the Navier–Stokes/Darcy coupled problem. *Comput. Math. Appl.* **80** (2020) 1944–1963.
- [25] V. Girault and B. Rivière, DG approximation of coupled Navier–Stokes and Darcy equations by Beaver–Joseph–Saffman interface condition. *SIAM J. Numer. Anal.* **47** (2009) 2052–2089.
- [26] V. Girault and M.F. Wheeler, Numerical discretization of a Darcy–Forchheimer model. *Numer. Math.* **110** (2008) 161–198.
- [27] P. Houston, D. Schötzau and X. Wei, A mixed DG method for linearized incompressible magnetohydrodynamics. *J. Sci. Comput.* **40** (2009) 281–314.
- [28] D. Kim, L. Zhao, E.T. Chung and E.-J. Park, Pressure-robust staggered DG methods for the Navier–Stokes equations on general meshes. Preprint [arXiv:2107.09226](https://arxiv.org/abs/2107.09226) (2021).
- [29] A. Linke, On the role of the Helmholtz decomposition in mixed methods for incompressible flows and a new variational crime. *Comput. Meth. Appl. Mech. Eng.* **268** (2014) 782–800.
- [30] A. Linke and C. Merdon, On velocity errors due to irrotational forces in the Navier–Stokes momentum balance. *J. Comput. Phys.* **313** (2016) 654–661.
- [31] J. Liu, Y. Liu and L. Zhao, Analysis of the staggered DG method for the quasi-Newtonian Stokes flows. *J. Sci. Comput.* **102** (2025) 14.
- [32] G.J. Minty, On a monotonicity method for the solution of nonlinear equations in Banach spaces. *Proc. Nat. Acad. Sci.* **50** (1963) 1038–1041.
- [33] P.A. Nguyen and J.-P. Raymond, Boundary stabilization of the Navier–Stokes equations in the case of mixed boundary conditions. *SIAM J. Control Optim.* **53** (2015) 3006–3039.
- [34] G. Roland and A. Marroco, Sur l’approximation, par éléments finis d’ordre un, et la résolution, par pénalisation-dualité d’une classe de problèmes de Dirichlet non linéaires. *Anal. Numer.* **9** (1975) 41–76.
- [35] P.G. Saffman, On the boundary condition at the surface of a porous medium. *Stud. Appl. Math.* **50** (1971) 93–101.
- [36] L. Zhao and E.-J. Park, A lowest-order staggered DG method for the coupled Stokes–Darcy problem. *IMA J. Numer. Anal.* **40** (2020) 2871–2897.
- [37] L. Zhao and S. Sun, A strongly mass conservative method for the coupled Brinkman–Darcy flow and transport. *SIAM J. Sci. Comput.* **45** (2023) B166–B199.
- [38] L. Zhao, E.T. Chung and M.F. Lam, A new staggered DG method for the Brinkman problem robust in the Darcy and Stokes limits. *Comput. Meth. Appl. Mech. Eng.* **364** (2020) 112986.
- [39] L. Zhao, E.T. Chung, E.-J. Park and G. Zhou, Staggered DG method for coupling of the Stokes and Darcy–Forchheimer problems. *SIAM J. Numer. Anal.* **59** (2021) 1–31.



Please help to maintain this journal in open access!

This journal is currently published in open access under the Subscribe to Open model (S2O). We are thankful to our subscribers and supporters for making it possible to publish this journal in open access in the current year, free of charge for authors and readers.

Check with your library that it subscribes to the journal, or consider making a personal donation to the S2O programme by contacting subscribers@edpsciences.org.

More information, including a list of supporters and financial transparency reports, is available at <https://edpsciences.org/en/subscribe-to-open-s2o>.